

Industrial Simulation



Bachelorwork

Simulation of nano composite materials

Executed at advanced technical college of bachelor program
Industrial Simulation
at the college of St.Pölten/Austria

under the direction of

FH-Prof. Dr. techn. Thomas Schrefl

executed by

Markus Gruber
id101006

St. Pölten at July 23, 2013

Ehrenwörtliche Erklärung

Ich versichere, dass

- ich diese Bachelorarbeit selbständig verfasst, andere als die angegebenen Quellen und Hilfsmittel nicht benutzt und mich sonst keiner unerlaubten Hilfe bedient habe.
- ich das Thema dieser Arbeit bisher weder im Inland noch im Ausland als Prüfungsarbeit vorgelegt habe.
- diese Arbeit mit der vom Begutachter/von der Begutachterin beurteilten Arbeit übereinstimmt.

3. Juni 2013

Markus Gruber

.....
Ort, Datum

.....
Unterschrift

Zusammenfassung

Das Erstellen von Hysteresis-Kurven gehört zu den wichtigsten Techniken um Magnete zu charakterisieren. Hysteresis Kurven werden auch BH-Kurven oder Schleifen genannt weil diese den Zusammenhang zwischen den äußeren anliegenden Feld (H) und der resultierenden Flussdichte (B) zeigen. Das äußere anliegende Feld (H) ist vergleichbar mit einem elektrischen Strom bzw. ist es ein Vielfaches von dem was durch einen Leiter fließt. Das anliegende Feld induziert ein Magnetfeld in einem Material. Die Stärke des entstandenen Magnetfeldes variiert von Material zu Material was wiederum zu verschiedenen Hysteresis-Kurven führt. Diese BH - Kurven geben die Möglichkeit um magnetisches Material zu unterscheiden, welches sich in ihren Zusammensetzungen variiert. Diese Unterschiede sollten es möglich machen jeden Supermagnet und jeweilige Materialkombination zu identifizieren. Mit der Hilfe von Hysteresis - Kurven kann man auch die Eigenschaften von Supermagneten verbessern, diese Supermagnete oder auch Nano Composite Magnete sind immer aus einer hartmagnetischen und weichmagnetischen Phase wobei der weichmagnetische Anteil aus α - Fe und der hartmagnetische Anteil aus $Nd_2Fe_{14}B$ besteht. Einige Simulationen haben bereits gezeigt, dass der Einfluss des hartmagnetischen Anteils gleich bleibt selbst wenn sich das jeweilige Volumen stark verändert, im Gegensatz dazu hat das Volumen der weichmagnetischen Phase auf das Verhalten von Supermagneten einen großen Einfluss. Das Hauptproblem von Simulationen mit finiten Elementen ist, dass es sehr viele Ressourcen benötigt, daher ist es fast unmöglich für jede Materialkombination eine Berechnung zu machen, jedoch kann man aus verschiedenen Berechnungen den jeweiligen Verlauf zeigen und so Rückschlüsse auf das Verhalten machen. Diese Arbeit soll zeigen, dass mit verschiedenen Materialkombinationen bestehend aus verschiedene Geometrien und Volumensverhältnissen der weich und hartmagnetischen Phase auch verschiedene Hysteresis - Kurven entstehen können. Der Hauptteil dieser Arbeit beschränkt sich auf die Erforschung der Auswirkung der Volumen von hart und weichmagnetischen Materialien auf die BH-Kurven, und ob neben den Volumen auch Geometrie, Korngrößen eine Rollen spielen welche zu verschiedenen Hysteresis Kurven führen können. In dieser Arbeit wird ebenfalls gezeigt wie sich die Korngröße der weichmagnetische Phase und der jeweiligen Geometrie von Supermagneten auf die Hysteresis Kurven auswirkt.

Abstract

Hysteresis-loops are one of the most important technique of magneto static characterization. In a lot of scientist works hysteresis-loops are also called BH-curves or loops, because they show the correlation between the external magnetic field (H) and the associated flux density(B). The external field(H) is similar to the current which flows around the material into a conductor where as the resulted flux density(B) is like the magnetic field. The inducted flux density vary from material to material which leads to different BH-curves. Those hysteresis loops give the possibility to differ magnetic materials at some properties. It's more like a fingerprint of every tie which gives every magnets distinct features shown in charts. These features differ in some ways which should make it possible to identify combinations of magneto static materials by this way. These loops are just more than simple characterization tools, at nano-composite magnets where the most common materials are α – Fe / Nd₂Fe₁₄B and FeCo / Nd₂Fe₁₄B. BH-loops reveals some possibilities to optimize the behaviour of those super-magnets, because different geometrical shapes and material properties leads to different distinct features. Nano-composite magnets always consist of two phases in different alignments where the soft phase is α – Fe / FeCo and hard phase is Nd₂Fe₁₄B. Some Simulations show that there is a connection between the volume of the hard and the soft phase, the effect of the hard shape is nearly almost the same but if the volume of the soft shape vary there is a big influence on the magneto static behaviour and moreover on the response BH-loops. The main problem with computing finite elements is, that it takes a lot of time to compute such curves, it's nearly impossible to compute every material composition. One way is to do some time consuming computation on many core systems and calculate these curves on big server clusters. This study should show that is suitable to differ several material combination with different properties like geometry, grain size, soft and hard magnetic content which lead to different curves. The main part of this study is to do different simulations to prove if there is a corresponding between the total volume of α – Fe /Nd₂Fe₁₄B and FeCo / Nd₂Fe₁₄B or beside of the total volume also geometry, grain size about the soft magnetic material are same important which results to different hysteresis loops. At this work there are different simulations to show the influence of the grain size and geometry of the soft phase.

Contents

1	Introduction	2
1.1	Characterization of super magnets	2
1.2	Definition of rare earth	3
2	Material science of nano composite magnets	4
2.1	Introduction to $\text{Nd}_2\text{Fe}_{14}\text{B}/\alpha - \text{Fe}$ - magnets	4
2.2	The hysteresis loop and magnetic properties	5
2.2.1	Introduction	5
2.2.2	Measuring the B-H loop	5
2.2.3	The maximum energy product $(\text{BH})_{(\max)}$	7
2.2.4	The goal of combination soft and hard magnetic materials	8
3	Sphere packing problem	9
3.1	Sphere Packing, how to replace space by spheres	9
3.1.1	Cannonball problem	9
3.1.2	Simple, face-centred cubic packing (fcc) and hexagonal cubic packing (hcp)	10
3.1.3	Sphere packing and response density	11
4	Meshing and quality	15
4.1	Overview of meshing	15
4.2	Meshing quality	15
4.3	Calculation of the mesh quality	17
4.3.1	Mesh smoothing	19
4.3.2	Comparison of different mesh qualities (1/2)	21
4.3.3	Comparison of different mesh qualities (2/2)	23
5	Goals,structure and post processing of all simulations	25
5.1	Goals	25
5.2	Structure	26
5.3	Python scripts	28
5.4	Post processing and calculating the hysteresis curves (BH-loop)	31
6	Some trials with magnetic materials	36
6.1	Determine the required mesh size	36
6.1.1	Introduction	36

6.1.2	Low density packed spheres	37
6.1.3	Low density packed spheres - Mesh of simulation 1 (57k)	38
6.1.4	Low density packed spheres - Mesh of simulation 4 (362k)	38
6.1.5	Low density packed spheres - BH-loops of first parameter set (par1) (Spheres=28; Radius=15nm)	39
6.1.6	Low density packed spheres - Comparison of all BH-loops within the first parameter set (par 1) (Spheres=28; Radius=15nm)	40
6.1.7	Low density packed spheres - BH-loops of second parameter set (par2) (Spheres=28; Radius=15nm)	41
6.1.8	Low density packed spheres - Comparison of all BH-loops within the second parameter set (par2) (Spheres=28; Radius=15nm)	42
6.2	High density close packed spheres	43
6.2.1	High density close packed spheres - Mesh of simulation 1 (57k) . . .	44
6.2.2	High density close packed spheres - Mesh of simulation 4 (362k) . . .	44
6.2.3	High density close packed spheres - BH-loops of first parameter set (par1) (Spheres=28; Radius=15nm)	45
6.2.4	High density close packed spheres - Comparison of all BH-loops within the first parameter set (par1) (Spheres=28; Radius=15nm) . .	46
6.2.5	High density close packed spheres - BH-loops of second parameter set (par2) (Spheres=28; Radius=15nm)	47
6.2.6	High density close packed spheres - Comparison of all BH-loops within the second parameter set (par2) (Spheres=28; Radius=15nm)	48
6.3	High density loose packed spheres	49
6.3.1	High density loose packed spheres - Mesh of simulation 1 (57k) . . .	50
6.3.2	High density loose packed spheres - Mesh of simulation 4 (326k) . . .	50
6.3.3	High density loose packed spheres - BH-loops of first parameter set (par1) (Spheres=48;max Radius=15nm)	51
6.3.4	High density loose packed spheres - Comparison of all BH-loops within the first parameter set (par1) (Spheres=48;max Radius=15nm)	52
6.3.5	High density loose packed spheres - BH-loops of second parameter set (par2) (Spheres=48; max Radius=15nm)	53
6.3.6	High density loose packed spheres - Comparison of all BH-loops within the second parameter set (par2) (Spheres=48;max Radius=15nm)	54
6.3.7	What's the best mesh size ?	55
7	Comparison of high close/high loose/low-density packed spheres	56
7.1	Comments to the simulations	56
7.2	Comparison of different geometries	57
7.2.1	Comparison of low/high close/high loose - packed spheres (par1) . .	58
7.2.2	Comparison of low/high close/high loose - packed spheres (par2) . .	59
8	Influence of soft magnetic material	60
8.1	Effect of soft magnetic material at equal volume parts	60
8.1.1	Computed BH-loops with 135 spheres and grain size with radius of 10nm (volume ratio of intersected cube/spheres = 53/47)	61

8.1.2	Comparison of computed BH-loops with 135 spheres and grain size with radius of 10nm (volume ratio of intersected cube/spheres = 53/47)	62
8.2	Effect of unequal volume ratios	63
8.2.1	Computed BH-loops with 294 spheres and grain size of radius with 10nm (volume ratio of intersected cube/spheres = 40/60)	64
8.2.2	Comparison of computed BH-loops with 294 spheres and grain size of radius with 10nm and volume ratio of 40/60	65
9	Influence of grain size and volume ratio	66
9.1	Description	66
9.2	Influence of grain size and volume ratio	67
9.2.1	Soft magnetic material with grain size of $r=10\text{nm}$ and different vol- ume ratios	68
9.2.2	Soft magnetic material with grain size of $r=12.5\text{nm}$ and different volume ratios	69
9.2.3	Soft magnetic material with grain size of $r=15\text{nm}$ and different vol- ume ratios	70
9.2.4	Comparison of $(BH)_{\max}$ and corresponding H_C values	71
9.2.5	Summary	72
10	Compendium and prospects	73
Bibliography		76
Appendices		77
.1	First Appendix	78

List of Tables

3.1	Possible methods of sphere packing	14
4.1	Computation time and response accuracy	17
6.1	Parameter sets for the simulations	36
9.1	Usage of iron at three different grain sizes(soft magnetic)	66

List of Figures

1.1	Production of rare earth minerals over the world from	3
2.1	Comparison of soft and hard magnetic materials	5
2.2	BH-loops of magneto-static materials	6
2.3	$(BH)_{(\max)}$ - soft magnetic materials	7
2.4	The development of permanent magnets in the 20th Century.	8
3.1	Cannon ball problem	9
3.2	Simple,fcc,hcp - sphere packing	10
3.3	Simple cubic packing	11
3.4	Face-centred cubic(fcc) packing	12
4.1	Simple example of meshing	15
4.2	Shapes for meshing	19
4.3	Smoothing a mesh to improve the quality.	20
4.4	Before meshing,...(1/2)	21
4.5	After meshing,...(1/2)	21
4.6	Mesh quality with lower amount of elemens (1/2)	22
4.7	Mesh quality with higher amount of elements (1/2)	22
4.8	Before meshing,...(2/2)	23
4.9	After meshing (mesh),...(2/2)	23

4.10	Mesh quality with lower amount of elements (2/2)	24
4.11	Mesh quality with higher amount of elements (2/2)	24
5.1	Structure	26
5.2	How to compute M(J)H-curves	33
5.3	How to compute BH-curves	34
6.1	Low density packed spheres - top view	37
6.2	Mesh of simulation 1 with max mesh size = 4.5 and min mesh size = 0.5 . .	38
6.3	Mesh of simulation 4 with max mesh size = 2.05 and min mesh size = 0.5 . .	38
6.4a	Demagnetization curve for a composite magnet (1/2) -cube(hard)/spheres(soft)	39
6.4b	Demagnetization curve for a composite magnet (2/2) -cube(hard)/spheres(soft)	39
6.5	Low density packed spheres - Comparison of all BH-loops where the intersected cube consist of hard magnetic material	40
6.6a	Demagnetization curve for a composite magnet (1/2) -cube(soft)/spheres(hard)	41
6.6b	Demagnetization curve for a composite magnet (2/2) -cube(soft)/spheres(hard)	41
6.7	Low density packed spheres - Comparison of all BH-loops where the intersected cube consist of soft magnetic material	42
6.8	High density close packed spheres - top view	43
6.9	Mesh of simulation 1 with max mesh size = 4.5 and min mesh size = 0.5 . .	44
6.10	Mesh of simulation 4 with max mesh size = 2.05 and min mesh size = 0.5 . .	44
6.11a	Demagnetization curve for a composite magnet (1/2) -cube(hard)/spheres(soft)	45
6.11b	Demagnetization curve for a composite magnet (2/2) -cube(hard)/spheres(soft)	45
6.12	High density close packed spheres - Comparison of all BH-loops where the intersected cube consist of hard magnetic material	46
6.13a	Demagnetization curve for a composite magnet (1/2) -cube(soft)/spheres(hard)	47
6.13b	Demagnetization curve for a composite magnet (2/2) -cube(soft)/spheres(hard)	47
6.14	High density close packed spheres - Comparison of all BH-loops where the intersected cube consist of soft magnetic material	48
6.15	High density loose packed spheres - top view	49
6.16	Mesh of simulation 1 with max mesh size = 4.5 and min mesh size = 0.5 . .	50
6.17	Mesh of simulation 4 with max mesh size = 2.05 and min mesh size = 0.5 . .	50
6.18a	Demagnetization curve for a composite magnet (1/2) -cube(hard)/spheres(soft)	51
6.18b	Demagnetization curve for a composite magnet (2/2) -cube(hard)/spheres(soft)	51
6.19	High density loose packed spheres - Comparison of all BH-loops where the intersected cube consist of hard magnetic material	52
6.20a	Demagnetization curve for a composite magnet (1/2) -cube(soft)/spheres(hard)	53
6.20b	Demagnetization curve for a composite magnet (2/2) -cube(soft)/spheres(hard)	53
6.21	High density loose packed spheres - Comparison of all BH-loops where the intersected cube consist of soft magnetic material	54
6.22	Comparison of two different mesh sizes at the same model	55
7.1	Comparison of all different geometries from chapter 5	57
7.2	Comparison of low/high close/high loose packed spheres where the intersected cube is hard magnetic	58
7.3	Comparison of low/high close/high loose packed spheres where the intersected cube is soft magnetic	59

8.1	Mesh of hexagonal placed spheres and equal volume ratios	60
8.2	BH-loop, the cube is hard magnetic, with equal volume ratios	61
8.3	BH-loop, the cube is hard magnetic, with equal volume ratios	61
8.4	Comparison of two BH-loops with volume ratio of 53/47	62
8.5	Mesh of hexagonal placed spheres and unequal volume ratios	63
8.6	BH-loop, the cube is hard magnetic, with unequal volume ratios	64
8.7	BH-loop, the cube is soft magnetic, with unequal volume ratios	64
8.8	Comparison of two BH-loops with volume ratio of 40/60	65
9.1	Top view different amount of iron with grain size 10nm(soft magnetic) . . .	67
9.2	Top view different amount of iron with grain size 12.5nm(soft magnetic) . .	67
9.3	Top view different amount of iron with grain size 15nm(soft magnetic) . .	67
9.4	BH-loops with grain size of 12nm and different amount of iron	68
9.5	BH-loops with grain size of 12.5nm and different amount of iron	69
9.6	BH-loops with grain size of 15nm and different amount of iron	70
9.7	Mesh of simulation 1 with max mesh size = 4.5 and min mesh size = 0.5 . .	72
1	Comparison of all BH-loops with the grain size of r=5nm	78
2	Comparison of all BH-loops with the grain size of r=5nm	78
3	Comparison of all BH-loops with the grain size of r=7.5nm	79
4	Comparison of all BH-loops with the grain size of r=10nm	79
5	Comparison of all BH-loops with the grain size of r=10nm	80
6	Comparison of all BH-loops with the grain size of r=12.5nm	80
7	Comparison of all BH-loops with the grain size of r=155nm	81
8	Comparison of all BH-loops with approximately 8% $\alpha - Fe$	81
9	Comparison of all BH-loops with approximately 19% $\alpha - Fe$	82
10	Comparison of all BH-loops with approximately 28% $\alpha - Fe$	82
11	Comparison of all BH-loops with approximately 33% $\alpha - Fe$	83
12	Comparison of all BH-loops with approximately 45% $\alpha - Fe$	83
13	Comparison of all BH-loops with approximately 60% $\alpha - Fe$	84

Chapter 1

Introduction

1.1 Characterization of super magnets

Super-magnets are applied at many scopes, and have a big economic and technological importance in different areas of the industry, like automotive industry, wind energy, hydrodynamic power. The power of super magnets comes from special materials which are also called noble earth. Those materials are really expensive and are of great politically interest. According to these facts companies are really anxious to improve the behaviour of those super magnets. One possibility is to increase the effectiveness which also leads to decrease the dependence of noble earth and furthermore to decrease the total costs . Super-magnets are also called nano composite magnets, they are applied at different applications, the impact of increasing the effectiveness of super magnets would lead to a bigger application spectrum. Those nano composite materials which are made of noble earth are characterized by extreme performance data. They have the ability to bear a weight which is 1000-times bigger than their own.[15][6][23]

Properties of nano-composite magnets

- Remanence M_R up to 1.5 Tesla, is the residual magnetism without any external field and external influence.
- Biggest maximum of energy product with $BH_{max} = 512 \text{ kJ/m}^3$, is the peak value about how much energy is a magnet able to save.
- Saturation magnetisation of $J_s=1,61\text{T}$, is the maximum reachable magnetism if the magnetic field is fully aligned into one direction.
- Coercive field strength H_c about 750kA/m , the value to change the direction of the magnetic field into the opposite.
- Curie-temperature of $T_c=586\text{K}$, below this point the magnet is not negatively influenced by the temperature above it is.

These presented values are peak values and depend on a lot of factors only a few of these can be achieved. Magnets with high rating are able to achieve some peak values.[13][15]

Materials of nano-composite magnets

- Nd ... Neodymium
- Dy ... Dysprosium
- Pr ... Praseodymium

These materials are really expensive and influence the effectiveness of every nano-composite magnet. Some studies show that the influence can be decreased with the awareness of the geometry, better manufacturing process, alloys and improvement of the grain boundaries. The goal of making super-magnet must be to use as less as possible of rare earth material but to be still powerful with less temperature dependency. The goal must be to explore much more powerful material combinations as well applying new principles of making nano-composite magnets but some material combinations are already established. At the moment super magnets where materials of neodymium, iron and boron are used are in focus because these material combination are cost effective but still powerful.

1.2 Definition of rare earth

The definition of rare earth comes from the fact that those deposits of these minerals are not exploitable commercially. Rare earth minerals or also called noble earth which are located on the periodic table. Those minerals which are mainly used at high-tech industry and clean energy. Noble earth elements are not really plenty on the earth crust's, but not really uniform distributed over the world. One another fact is that 97 percent of rare earth minerals come from China, so most of the companies which aren't in those countries with well occurred sources want to weaken the dependency from other countries. Because of none uniform distribution there are only several countries where rare earth occur. China has one third of the total amount of rare earth over the whole world, other countries where rare earth appear are in the north of America, Greenland, Mongolia and Australia.[6]

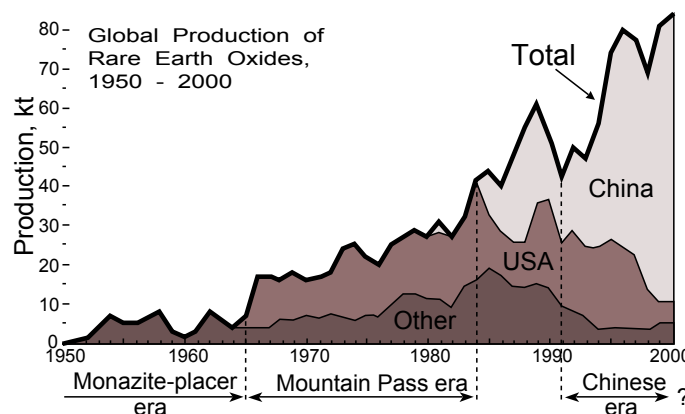


Figure 1.1: Production of rare earth minerals over the world from 1960 to 2000 with the greatest supplier of noble earth, this picture also shows that most of delivered noble earth comes from China and the total amount of rare earth is still rising.[7]

Chapter 2

Material science of nano composite magnets

2.1 Introduction to $\text{Nd}_2\text{Fe}_{14}\text{B}/\alpha - \text{Fe}$ - magnets

First of all we differ between hard and soft magnetic materials. Super-magnets are always made of some kind of noble earth, at most cases Neodymium(Nd) is used with a big amount of Iron (Fe) and a small amount of Boron (B). This material combination is called Nd-Fe-B magnets which is really stable and leads to really strong magnets. During the activity of the manufacturing process always hard and soft magnetic phases arise. Soft magnetic materials are really easy to magnetize, but they are not able to carry a lot of magnetization energy, beside the facts of soft magnetic materials also hard magnetic materials exist, hard magnetic materials are really hard to magnetize, but they are able to carry a lot of magnetization energy. At Nd-Fe-B magnets, the hard magnetic part consists of the material Neodymium (Nd) and the soft magnetic part is Iron (Fe), the material Boron (B) is just used for the improvement of the grain boundaries and to stable these combination of Neodymium and Iron. On the other side Boron (B) is really important for decreasing the amorphous phase (none crystalline phase) which negatively influences the behaviour of nano composite magnets. This composition is build up with about 60-70 percent Iron by 35-25 percent of Neodymium and only 5 percent Boron.[15][23][14] [27]

Hard magnetic phase ($\text{Nd}_2\text{Fe}_{14}\text{B}$): The material combination of Neodymium, Iron, Boron, is just the base of powerful super magnets. These materials are also combined with some alloys. Nevertheless during the manufacturing process hard magnetic phases arise. These phase consists of Neodymium, Iron, Boron but with the distribution of 2:14:1 (Nd-Fe-B). The main properties of hard magnetic materials are less residual magnetism power (M_R , B_R) but high coercive field strength (H_C).[29][23][15][17]

Soft magnetic phase ($\alpha - \text{Fe}$): During the manufacturing process also soft magnetic phases arise. This phase consists at most cases only of Iron (Fe) and Boron (Br). Soft magnetic materials are easier to magnetize but they are not able to carry more magnetization energy in difference to hard magnetic materials. The properties of soft magnetic materials are high residual magnetism power (M_R , B_R) but less coercive

field strength (H_C).[29][23][15][17]

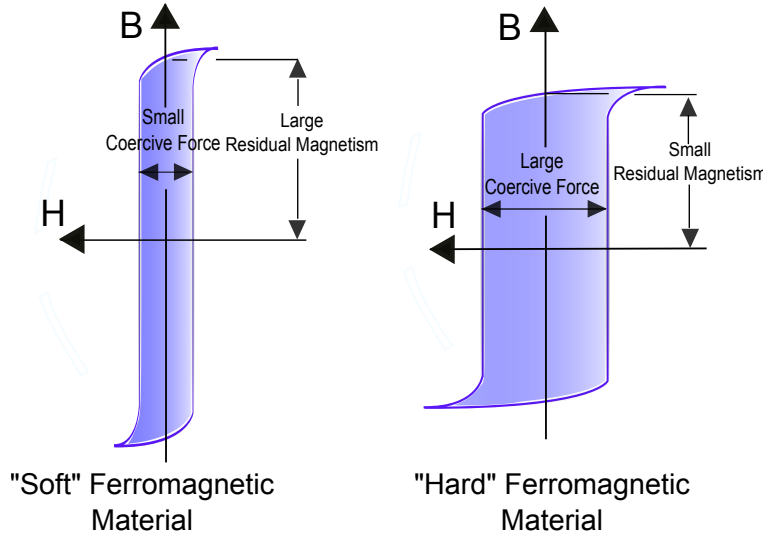


Figure 2.1: Comparison of soft and hard magnetic materials with different coercive forces (H_C 's), the value of H_C is one property of magneto static materials which is the main feature to distinguish between hard and soft magnetic materials.[25]

2.2 The hysteresis loop and magnetic properties

2.2.1 Introduction

A lot of informations can be learned from hysteresis loops, hysteresis loops show the behaviour of every magnetic material, this graph is really important for material science and related magnetic properties. Despite the fact that different material combinations lead to nearly same behaviours, hysteresis loops have significant points which show the main features of every magnetic material. Hysteresis loops are almost called BH-loops because hysteresis loops show the relationship between the flux density (B) and the magnetizing force (H), so every flux density (B) value has an corresponding magnetizing force (H) value.

2.2.2 Measuring the B-H loop

The loop is generated by changing the magnetic force (H) and measuring the flux density (B). First of all, all hysteresis loops start at the origin point, where the magnetizing force is zero (H), if the ferromagnetic material has never been previously magnetized or has been thoroughly demagnetized, all flux density (B) values will follow the dashed line if the magnetizing force (H) increases. At the saturation point "a", almost all magnetic domains are aligned into the same direction, and it's not possible to increase the flux density (B) over this point. If the magnetizing force (H) is reduced to zero, the curve will move from point "a" to point "b" this point is called the residual magnetism, some magnetic domains are aligned but some have lost their alignment. If the magnetizing force is reversed, the curve moves to point "c" this point is called the coercive force. The coercive force is the

point where the flux density is zero, it's just the force which is needed to flip the direction of all magnetic domains. On the other side of the x-axis there is the saturated point "d", it's the same amount of flux density (B) of point "a", but into the mirrored direction, this point becomes active after increasing the magnetizing force into the negative direction. After reducing the magnetizing force to zero the point "e" occurs, it's the residual magnetism power into the other direction, nearly equal to point "b". Increasing the magnetizing force (H) back in the positive direction will return the flux density B to zero. Notice that the curve did not return to the origin of the graph because some force is required to remove the residual magnetism. The curve will take a different path from point "f" back to the saturation point where it completes the loop.[2][25]

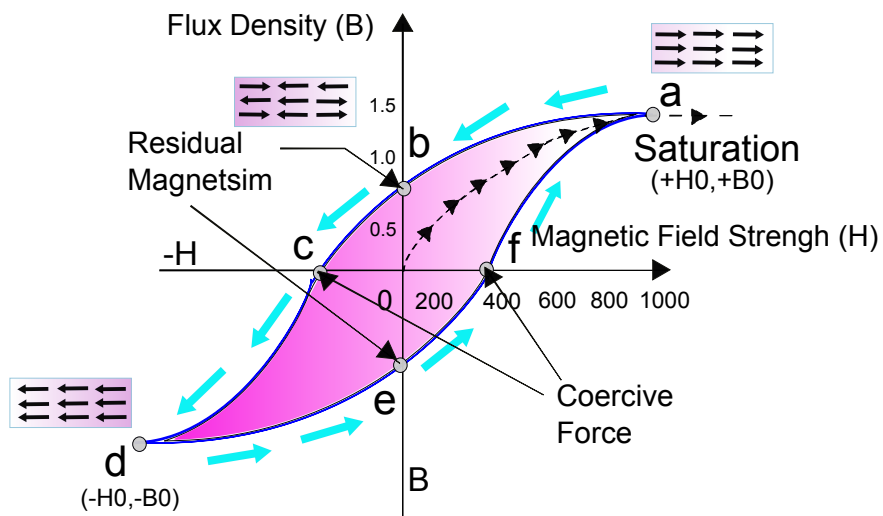


Figure 2.2: BH-loops of magneto-static materials which shows the main features of every magnetic material, BH-loops are really import for materials science, many material composition leads to distinct BH-loops, hysteresis loops are also important to distinguish between hard and soft magnetic materials.[25][3]

Retentivity, M_R : A measure of the residual flux density corresponding to the saturation induction of a magnetic material. In other words, it is a material's ability to retain a certain amount of residual magnetic field when the magnetizing force is removed after achieving saturation. (The value of B at point "b" on the hysteresis curve.)

Residual magnetism or residual flux, M_R , B_R : The magnetic flux density that remains in a material when the magnetizing force is zero. Note that residual magnetism B_R and retentivity B_R are the same when the material has been magnetized to the saturation point. However, the level of residual magnetism may be lower than the retentivity value when the magnetizing force did not reach the saturation level.

Coercive force, H_C The amount of reverse magnetic field which must be applied to a magnetic material to make the magnetic flux density return to zero. (The value of H at point "c" on the hysteresis curve.)

Reluctance: Is the opposition that a ferromagnetic material shows to the establishment of a magnetic field. Reluctance is analogous to the resistance in an electrical circuit.

Magnetizing force, (H): That part of the magnetic induction that is determined at any point in space by the current density and displacement current at that point independently of the magnetic or other physical properties of the surrounding medium. The magnetizing force is a multiple of the current, where n is the number of coils and l the length of the conductor. $H = I * \frac{n}{l}$

Permeability, μ : Magnetic permeability is the distinguishing property of the matter, every matter has a specific permeability. It's the relation between magnetizing force (H) and flux density (B). $\mu = \frac{B}{H}$

Flux density, (B): Magnetic flux density is the amount of magnetic flux per unit area of a section, perpendicular to the direction of flux energy. $B = \mu * H$

2.2.3 The maximum energy product $(BH)_{(\max)}$

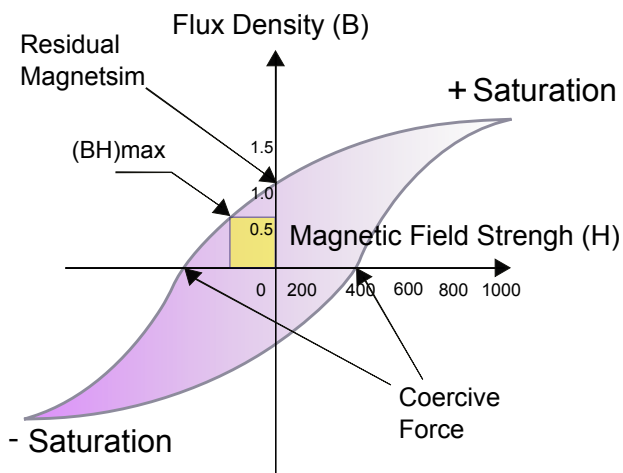


Figure 2.3: Calculation the $(BH)_{(\max)}$ of **soft magnetic materials** and **hard magnetic materials** the main features like the associated coercive force (H_C) and the residual magnetism (M_R) can lead to the same energy product $((BH)_{(\max)})$.[4]

The maximum energy product $(BH)_{(\max)}$ is one of the most important properties of every super-magnet. It's just the ability to store magnetization energy. The $(BH)_{(\max)}$ is just maximum of the product magnetizing force (H) multiplied by the flux density (B). The maximum energy product is the area of the largest rectangle in the second quadrant of the hysteresis-loop. A lot of applications require high $(BH)_{(\max)}$ values, at most cases it's not possible to reach this value, because of the cost of used materials, the manufacturing process and the temperature addiction. For every single problem there is just a possible solution but it affects other terms too. Just for example if you just want to decrease the costs of super-magnets one possible solution might be to use more Iron but at the opposite of this it leads to increase the temperature dependency too, to improve the temperature

behaviour it's recommended to use some alloys. According to soft/hard magnetic the value of $(BH)_{(max)}$ and it's strength of those materials relies on two properties. So the $(BH)_{(max)}$ of soft magnetic material depends mainly on the coercive force (H_C) on the opposite the strength of hard magnetic materials is heavily influenced by the value of the residual flux (M_R , B_R). Just to mention if soft magnetic materials mainly rely on the coercive force (M_R) the residual magnetism must be high, so for hard magnetic materials the coercive force (H_C) must be high in comparison to the remanence (M_R , B_R) to achieve the same $(BH)_{(max)}$. At figure 2.3 and 2.4 the magnetic materials achieve the same $(BH)_{(max)}$ but with different properties, which leads to the next step of nano composite magnets, there must be some possibilities to achieve the same $(BH)_{(max)}$ with the usage and combination of those two kinds of materials. [23][27]

2.2.4 The goal of combination soft and hard magnetic materials

The goal of nano composite super magnets must be to use as much as Iron possible with less dependency to temperature, but to accomplish a high maximum energy product $(BH)_{(max)}$. While decreasing the cost of nano composite magnets it's recommended to replace as much as possible volume by Iron, which costs are less but influence the behaviour of hard magnetic materials negatively. One goal of researches might be to find new ways to decrease the effects of Iron on hard magnetic materials and also on the resulting BH-loops, there a lot of possibilities which aren't figured out yet to decrease the influence of Iron on nano-composite magnets, like the grain boundaries or the alignment of iron in three dimensional space. On another goal of nano-composite magnets might be to decrease the total weight to use super magnets at much more applications, there a lot of problems and factors which influence the behaviour of those magnets which means that the properties and material combinations must be adapted in every single case.

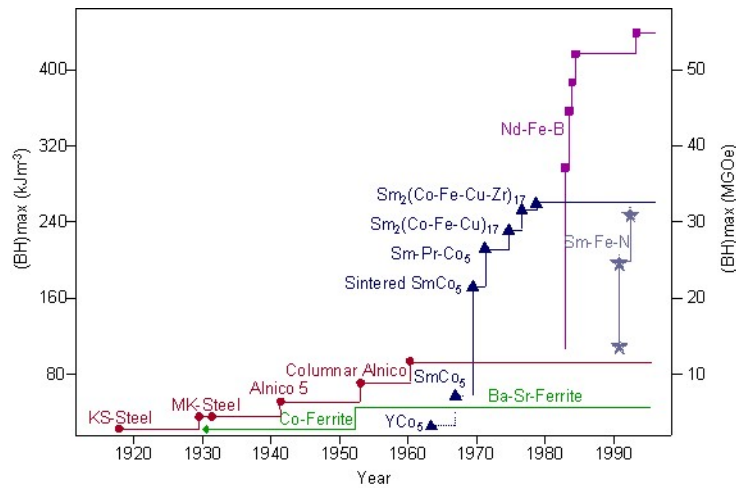


Figure 2.4: The development of permanent magnets in the 20th Century. The value of $(BH)_{(max)}$ has improved exponentially, doubling every 12 years. The material combination of super magnets has changed from one generation to another, due the limitation of the maximum reachable energy product $(BH)_{(max)}$.[2]

Chapter 3

Sphere packing problem

3.1 Sphere Packing, how to replace space by spheres

3.1.1 Cannonball problem

The problem of close packing spheres was first figured out by Thomas Harriot around 1587. At this case the problem was how to transport as much as possible cannon balls with a ship. The main issue is how to stack as much as possible spheres together without the need of too much space or to replace as much as possible space with any geometry. Cannon balls are usually put together in a rectangular or triangular, both arrangements produce a face to face orientation. It's not feasible to fill the volume of a cubic with same spheres, because there is always a gap between spheres. There are some different ways how to fill a cube with spheres but all alignments have the same problem. There is a limitation for the count of spheres and as follows for the maximum reachable density with equal sized spheres. Carl Friedrich Gauss([9]) mathematically proved that the highest average density of close packing spheres is $\frac{\pi}{3\sqrt{2}} = 0.74048$, this result was confirmed by Thomas Hales([11],[12]). How to closely pack spheres is really important for analysing structures which consists of any kind of particles. It's possible to replace space by any given geometric shape, at this study there are spheres used. There are lot of different solutions how to replace space some are with analytical and mathematical procedures, several may use methods with random numbers. A lot of scientist have proved the maximum reachable dense with spheres.



Figure 3.1: Cannon ball problem figured out by Thomas Harriot and Karl Gustav Gauss([9]). It describes the problem how to replace space by any geometric body. The cannonball problem is the main issue of replacing space by any shape. There are always some limitations about the maximum reachable dense.[1]

3.1.2 Simple, face-centred cubic packing (fcc) and hexagonal cubic packing (hcp)

There are three different ways how to reach high density packed spheres. One way is **called-face centred cubic (fcc)** alignment one another other way is **hexagonal close packing (hcp)**. Nevertheless each sphere has eight neighbours, for every sphere there is still a gap to the neighbour(s), with the hcp and fcc packing method. At the method of simple cubic packing spheres are aligned into a layer where each layer has the form of a quad which are formed into a cube so the length into each direction is equal. **Face-centred cubic packing** is similar to **hexagonal cubic packing**, those two alignments have the same fraction of about $P=0.7405$, so approximately 74 percent of space is replaced by spheres. Spheres which are aligned into a **triangle** are the base of **face centred cubic packing**, this alignment is stacked up with other spheres to build a pyramid. The **hexagonal cubic packing** is similar to face centred cubic packing but the base of this alignment is a quad, the amount of spheres at each layer is decreasing until to one if the amount of layers increase.

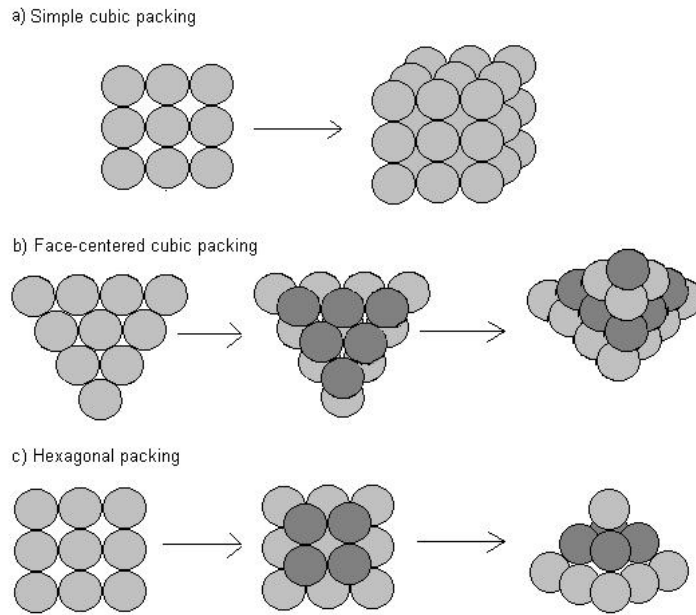


Figure 3.2: Comparison of simple, fcc and hcp lattice where each lattice is **regular aligned** with different shapes. At those alignments all spheres have equal sizes. **Figure "a"** shows the alignment with **simple cubic packing**, this alignment achieves a dense of $P=0.5224$. The base of simple cubic packing is quad at each layer, those layers are stacked to a cube so all lengths are uniform. The next **figure ("b")** illustrate packing spheres with **face-centred cubic packing**. The first layer of it (fcc) is a triangle and those layers are stacked to a pyramid. At the opposite a quad is used to shape the base of **hexagonal packing (hcp)** each layer of this pyramid has less spheres than the layer above, it's **figure "c"** of these possible alignments. Both, **face-centred cubic (fcc)** and **hexagonal cubic packing (hcp)** achieve the same dense of $P=0.7405$. [16]

Figure 3.2 shows the simple,hcp and the fcc lattice. At the hcp matrix there are always two layers where all spheres are in the same position. On the other side all three layers in the fcc stack are different. The fcc stacking can be converted by translation of the upper-most spheres. There is some differentiation how to pack spheres or any given body.

Regular packing - Particles are aligned to any kind of lattice.

Random packing - Particles are randomly packed together

3.1.3 Sphere packing and response density

At some simulations sphere packing is a big problem, because there are still some mathematically and geometrically limitations to the amount of reachable volume. So it's hard to do some simulations with high dense packed spheres but it's even harder to this at real. In simple cubic packing, each sphere is stacked directly on another sphere. We can visualize each sphere being contained within an individual cube. So we can easily calculate the efficiency of these methods by calculating the fraction of those two volumes like the spheres and the cube. So the density is given by calculating P with the volume of the cube (V_{Cube}) and the spheres ($V_{Spheres}$).

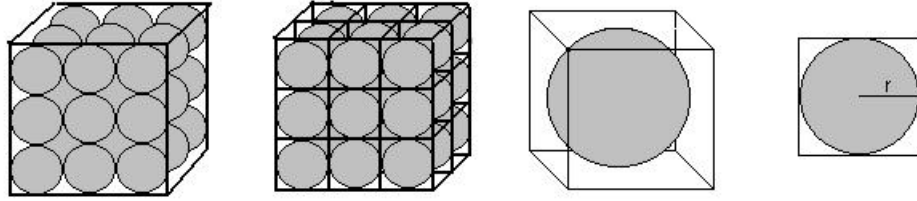


Figure 3.3: **Simple cubic packing** where each sphere is stacked directly on another sphere. It's the easiest way to replace any given space by spheres which are aligned to a grid, at this case the **maximum reachable dense** with equal spheres is $P=0.5224$. Simple cubic packing is one possible to align spheres in three dimensional space. So to calculate the dense of spheres one possible might be to split the space into smaller cubes where each length of the cube is equal. It makes it now possible to calculate the dense of one smaller cube with one single sphere in it. It's the same like to calculate the dense of the whole space, each length of the smaller cube is two times r ($l=h=w=2r$).[16]

For simple sphere packing , the volume of sphere is given by the formula

$$V_{Spheres} = \frac{4}{3}\pi r^3 \quad (3.1)$$

,where r is the radius of the sphere. The volume of the cube is given as

$$V_{Cube} = lwh \quad (3.2)$$

or length(l) times width(w) times height(h). The dimensions of the cube are exactly equal to the diameter, or twice the radius of the sphere, so we can calculate the volume of the

cube (V_{Cube}). The Sphere in it hits the boundary at all edges of the cube.

$$V_{Cube} = lwh = (2r)(2r)(2r) \quad (3.3)$$

We can therefore calculate the **packing density (P)** as

$$P = \frac{V_{Spheres}}{V_{Cube}} = \left(\frac{4}{3}\pi r^3\right)/8r^3 = \frac{1}{6}\pi = 0.5224 \quad (3.4)$$

, which is approximately **P=0.5224** , so **52.24 percent** of the cube are occupied by the spheres with **simple cube packing**.

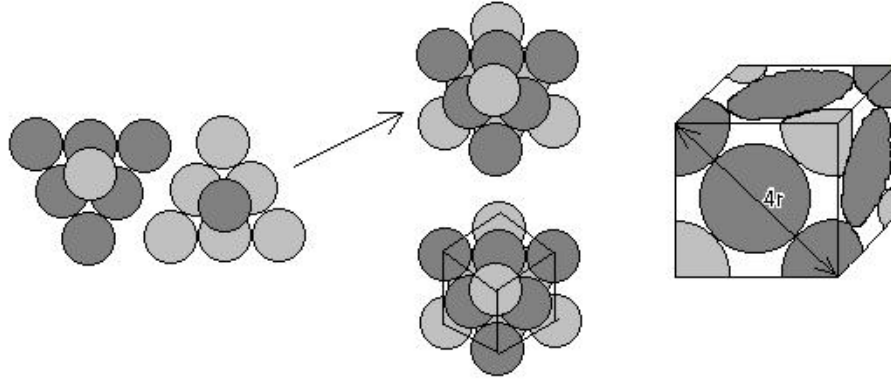


Figure 3.4: **Face-centred cubic(fcc) packing**, the cube contains eight 1/8 spheres and six 1/2 spheres, which response to the same dense like **hexagonal cubic packing (hcp)** with equal sized spheres, **fcc and hcp** leads to the **highest dense (P=0.7405)** of sphere packing. The simplest way to construct face centred cubic packing is to align spheres to a triangle, then put a single sphere on the top. The next step is to copy it and stack it on the opposite of the first triangle. At the face centred cubic packing one sphere must be in the middle of the cube, where each corner of it is in the origin of it's neighbours. It's also possible to use several cubes but the dense of this alignment is not changed.[16]

Calculating the density of **face-centred cubic packing** is almost the same like for calculating the density of simple sphere packing. First determine how many spheres fill an individual cube. So start with a group of 6 spheres which are aligned in an equilateral triangle, now put a sphere in center of it. Make another group of 7 spheres with the same formation but into the opposite direction. Now put each group back on back, a symmetrical group appear, with eight 1/8 spheres in each corner and six 1/2 spheres. The volume of all spheres is now calculated by the formula

$$V_{Sphere} = 8(1/8)\left(\frac{4}{3}\pi r^3\right) + 6(1/2)\left(\frac{4}{3}\pi r^3\right) = (1+3)\left(\frac{4}{3}\pi r^3\right) = 16/3\pi r^3 \quad (3.5)$$

, where r is the radius of a single sphere. Now we can calculate the volume of the cube, the diagonal length from one corner to another corner is $4r$ with appliance of the Pythagorean theorem ($c^2 = a^2 + b^2$, with $c=4r$ from one corner to another). It leads to

length=width=height= $2r\sqrt{2}$, each length of the cube must be equal.

$$16r^2 = 8r^2 + 8r^2 \quad (3.6)$$

$$16r^2 = 2(4r^2) + 2(4r^2) \quad (3.7)$$

$$(4r)^2 = (\sqrt{2}(2r))^2 + (\sqrt{2}(2r))^2 \quad (3.8)$$

So the volume of the cube (V_{Cube}) is calculated by the formula where each length is equal.

$$V_{Cube} = lwh = (2\sqrt{2})^3 \quad (3.9)$$

Now it is possible to calculate the **density (P)** of **face-centred cubic packing**, it is still the fraction of the volume by spheres divided by the volume of the cube. We can calculate the packing density as

$$P = V_{Spheres}/V_{Cube} = \frac{16/3\pi r^3}{(2r\sqrt{2})^3} = \frac{\frac{16}{3}\pi r^3}{2^3 r^3 (\sqrt{2})^3} = \frac{\pi}{3\sqrt{2}} = 0.7405. \quad (3.10)$$

In other words, with **face-centred cubic packing** the maximum of space which can be occupied by spheres is **74.05 percent** and 25.95 percent is unoccupied. **Hexagonal packing** is similar to face-centred cubic packing as a result the maximum density is also **P=0.7405**. The problem of sphere packing arise in different tasks of science. According to Kepler's conjecture (1611)([26]), proved by Thomas Hales (1998), the highest packing density of mono-sized spheres in the 3-dim space is $\frac{\pi}{3\sqrt{2}} = 0.7405$ with two different sizes the possible density is $1 - (1 - \frac{\pi}{\sqrt{18}})^2 = 0.93265$. Table 3.1 shows the methods and highest reachable density with sphere packing. In applications, where nano particles are randomly packed the density will be lower than regular packing with equal spheres. It is possible to replace much more space by using multi sized spheres which allow higher possible fractions. There also some different types of packing randomly particles together there is a distinction between random close and random loose packing. The procedure of random close packing means that all particles touch another particle at the opposite of this procedure is random loose packing which means that all particles are separated from each other.[11][12][9][16]

Random close packing -Shake the container after a random packing.

Random loose Packing -No shaking is given to the container.

Circle Packing

In two dimensional Euclidean space, the German mathematician Carl Friedrich Gauss([9]) figured out that the regular arrangement of circles in a lattice with the highest density is the hexagonal packing arrangement, in which the centres of the circles are arranged in a hexagonal and each circle touches another sphere. Every circle is surrounded by 6 other circles. The density of this arrangement is

$$\frac{\pi}{\sqrt{12}} \approx 0.9069 \quad (3.11)$$

Sphere packing

In three dimensional Euclidean space, Carl Friedrich Gauss ([9]) figured out that the regular arrangements of spheres with the highest density are two very similar arrangements called cubic close packing (or face centred cubic (fcc)) and hexagonal close packing(hcp). In both of these arrangements each sphere is surrounded by 12 other spheres, and both arrangements have an average density of

$$\frac{\pi}{\sqrt{18}} \approx 0.7408 \quad (3.12)$$

Irregular Packing

When spheres are randomly added to a container and then compressed, they will generally form what is known as an "irregular" or "jammed" packing configuration when they can be compressed no more. This irregular packing will generally have a density of about 64 percent. Recent research predicts analytically that it cannot exceed a density limit of 63.4 percent. This situation is unlike the case of one or two dimensions, where compressing a collection of 1-dimensional or 2-dimensional spheres (i.e. line segments or disks) will yield a regular packing.

Possible methods of packing spheres

This table 3.1 presents the most common methods of replacing space by spheres in 3d-space, it's possible to replace much more space with using only two dimensional space, due the fact that if the order of space is decreased also the complexity of the main problem is decreased. There are a lot of other possibilities to replace space by any geometry body figured out by some scientist. The maximum (theoretically) reachable dense is decreasing and most of them are not applicable, there might be some work to find the best grid for nano composite materials and also the best shape which should replace the space. The shape of nano particles could be an import factor which influences the behaviour of nano composite magnets too.[28]

PACKING	P	P	REFERENCE
loosest possible	-	0.0555	Gardner(1966)
tetrahedral lattice	$\frac{\pi\sqrt{3}}{16}$	0.3401	Hilbert and Cohn-Vossen (1999, pp. 48-50))
cubic lattice	$\frac{\pi}{6}$	0.5236	
hexagonal lattice	$\frac{\pi}{3\sqrt{3}}$	0.6046	
random	-	0.6400	Jaeger and Nagel (1992)
cubic close packing	$\frac{\pi}{3\sqrt{2}}$	0.7405	Steinhaus (1999, p. 202), Wells (1986, p. 29; 1991, p. 237)
hexagonal close packing	$\frac{\pi}{3\sqrt{2}}$	0.7405	Steinhaus (1999, p. 202), Wells (1986, p. 29; 1991, p. 237)

Table 3.1: Possible methods of sphere packing and maximum reachable densities with equal sizes in three dimensional space, figured out and proved by several scientist.[28]

Chapter 4

Meshing and quality

4.1 Overview of meshing

Finite element modelling is crucial to the capability to perform an engineering analysis of a model using a computer. The equations needed to determine the behaviour of an entire complex model are often so complicated that it would be impractical to derive or solve them. Meshing solves this problem by breaking the complex model into an assembled group of finite elements like small interconnected pieces. These elements in a finite element model often consist of geometric shapes such as rectangles, triangles, and tetrahedra which are all connected together to one group that's called a mesh. One single mesh also has connecting points to other meshes which are also called nodes, and assigned material and element properties. Those points are really important because each note is computed into a computer program or algorithm over some time where the appropriate model belongs to any mechanical or mathematical problem.

4.2 Meshing quality

Mesh quality is really critical for computing finite elements which influences the accuracy and calculation time of every computer program. Especially the mesh quality decides if the finite element program is able to compute these simulations or not. The program which

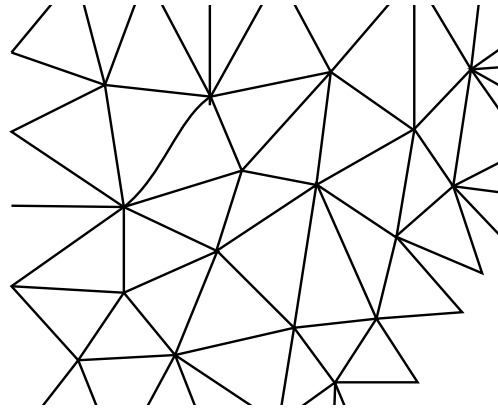


Figure 4.1: Simple example of meshing, each corner of those triangles is a note which influence the accuracy a lot, more notes lead to higher accuracy, meshing is the main method to discretize any shape of the real world to compute the model with any finite element method, the angle of each corner is really import for the mesh quality. Meshing is crucial for computing finite element methods with computer programs, it decides how long has the computation to be done and it's critical to the accuracy of the finished results. The distance from one note to next note of it is defined as the mesh size.[24]

has the duty to compute the differential equation system is sometimes called a solver, because it solves the problem with any finite element method inside a computer program. The issue always consist of the geometry and the generated equation system for different appliance like to calculate the magnetic field, mechanical analyses and other problems. In this study the solver has compute differential equation systems which belongs to micro magnetic problems. It's possible to try different solver at the same mesh or to improve the quality. It can be improved in different ways like to use another algorithm or to use more computation elements, there is always a trade off because using a better meshing algorithm always means that it takes maybe some more time than using other algorithm, it just depends on a lot of factors. It's recommended to use better mesh quality if the system of finite elements is really great. One another way to find the best clustering is to use several algorithm with different meshing parameters on the same model. That's just what happens on chapter 6, the same model is used with only one meshing algorithm but with different parameters (like maxsize(step) and minsize(step) of the mesh) just to find out if the results converge to the same values. If all calculated values are nearly the same with other (better) parameters then there is no improvement of this computation, so there is no need to use other algorithm (if the values are equal) with different solver or more points.

Kinds of solver

There are just two main methods of solver, one is able to solve the problem directly like the Gaussian method the other one computes the equation system iterative. The Gaussian method is able to solve the problem directly which also means that results have to converge to decent values. On the other side the iterative method is only able to compute the model one point after another point, which makes every computation really time exhausted. One another aspect of iterative methods is, that the computed results don't have to converge to any special value which leads at some models to no results, that's why the mesh quality must be high enough to achieve any result or even better data's. It is possible to calculate the mesh quality of every single point and visualize it, like with the program paraview. At all simulations the algorithm NETGEN is used but with different parameters like max size(step) and min size(step) of the mesh. NETGEN is just an automatic 3d tetrahedral (figure 4.2) mesh generator which is used at several programs. The NETGEN algorithm is one possible way to generate meshes from shapes.[10][20]

Direct solver -For small systems, the equation system is solved directly with some matrix operations, really memory exhausted

Iterative solver -For great system, ever point has to be computed from one time step to the next time step, really time exhausted

The accuracy of every computations strongly depends on the amount of calculation elements, which are shown on tabular 4.2, higher accuracy of computation leads to more calculation time because of higher amount of calculations elements, the computer system has to calculate every note. The main sizes of all models and simulations in this work are equal, length, width and height of the model(cube) are 100nm(100nmx100nmx100nm). At tabular 4.2 the most important facts are summarized, just to the mention the geometry of

the model slightly influences the amount of those calculation elements too. The number of elements if triangle, tetrahedron or anything else is no guarantee for having high mesh quality, because it's possible if the maximum step size of the mesh decreases also the mesh quality gets poor due the used algorithm. It's common if the number of elements rises also the accuracy of computations increases if the level of quality is nearly same.

Summary of different mesh sizes, elements and computation time and response accuracy.

No.	MaxSize[nm]	MinSize[nm]	Elements	Compute time	Accuracy
sim1	4.5	0.5	≈57k	<1h	really low
sim2	2.5	0.5	≈270k	<3h	low
sim3	2.15	0.5	≈340k	<6h	low
sim4	2.075	0.5	≈362k	<6h	low
sim5	2.02	0.5	≈664k	<12h	average
sim6	1.5	0.5	≈1350k	<1d-2d	high
-	1.25	0.5	≈2500k	<3d	really high
-	1.00	0.5	≈4000k	>6d	really high

Table 4.1: In this table by far all import facts are summarized with all parameters, which are changed during all simulations in chapter 6, 7 and chapter ???. This table also shows the needed computation time and response accuracy. The simulation time increases if the accuracy of the calculations improves, the real mesh sizes must be figured out by several computations with different mesh parameters. The size of the used model is always the same size, each length of the cube is 100nm long.

4.3 Calculation of the mesh quality

The mesh quality can have a serious impact on the computational analysis in terms of the quality of the solution and computation time of the result. This aspect becomes especially important if poorly conditioned problems, non-linear, and/or transient analysis or stiff systems are considered. To calculate the mesh quality of a model could be very useful because it shows how far the mesh fits to the problem and numeric solved solution. The quality of the mesh is an indicator of the grade about the finished solution. There are several ways how to compute the quality of individual elements and how to quantify the overall quality of a mesh. In the following text, three elementary criteria are narrate.

The first one evaluates the element quality with respect to the equilateral simplex (as the best possible element). The **triangular element** (figure 4.2) is used at different mesh algorithm, the quality is of a single element is expressed with formula as

$$q = f \frac{A}{a^2 + b^2 + c^2} \quad (4.1)$$

where A is the area of the triangular and a, b, c are the length of it's side. The factor $f = 216 * 3^{1/2}$ is the normalizing factor which represents the best quality of an equilateral triangular. Similar to this formula the quality of a single **tetrahedron** (figure 4.2) element is calculated. This formula

$$q = f1 \frac{V}{A^{3/2} + B^{3/2} + C^{3/2} + D^{3/2}} \quad (4.2)$$

or the most appropriate (more sensitive to poor elements) form

$$q = f2 \frac{V}{\left(\left(\frac{(A^2+B^2+C^2+D^2)}{4}\right)^{1/2}\right)^{3/2}} \quad (4.3)$$

presents the quality of an single tetrahedron element, where V respects the total volume of the tetrahedron and A, B, C, D the areas of its faces. The factor $f1 = 18^{1/2} * 27^{1/4}$ and $f2 = \frac{3}{2} * \frac{27^{1/4}}{2^{1/2}}$ are still the normalizing factor to the best quality of an equilateral tetrahedron which quality is equal to 1. The normalizing or form factor f can be calculated by comparing equilateral and general triangle same like tetrahedron. All forms of equations are naturally based on the volume ratio of areas(volumes) of circles(spheres) inscribed and circumscribed to a triangle (tetrahedron). The total mesh quality is measured by summarizing the quality of every single mesh of each element (at this case of every triangular and tetrahedron). There are just two possibilities ways how to calculate the total mesh quality.

The standard form

$$Q_a = \frac{1}{N} \sum_{i=1}^N q_i \quad (4.4)$$

or as the **harmonic mean** by

$$Q_h = N / \sum_{i=1}^N \frac{1}{q_i} \quad (4.5)$$

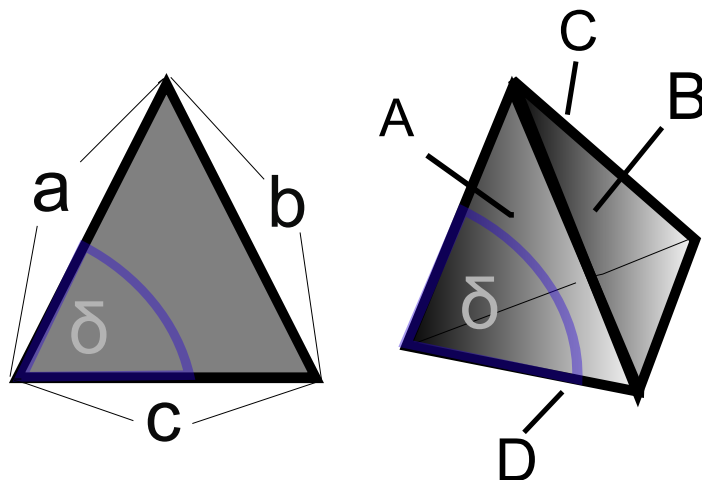
where N stands for the number of elements (of a particular type) and q for the mesh quality of each element with the index i and Q is the resulted quality over the whole mesh. The harmonic formula considers the mesh quality of every single element in a very sensitive way, so if at one single mesh the quality is really poor the overall mesh quality is also worse. In comparison to the standard form the harmonic formula picks up the worst elements of the mesh and bring it to appear, the harmonic mesh quality is really sensitive to poor elements of the mesh. The standard form doesn't consider each element in such a way, it only calculates the overall mesh quality without any quantifier. At the standard form the overall quality resides even when some elements are really bad.

One another criterion of quality is to calculate the dihedral angles (δ) looking for the minimum and maximum extremes and calculating the average. It's also the **second criterion** of mesh quality. The distribution of the dihedral angles (δ) offers a valuable indication about the quality. The optimal angle relies on it's simplicity of the geometry like at the equilateral triangular or tetrahedron. It is also possible to calculate the mesh

quality with dihedral angles of each element with the formula, the optimal dihedral angles of the equilateral simplices are 60° (triangle) and 70.53° (tetrahedron)

$$q = \frac{\delta_{min}}{\delta_{max}} \quad (4.6)$$

where δ_{min} is the minimal and δ_{max} the maximal dihedral angle in a single element. The **third criterion** is based on the mesh connectivity and evaluates the valency (number of connected edges) for nodes classified either to a region or to a surface, patch, or shell. Each uniform triangle should have exactly 6 neighbours, but only the approximate value of 12 is available for the tetrahedral shape. As much the valency differ from the optimal value the mesh becomes more irregular in the neighbourhood of that node.[22][21][19]



(a) Shape of a single triangle. (b) Shape of a single tetrahedron.

Figure 4.2: Shows the two possible kinds of shapes mentioned in this chapter, the shape of a triangle can only be used in two dimensional space for meshing because they are flat in the opposite tetrahedrons are often used in three dimensional space, the quality of meshing strongly depends on the difference to its equilateral form of the shape. All criterion of mesh quality come naturally based on the volume ratio of areas(volumes) of circles (spheres) inscribed and circumscribed to a triangle (tetrahedron). The variables a , b , c are the length of the triangle whereas A , B , C , D are the area of a tetrahedron used to calculate the mesh quality. One another criterion is the dihedral angle (δ) where the minimum and maximum extrema are used to calculate the quality of single element or overall mesh quality.[22][21][19]

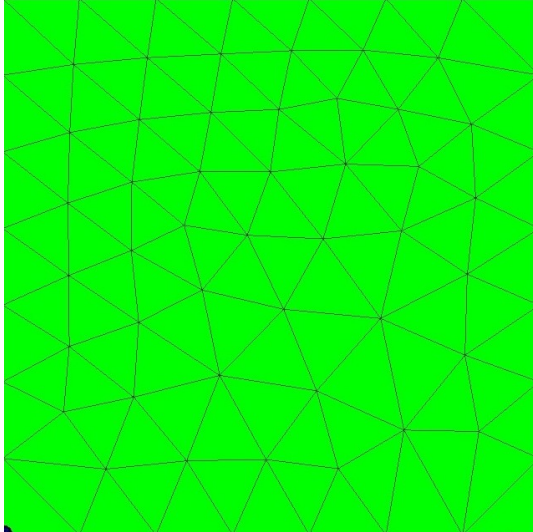
4.3.1 Mesh smoothing

Mesh smoothing is the way how to improve the quality of the overall mesh and each element. The position of the element is changed but the overall topology remains unchanged with mesh smoothing high frequents are blocked out which effect the mesh quality negatively.

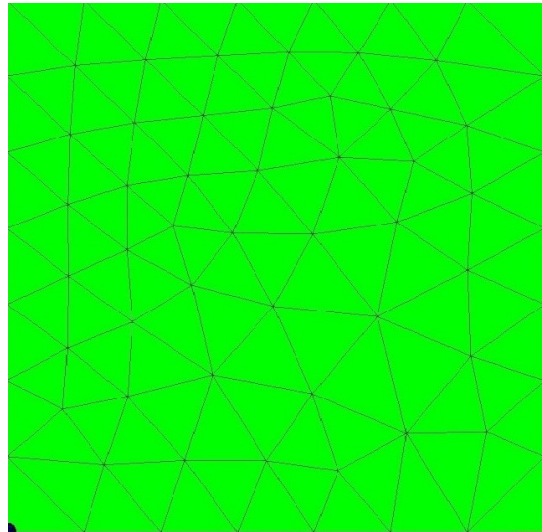
Changing the position of a single element can widely effect the mesh quality. There are some different methods how to smooth the mesh, but most of them are based on the same principles where each position of one point is changed with holding the position of surrounding points and quantified this two requirements are used to calculate a new point. These methods of mesh improving are really similar to methods of smoothing pictures, where each color of all surrounding points are quantified to calculated a new color so failures(high frequents) are blocked out. Only with a few iterations over the mesh the quality can improved drastic. One of the most common methods is Laplacian smoothing where a mesh point is moved to be center of the surrounding points. This formula calculates

$$P = \frac{1}{N} \sum_{i=1}^n \alpha_i P_i \quad (4.7)$$

a new point according to the **Laplacian smoothing**, where N is the total number of surrounding points and α_i the associated weighting coefficient of all points (P_i), the variable P_i inherit the coordinates (x,y,z) of those points and i is just the index of each element. There are some other smoothing algorithm with different number of points and weighting coefficients but they are still similar. The effect of mesh smoothing is shown on figure 4.3 where the mesh is displayed without smoothing and after applying smoothing the Laplacian algorithm.[5][18][8]



(a) Before smooting a mesh.



(b) After smooting a mesh.

Figure 4.3: These two pictures to show the effect of smoothing a mesh, which can improve the quality of a mesh a lot. Smoothing also means changing positions of some notes. A lot of mesh algorithm are optimized to improve the quality during computation the mesh .At this case only a few positions are changed because the mesh was optimized before doing mesh smoothing. The effect of smoothing is really less but some areas are smaller and some are greater which means that the position of some notes has changed to improve the quality of the mesh.

4.3.2 Comparison of different mesh qualities (1/2)

The quality can be effected by many factors especially by the used algorithm but before computing any model, the mesh has do be done. The number of elements is also influenced by the geometry. It's possible to achieve high mesh quality even with less amount of notes. The following model used to compare the mesh quality with different amounts of elements.

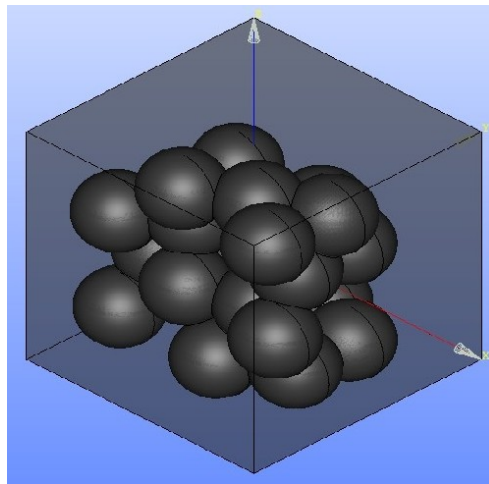


Figure 4.4: Before meshing, the geometry of each model has to be made at this case the model is constructed with the program salome. This program is not a dedicated construction program, it's mainly used for meshing. There are some tools in this program which give the ability to construct simple geometries.

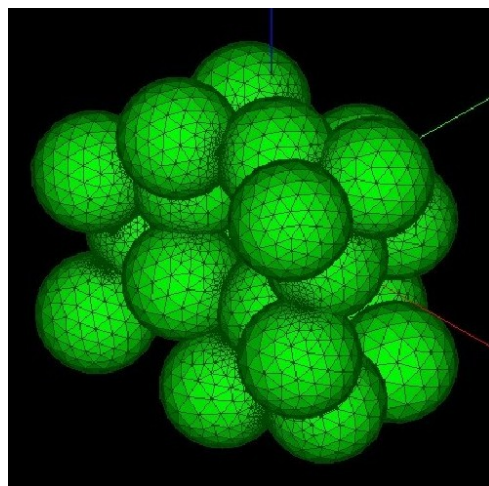
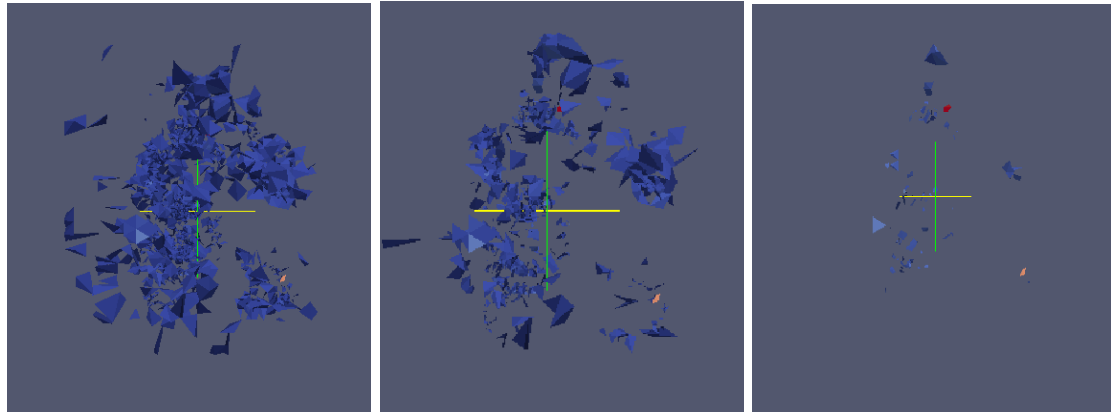


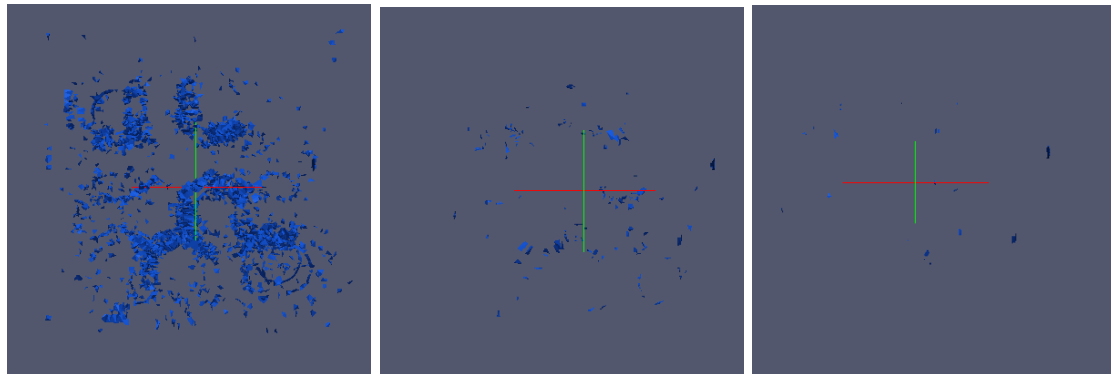
Figure 4.5: After meshing, there is a grid with shapes which are connected throw points called notes. They are really important because each note is a single point where the finite element method is trying to solve the equation system. The way how all notes are connected is crucial to this method. (Only the mesh of spheres is shown.)

The mesh quality can be easily visualized with paraview and with the usage of the filter mesh quality and threshold value, it only shows the needed steps of quality levels.



(a) Mesh quality with the threshold level of lower bound=3. (b) Mesh quality with the threshold level of lower bound=4. (c) Mesh quality with the threshold level of lower bound=10.

Figure 4.6: This figure presents the quality of the same model like at figure 4.11 with less mesh quality and the parameters of $\text{maxsize}=4.5$ and $\text{minsize}=0.5$ and different threshold steps, which means that with increasing the lower limit only worse quality levels are shown (approximately 57k elements).



(a) Mesh quality with the threshold level of lower bound=2. (b) Mesh quality with the threshold level of lower bound=3. (c) Mesh quality with the threshold level of lower bound=4.

Figure 4.7: This figure presents the quality of the same model like at figure 4.10 with higher mesh quality and the parameters of $\text{maxsize}=1.5$ and $\text{minsize}=0.5$ and different threshold steps, which means that with increasing the lower limit only worse quality levels are shown (approximately 1350k elements).

Figure 4.6 and figure 4.7 show that with increasing the number of mesh notes the quality could be dramatically increased, but the mesh should be still considered even with higher amounts of elements because the quality could still be worse.

4.3.3 Comparison of different mesh qualities (2/2)

The quality can be effected by many factors especially by the used algorithm but before computing any model, the mesh has do be done. The number of elements is also influenced by the geometry. It's possible to achieve bad mesh quality even with high amount of notes. The following model used to compare the mesh quality with different amounts of elements..

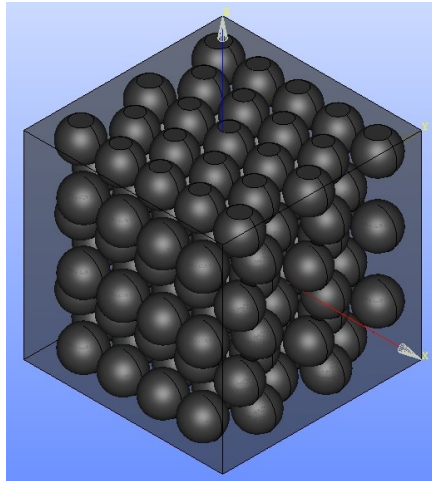


Figure 4.8: Before meshing, the geometry of each model has to be made at this case the model is constructed with the program salome. This program is not a dedicated construction program, it's mainly used for meshing. There are some tools in this programm which give the ability to construct simple geometries.

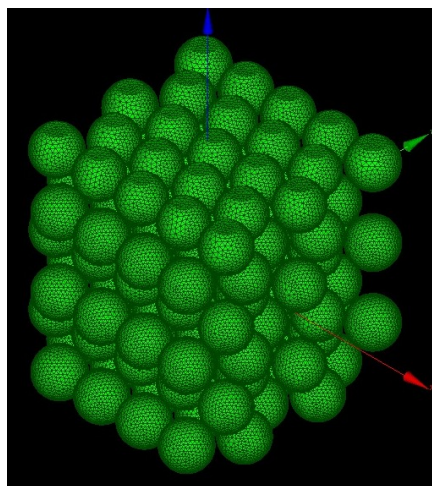
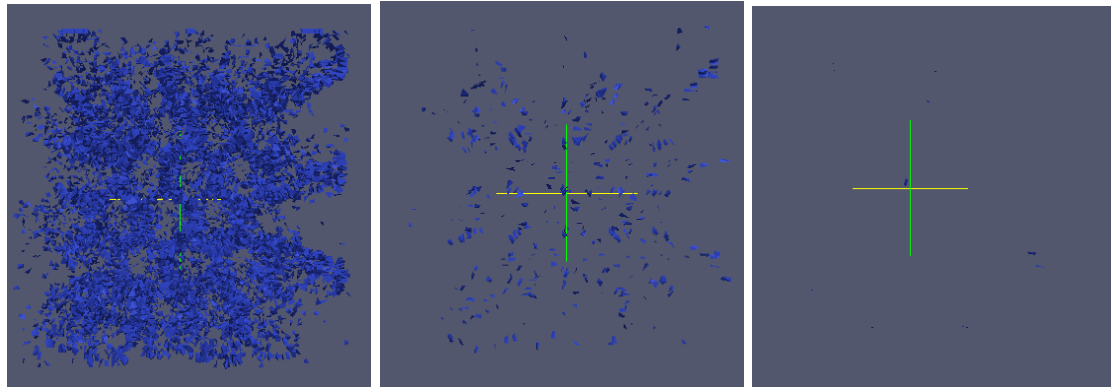


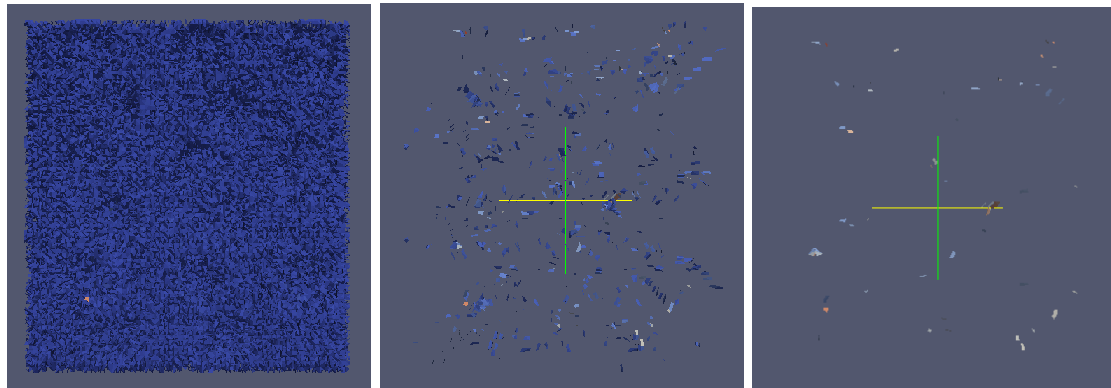
Figure 4.9: After meshing, there is a grid with shapes which are connected throw points called notes. They are really important because each note is a single point where the finite element method is trying to solve the equation system. The way how all notes are connected is crucial to this method. (Only the mesh of spheres is shown.)

The mesh quality can be easily visualized with paraview and with the usage of the filter mesh quality and threshold value, it only shows the needed steps of quality levels.



(a) Mesh quality with the threshold level of lower bound=3. (b) Mesh quality with the threshold level of lower bound=4. (c) Mesh quality with the threshold level of lower bound=10.

Figure 4.10: This figure presents the quality of the same model like at figure 4.11 with higher mesh quality and the parameters of $\text{maxsize}=1.5$ and $\text{minsize}=0.5$ and different threshold steps, which means that with increasing the lower limit only worse quality levels are shown (approximately 1600k elements).



(a) Mesh quality with the threshold level of lower bound=2. (b) Mesh quality with the threshold level of lower bound=10. (c) Mesh quality with the threshold level of lower bound=40.

Figure 4.11: This figure presents the quality of the same model like at figure 4.10 of the same model with lower mesh quality and the parameters of $\text{maxsize}=1.4$ and $\text{minsize}=0.5$ and different threshold steps, which means that with increasing the lower limit only worse quality levels are shown (approximately 2500k elements).

Figure 4.10 and figure 4.11 show that with increasing the number of mesh notes the quality could be dramatically decreased, so the mesh should be still considered even with higher amounts of elements because the quality could be worse.

Chapter 5

Goals,structure and post processing of all simulations

5.1 Goals

Super magnets always consist of hard magnetic and soft magnetic materials, one goal of this study is to figure out how the soft phase influences the behaviour of all BH-loops. The grain sizes and especially the properties of the soft magnetic part is really critical to the values of the coercive force (H_C) and the maximum energy product ($(BH)_{\max}$). So this study shows how the soft phase effects these two values. Chapter 3 was introduced because at all these simulations in this study the geometry of spheres and a cube is used. Spheres which are different aligned and applied with different counts to replace space from the cube. At this study spheres become hard magnetic and soft magnetic and the intersected cube becomes the opposite of the used material,to figure out the best alignment. The main reason why spheres are used is, that this geometry influences the behaviour of the computed BH-loops less. Each corner of another geometric body like a quad or tetrahedron will generate magnetic fields which influence the behaviour negative, that's why spheres are used because there are no corners. According to chapter 3 there are only a few possible alignments for packing spheres together so there are some limitations because of the applied geometry. This is another reason why this chapter was introduced because it's not possible to replace as much space as wanted. So the goals of this work are how does **grain size, volume ratio, and geometry** effect super magnets and the associated magnetic field. The first aim about all computations was to determine the right mesh size. At chapter 6 there are some simulations done with different geometries but at each model also different mesh parameters are tested, to determine the maximum and minimum step size of the mesh and to achieve high accuracy at the computations. This leads to the next point that all simulations are compared at chapter 7, to show the effect of the soft phase to all computed BH-loops. In this study there are also two simulations to show the effect of wide areas of the soft phase, this is another goal of this work which is summarized at chapter 8. At chapter 9 a set of simulations is computed with three different grain sizes , to show the effect of soft magnetic phase if the grain size and volume ratio vary.

5.2 Structure

At this section the structure of all simulations is mentioned it's only a short overview but it shows how to create all simulations with the used models and parameters. It also illustrates the main programs which are used in this study. All models and the post processing is done with five different programs each program has it's own emphasis into this work. So let's start with the first one, it's called YADE (Yet Another Dynamic Engine). It's main responsibility is to generate the coordinates of the spheres which are different aligned the coordinates are saved to text files which are used to generate the geometry and the mesh. At YADE it is also possible to define the boundary where all spheres are placed. The next program is called Salome it's just a program which is used to generate the model and to compute the mesh for all these simulations. Users are also capable to write different scripts for the program Salome and YADE with programming language Python. One another program at this study is the program FEMME (Finite Element Micro Magnetics) it's just the solver to compute the model(problem) about micro magnetics. FEMME is used to calculate the complex differential equation with finite element methods. The last one is needed for post processing, it's a open framework program which is called Matplotlib. Some programs mentioned in this section are working with the interface and programming language Python. FEMME and convert2ucd are executables with different inputs and outputs at the opposite (YADE,Salome,Matplotlib) the interface of Python(*.py) is used.

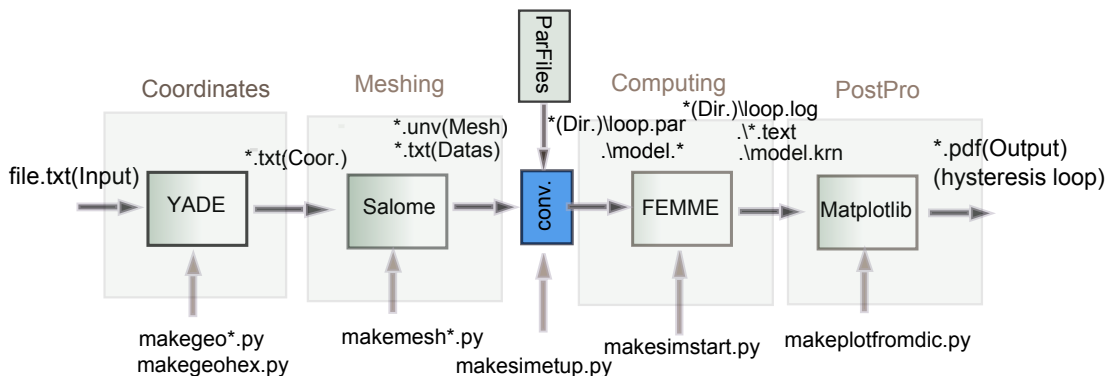


Figure 5.1: This figure just describes the four main stages of this work where all important scripts and programs are mentioned. At the first stage the coordinates of the spheres are computed with the program YADE. After generating geometry and the mesh with the program Salome, the Python script makesimetup.py is used to do the structure of all files and the computations with FEMME. It also converts the model and copy the text file for post processing. This script has also the duty to do all directories and subdirectories for the simulations. The file names in this directory are equal (model.*) because at the parameter file (loop.par) the problem name is denoted. The next step is just to compute the model with FEMME on any cluster system. After computing the model the hysteresis loops are generated with Matplotlib. At each stage of the process different files are created, but the last file is just a pdf with the hysteresis loop.

Remark The character * means arbitrary because the file names depends one the input and there is too less space to show every used file.

YADE (Yet Another Dynamic Engine)

YADE or Yet Another Dynamic Engine is a particle simulation program, which is used at this study to generate all coordinates of the spheres. The main interface of YADE is the programming language Python but this program is written in C++. There are two main commands which are used to generate the coordinates of the spheres. The command **makeCloud** is used to determine the boundary and the properties of spheres. At this study the boundary is a cube. Another command is **regularHexa** this command defines a grid where all spheres are aligned into hexagonal lattice within a boundary. The output of YADE are text files with the coordinates of the spheres and the cube. The command **RandomDensePack** generates spheres which are close together and maybe intersect them.

Salome

Salome is just a program for generating geometries and meshing. It is also possible to write different scripts for Salome. At this study its input is a text file generated from YADE. The main data which are extract from this text file are the boundary of the cube and the coordinates and radius of each spheres. After reading those datas the Salome script generate the geometry and computes the mesh with some parameters like the maximum mesh size and minimum mesh size. The interface of Salome is just Python but it's also possible to control the program from a graphical user interface. The main outputs of the script are the mesh (*.unv) and one text files (*.txt) which includes some data used for post processing.

FEMME (Finite Element MicroMagnEtics)

FEMME is just the solver which calculates the micro magnetic field of the model. The program FEMME needs the converted mesh in the right format (*.ijk) and some parameters files. The parameter files are just simple text files which defines the material properties (*.krm), alignment of the magnetic field (*.ini) and the parameters for computation the hysteresis loop (*.par). The main output is one single file (*.log) where informations of the computed BH-loops are stored.

convert2ucd

The tool convert2ucd is just a program to convert the generated unv file from Salome to another format for FEMME (*.ijk, *.inp). The mesh (*.unv) has to be converted because the solver needs another format to compute differential equation system.

Matplotlib

Matplotlib is the plotting tool which generates all the hysteresis loops in this study. The main input are the log (*.log) file from the program FEMME and material properties (*.krm) which are used during the computation and text file from the program salome where the volume of the spheres and the intersected cube are stored. This file is used to get volume fraction of the soft and hard phase and also some meshing properties. The script for Matplotlib generates plots for all the needed hysteresis loops. Its output are pdf files which are used to write this study.

5.3 Python scripts

This section is just to give a short overview, not to explain everything. Those explanation are for people who are familiar with the used programs, scripting with Python and server structure. All scripts are used to operate with the these programs.

Remark It's recommended that each script has it's own working directory. Scripts and working directories should be arranged in the same main directory. So it's advantageous to have the following structure.

Directory \...

- .\makegeo (Directory of the different text files for the used models.)
- .\makegeo*.py (YADE script for the sphere packing problem.)
- .\makemesh (Directory where the files for the mesh have to be stored.)
- .\makemesh*.py (Salome script for doing the geometry and the mesh.)
- .\makesimsetup (Directory with subdirectories for different meshes and parameter files.)
- .\makesimsetup.py (Creates subdirectories and converts the meshes.)
- .\finished (All finished computation from FEMME.)
- .\makeplot (Directory where to save all generated plots.)
- .\makeplotfromdic.py (Script for doing the plots with Matplotlib)
- .\makeplotfromfile.py (Included file needed for makeplotfromdic.py)

Yade script - makegeo*.py

The main purpose of the makegeo scripts is, to generate files where the boundary of the cube is defined and the coordinates of the spheres. The input file just has a simple structure

Input file:

```
B S R V
100 95 10 0
```

At the first line only variables for names are used (B..Block,S..Spheres,R..Radius,V...Variance) and on the second line the real parameters for calculating the sphere packing problem are mentioned. The first number (100) just stands for the dimensions of the block in each direction, followed by 95, this is just the number of spheres which have to be placed within the cube and 10 is the average radius, where as 0 just stands for the variance. So the YADE script just generates another directory within the directory makegeo which has the name of the input file, the number of files which are computed depends on how much lines are added to the input file. This script will now generate the output file.

Output file:

```

91.0 10.0 0.0
100.0 100.0 100.0
-42.7167956184 -33.7212333435 37.2189794751 10.0
-18.0260566924 18.0651146896 21.1519270568 10.0
-0.969388833551 -24.1364406599 38.0797303421 10.0
-7.18251143606 -40.3415494234 -44.8788748278 10.0
....
```

The output file is just similar to the input file but at the first line the number 91 stands for how much spheres YADE was able to put in the cube where as 10 stands for the average radius and 0 for the variance. Followed by the next line 100 is the size of cube in each direction. After the main properties the coordinates of spheres are stored and the radius at each line. The output file has the name `__B_100__S_100__R_10__V_0.txt`. There are three different scripts which will generate different kinds of packed spheres.

- makegeo.py** Yade - Command "MakeCloud(...)", spheres are well separated.
- makegeo1.py** Yade - Command "randomDensePack(...)",spheres are close together.
- makegeohex.py** Yade - Command "regularHexa(...)",spheres are aligned regular.

Each script must be started with command `yade -x scriptname`, it's recommended to use the operating system Linux because it is easier to install.

Salome script - makemesh*.py

The scripts for Salome have the duty to compute the geometry and to do the mesh for all the models. They are really simple to use because only the input file and the directory where the output has to be stored be must defined , so at this case the output directory is makemesh. The file name is generated from the input file, it looks like this `__B_100__S_100__R_10__V_0.txt` , so it means that the size of the cube is 100, there should be 100 sphere in it(maybe) with radius of 10 and the variance of zero. After reading this file the scripts generates two files at the directory. The first one is the generated mesh (`__B_100__S_100__R_10__V_0.unv`) and the second one some data for post processing (`__B_100__S_100__R_10__V_0.txt`). That leads to next step to make the structure of the the computations. There are also some different scripts because of different types of geometries. The scripts can be open from the graphical user interface or from the command line. It's recommended to use the operating system Linux because Salome is more stable on it and can handle much more data.

- makemesh.py** Salome - script for doing spheres which are aligned well.
- makemesh2.py** Salome - script for common spheres.
- makemesh3.py** Salome - script for doing a hexagonal grid.

Python script - makesimsetup.py

The Python script makesimsetup.py is written to make the structure of all simulations. It's similar to all other scripts which are used in this study. For doing the directories and subdirectories only the place where the meshes(*.unv) and post processing files(*.txt) are stored have to be defined and also the path of the output directory. For computing the models the parameter files have to be stored into the same subdirectory where and text and mesh files are saved. The parameter files should have following files in it.

loop.par (Paramter file for FEMME, for computing the hysteresis loop)

run (For the cluster system, to specify how much resources are allowed to use)

model.krn (The properties of the used materials at the mesh(model).)

model.ini (The alignment of the magnetic field at the start of the simulation.)

The script just makes several subdirectories, each of these has a combined name from the directory of the parameter files and the used mesh file (*.unv). So if directory of those parameters files has the name **par1** and the mesh is called **__B_100__S_32__R_15_0__V_0.unv** the script will make a new name to create the directory (**par1__B_100__S_32__R_15_0__V_0**) where the files and problem is saved. After doing this, the script will copy each file from the directories of the used parameter files(Parfiles) into the new directory and will also convert the mesh(*.unv) into a new format(*ijk,*inp). It is also possible to use several directories for the parameter files and different unv files. The script will generate for each mesh(*.unv) file a new directory with the used parameter files. It will also rename all files which are copied from the directory of the parameter files and also the mesh(*.unv), because at the file **loop.par** the name of the computation is defined so the name mentioned in **loop.par** and the used name of converted the mesh(*.ijk) and parameter files must be equal. At this case the script will rename the prefix of all files into **model.*** excluded **loop.par**. The problem name must specified at **loop.par** and at this script.

Python script - makesimstart.py

This script is just written to start the computation at each subdirectory onto the cluster system, it's really simple and short. The upper path of the subdirectories must be defined and this script will execute every problem into those subdirectories. The command of this scrip is **qsub run** it means that cluster system will execute the problem (model) with the name mentioned in this file (run) and will search for the parameter files of the hysteresis loop(**loop.par**). This script will also start all simulation for FEMME.

Matplotlib script - makeplotfromdic.py

After finishing the computations the generated data from FEMME have to be analysed. This script is searching for subdirectories and passes the path to **makeplotfromfile.py** . It generates for each subdirectory different plots with the usage of **loop.log**(computed values from the model),**model.krn**(properties of the used materials) and the generated text file (data for post processing) from Salome which are stored in this subdirectories. If one of those files is not existing this script will not generated the associated plot.

5.4 Post processing and calculating the hysteresis curves (BH-loop)

To compare all the different models with different properties and features the BH-loops must be done. The script makeplotfromdic.py is just used to do all hysteresis loops, but there are three files which are needed to generate all the hysteresis loops for each computed problem. Post processing is the last stage at this work of generating new data, after computing the model and after plotting these BH-loops must be analysed and interpreted.

- *.log (Stored data of the computed the model)
- *.krn (The properties of the used materials at the mesh(model).)
- *.txt (The generated text file from Salome for post processing.)

This script will search for each file at the subdirectories which are mentioned in the input path of the script.

```
if(len(sys.argv))> 1:
    dir_name_in=sys.argv[1]
else:
    dir_name_in=_char+'finished\FORC\FORC1'
```

This means the script will search for files at the subdirectory of FORC1 and will generate the output file. The path where all files have to be stored is also denoted in the script.

```
if(len(sys.argv))>2:
    dir_name_out=sys.argv[2]
else:
    dir_name_out=_char+'makeplot',
```

This script will save all pdf files into the subdirectory of makeplot called FORC1. After searching for all three files(*.log, *.krn, *.txt) into the list of all subdirectories (`list_subdir`) within the input path.

```
for i in range(len(list_subdir)):
    for filename in os.listdir(list_subdir[i]):
        file_txt=""
        if fnmatch.fnmatch(filename, '*.txt'):
            file_txt=os.path.join(list_subdir[i],filename)
            filelist_txt_full_path[i]=file_txt
            print file_txt
        file_log=""
        if fnmatch.fnmatch(filename, '*.log'):
            file_log=os.path.join(list_subdir[i],filename)
            filelist_log_full_path[i]=file_log
            print file_log
        file_krn=""
        if fnmatch.fnmatch(filename, '*.krn'):
```

```

file_krn=os.path.join(list_subdir[i],filename)
filelist_krn_full_path[i]=file_krn
print file_krn

```

The script will pass all located files to the printing functions which will do the hysteresis loop

```

make_plot(file_dic,_char)
make_plot_full(file_dic,_char)
make_plot_all_in_one_full(file_dic,_char)

```

where `file_dic` is just the array with the located files and `_char` the character for separating directories (\ or /). Each plotting function will iterate over the list and open these 3 files(*.txt, *.log, *.krn) and generate the plots for just each model (and subdirectory). Nevertheless the scripts are sometimes changed because of different requirements but the script `make_plot()` will plot one curve where as the function `make_plot_full()` will print the whole x-range of collected data. There is one special plotting function which will put all loops into one graph (`make_plot_all_in_one()`). Each function will open all three files(*.krn, *.txt, *.log) and plot the BH-curves.

```

def make_plot(file_dic,_char):
    for d in range(len(file_dic)):
        #reading from krn file
        f_3=open(file_dic[d][2],'r')

        #reading from txt file
        f_1=open(file_dic[d][0],'r')

        #reading from log file
        f_2=open(file_dic[d][1],'r')

        .
        .
        .

        plot(.....)

#function end

```

This form is equal at all plotting functions because each function will open those files and extract the data from it and will generate the hysteresis curve into a pdf. Each input file is different because the krn files stores the properties of the material, the txt file the volume of the intersected cube and the spheres and the log file the computed values for the BH-loop.

The **krn(material properties** files has the look of

```

0.0 0.0 0.0 0.0 2.14 2.5e-11 1.0 0.0
0.0 0.0 4.2e6 0.0 1.6 1.0e-11 1.0 0.0

```

where the material characteristics are stored. The first lines are the properties of the intersected cube and second line are the spheres. There are only two variables used, the value of $J_{S_{soft}} = 2.14$ and $J_{S_{hard}} = 1.6$ for doing the plots. $J_{S_{soft}}$ means this property belongs to soft and $J_{S_{hard}}$ to hard magnetic material. This two values are used to calculate the weighting factor f and the associated flux density (B), the weighting factor is explained later.

At the **txt (volume of spheres and the intersect cube)** file

```
Volume_intersected_block: 414334.682795 Volume_inserted_spheres: 585665.312917
```

there is a line where the volume of the intersected cube and spheres are stored. The volume of $V_{Cube} = 414334.68$ and $V_{Spheres} = 585665.312917$ are also used for the weighting factor f to calculate the flux density (B). This file is generated by the Salome script.

The computed **log (values of the BH-curves)** file from FEMME has the form of

```
#_1_inp_number 2_time ... 10_hextX 11_hextY 12_hextZ 13_htotal 14_mx 15_my 16_mz
.
.
.
.
```

where the number stands for the column, _hext for the external magnetic field (H) and _m for the magnetization (M) each value in Tesla (T) even (H) because of normalizing this variable for easier computing. The direction is mentioned with x(X),y(Y),z(Z). At this study the values of the z coordinates are used so the value 12_hextZ and 16_mz are needed, because the external magnetic field (H) is changed along this direction.

The first and easiest plots are where only the external field(H) and the magnetization(M) are shown, so the value of 12_hextZ and the associated 16_mz are illustrated. This is at chapter 6 and chapter 7 where the volumes are equal and the fraction is not important to the $M(J)H$ -loops to compare them.

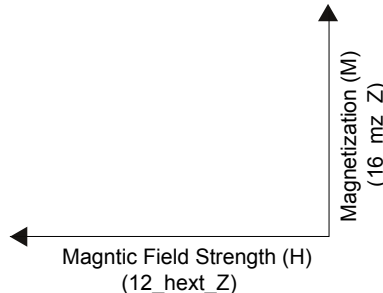


Figure 5.2: This figure illustrates the easiest kind of plotting, where the different volume fractions of the super magnet are not respected. It also shows which values are plotted so the magnetic field strength(H) is plotted from values of 12_hextZ and the associated magnetization (M) is plotted from the values of 16_mz which are stored into computed logging file(*.log) from FEMME. This curve is called a MH or JH-curve.

The second from is a little bit more tricky but it respects the volume fraction of the hard and soft magnetic material. The flux density (B) is illustrated at chapter 8 and 9. Before showing the flux density the weighing factor f must be calculated. This value is calculated with the formula

$$f = \frac{V_{Spheres} * J_{Spheres} + V_{Cube} * J_{Cube}}{V_{Spheres} + V_{Cube}} \quad (5.1)$$

where V considers the volume of the spheres and intersected cube , and J(saturation magnetism) is the property if hard or soft magnetic material is used($J_{S_{soft}} = 2.14$ and $J_{S_{hard}} = 1.6$). This leads to the next step to calculate the flux density (B). This script takes the two volumes from the text file(*.txt) and the material properties(*.krn) (J) and calculates the weighting factor f. After doing this it computes the flux density according to his formula.

$$B = \mu_0(H + M) \quad (5.2)$$

$$B = \mu_0 * H + \mu_0 * M \quad (5.3)$$

$$B = \mu_0 * H + J \quad (5.4)$$

$$B = 12_hextZ + f * 16_mz \quad (5.5)$$

So before calculating the flux density the weighting factor f must be calculated and multiplied with 16_mz and added to the value 12_hextZ.

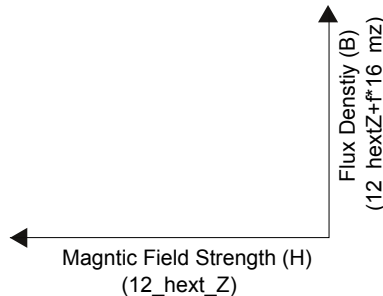


Figure 5.3: This figure illustrates the second kind of plotting in this study, where the volume fractions and material properties of the magnet are respected. It also shows which values are plotted so the magnetic field strength(H) is plotted from the values of 12_hexZ and the associated flux denstiy (B). The value of the flux density must be calculated with the weighing factor f . This curve is called a BH-curve or hysteresis loop.

One another value which is sometimes calculated in this work is the **maximum energy product**((BH)_(max)). This value is the maximum of the product with the flux density (B) and the external field (H) over all calculated values must be taken. So it is computed by this formula

$$(BH)_{max} = \max(H * B) \quad (5.6)$$

where H is normalized from FEMME(*.log) and in Tesla(T) and must must be converted to kA/m.

$$(BH)_{max} = \max(H * B) \quad (5.7)$$

$$12_hextZ = H * \mu_0 \quad (5.8)$$

$$(BH)_{max} = \max\left(\frac{12_hextZ * B}{\mu_0}\right) \quad (5.9)$$

At the script the value of the maximum energy product is calculated with iterating of those two values(H,B) and at each index a new value is calculated ((BH)_(max)) this value is compared with the computed value before and if the new value is bigger than the old value the old one will be replaced. The value of(BH)_(max) must be calculated in the second quadrant so the magnetization (M) must positive.

```
if((math.fabs(mz[i]*hz[i]) > BH_max) and (mz[i] > 0)):
    BH_max=math.fabs(mz[i]*hz[i])
```

The script for doing the post process must be adapted every time, or the functions within the script must be copied and changed because sometimes the magnetization(M) is shown and at another chapter the flux density. Like this lines of the script,

```
hz.append(float(tabele[11]))
#mz.append(float(tabele[15]))
mz.append(hz[i]+float(tabele[15])*f)
```

One line is not active because the flux density(B) is shown.

Chapter 6

Some trials with magnetic materials

6.1 Determine the required mesh size

6.1.1 Introduction

First of all the mesh size is a factor of the accuracy for computing finite elements and at this case important at calculating the demagnetizing curves, so there are several computations done to determine the required grid size for the used geometry. The number of tetrahedrons affects the accuracy of the computation and the hysteresis loop. There is no way to find the exact parameters for any amount of tetrahedrons, but it's possible to do some kind of pre-computing. Also just to mention meshing is also really time-consuming, so the best way is to try different parameters at the pre-computing for the mesh (min/max - size) before doing the real mesh. The first simulation has approximately 57k tetrahedrons and the last one approximately 1350k elements. If the count of tetrahedron is octuplicate the real mesh size is divide especially the maximum step size of the mesh. At all simulations there are two different sets of parameters, which means at the first set of parameter files (par1) the hard magnetic material is the intersected cube and at the second parameter set (par2) the soft magnetic material is replaced by spheres which consist of hard magnetic material. The total volume of the cube is 100 nm times 100 nm times 100nm = 10^6 nm^3 , the model of all simulations always consists of an intersected cube and some spheres.

parameter sets for next simulations

PARAMETER SET	BLOCK	SPHERES
par 1	hard magnetic shell	soft magnetic core
par 2	soft magnetic shell	hard magnetic core

Table 6.1: Parameter sets for the simulations

Table 6.1 presents the two parameter sets of all simulations, at all models there are two different computations done, which means at one simulation the spheres consist of hard magnetic material and at the second simulation the spheres consist of soft magnetic material.

6.1.2 Low density packed spheres

This name has nothing to do with the real dense (P) of packed spheres from chapter 3 only with the alignment of those spheres.

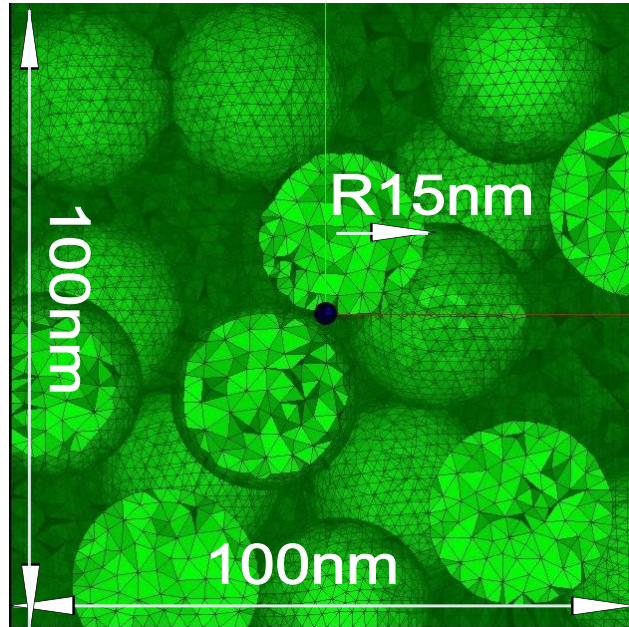


Figure 6.1: Top view - cut through the cube with low density packed spheres which shows the space between each sphere, they are all well separated, at this case all spheres are equal sized. Spheres which hit the boundary of the cube are cut. The volume ratio is still the same like at the other simulations of chapter 5 and each sphere has the same radius ($r=15\text{nm}$).

Explanation

This first attempt was to determine the required mesh size for all the next simulations. At this point it wasn't clear that there is a big trade off between geometry, packing density and sphere size. At this simulation all spheres within the intersected cube have the radius of 15nm, they are all well separated and each sphere doesn't touch any other sphere. Areas of spheres which are outside the cube are cut so that the overall geometry is still a cube and it makes it easier to compare this run with next simulations because of the same volume. The method of low (random) density packed spheres makes it possible that only approx. 35 percent of the total volume can be replaced by spheres if the spheres have equal sizes. If the radius of those spheres is decreased the density of spheres could be slightly higher but with the problem of computing time and meshing awareness. All next simulations are done with density of 0.3 so the spheres replace approximately 30 percent of the intersected cube. There are two sets of parameters used, at first parameter set (par1) the hard magnetic material is the cube and the spheres within the cube consist of soft magnetic material. The second parameter set is used for the case that hard magnetic material is inside the cube and soft magnetic material is at the outside.

6.1.3 Low density packed spheres - Mesh of simulation 1 (57k)

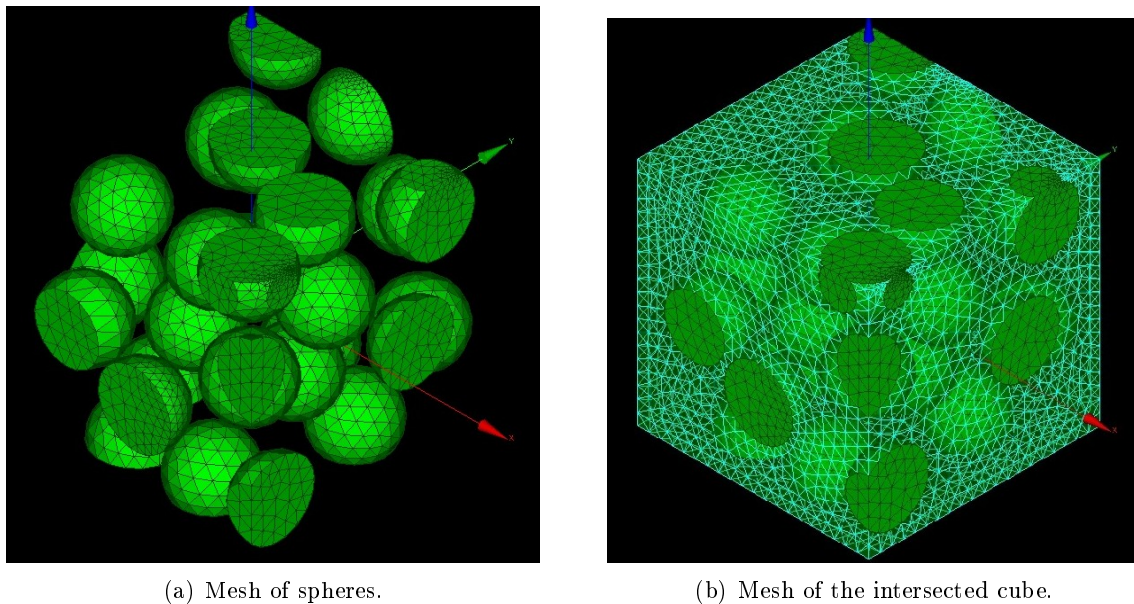


Figure 6.2: Shows the two meshes used for the first simulation of low density packed spheres with low mesh quality, this mesh is used to compare the computed results.

6.1.4 Low density packed spheres - Mesh of simulation 4 (362k)

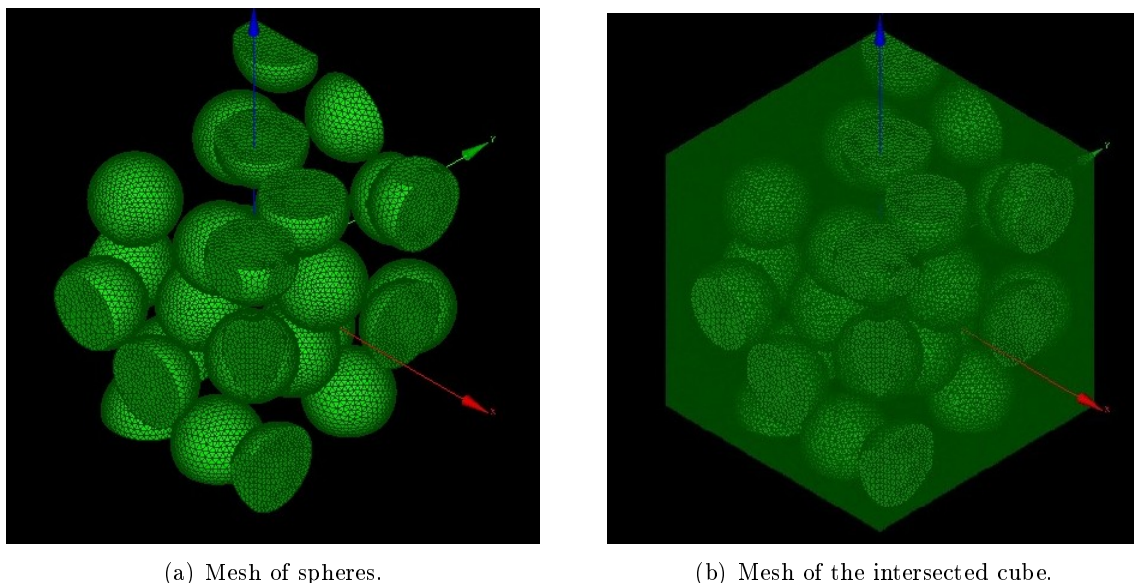


Figure 6.3: Shows the two meshes used for the fourth simulation of low density packed spheres with higher mesh quality, this mesh is used to compare the computed results.

6.1.5 Low density packed spheres - BH-loops of first parameter set (par1) (Spheres=28; Radius=15nm)

At these simulations the geometry of low density packed spheres is used. The intersected cube consist of hard magnetic material and 30 percent of space is replaced by soft magnetic material. All spheres are well separated from each other.

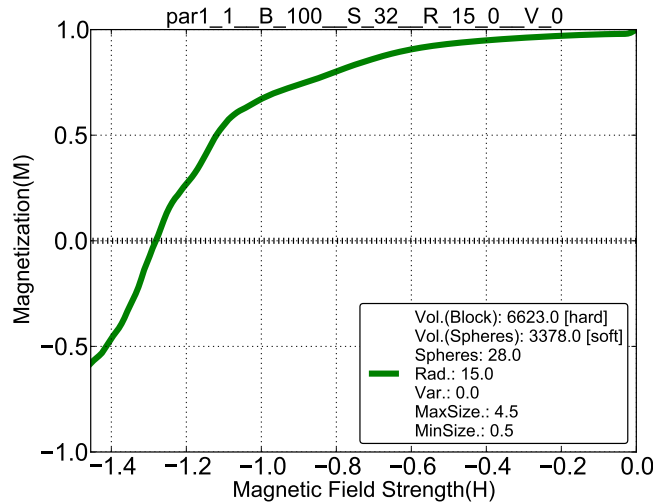


Figure 6.4a: Demagnetization curve for a nano composite magnet with volume fraction of soft about 0.3, soft sphere size with the radius of 15nm and max mesh size by 4.5nm.

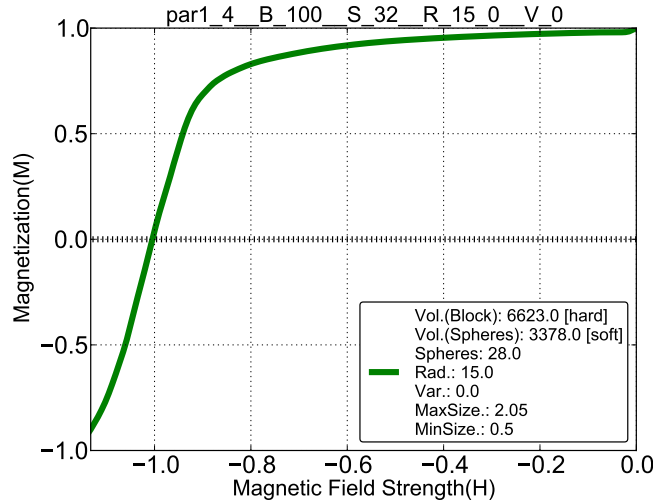


Figure 6.4b: Demagnetization curve for a nano composite magnet with volume fraction of soft about 0.3, soft sphere size with the radius of 15nm and max mesh size by 2.05nm.

Figure 6.4a up to 6.4b show some BH-loops of low density packed spheres with the first parameter set and some significant points where these curves differ because of different amount of calculations elements at the mesh.

6.1.6 Low density packed spheres - Comparison of all BH-loops within the first parameter set (par 1) (Spheres=28; Radius=15nm)

At this attempt most of the volume consist of hard magnetic material and approximately 30 percent of the cube is replaced by spheres which consist of soft magnetic material. At figure 6.5 all computations are compared with different mesh parameters to figure out the best parameters with low computation time but and high accuracy.

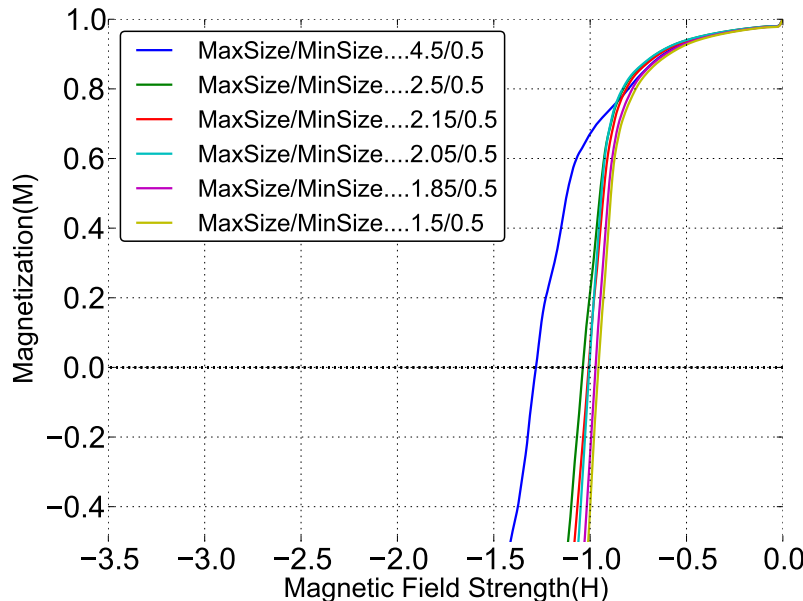


Figure 6.5: Comparison of all BH-loops within parameter set 1 with different tetrahedron count at this case the spheres consist of soft magnetic material and the intersected cube of hard magnetic material, approximately 30 percent of the total volume is replaced by spheres. The geometry is low density packed spheres, all spheres have equal sizes ($r=15\text{nm}$).

Conclusion

According to figure 6.5 there is a big shift between the simulation 1 with only 57k elements and those simulations between 200k up to 1.4m elements. The fist simulation only took approximately 30 minutes to compute on the other side the simulation with 1.4 million elements was finished after one and a half day. Just to mention the real mesh size is divide from simulation 1 to simulation 4, so if the mesh size is divide the elements must be multiplied with the factor 2^3 because of the fact that the model of these computations consists of three lengths in each direction of space . Simulations with higher amout of tetrahedrons differ less but computations with higher accuracy take a lot more time. There is always a trade off between higher accuracy and computation time, computation time is not relevant as long as the account of simulation is less, but if the number of simulations rises it could be big problem if the accuracy is too high.

6.1.7 Low density packed spheres - BH-loops of second parameter set (par2) (Spheres=28; Radius=15nm)

At these simulations the geometry of low density packed spheres is used. The intersected cube consist of soft magnetic material and 30 percent of space is replaced by hard magnetic material. All spheres are well separated.

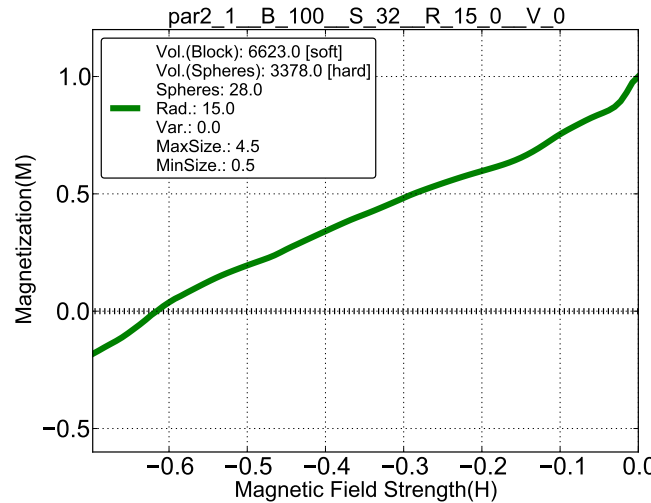


Figure 6.6a: Demagnetization curve for a nano composite magnet with volume fraction of hard about 0.3, hard sphere size with the radius of 15nm and max mesh size by 4.5nm.

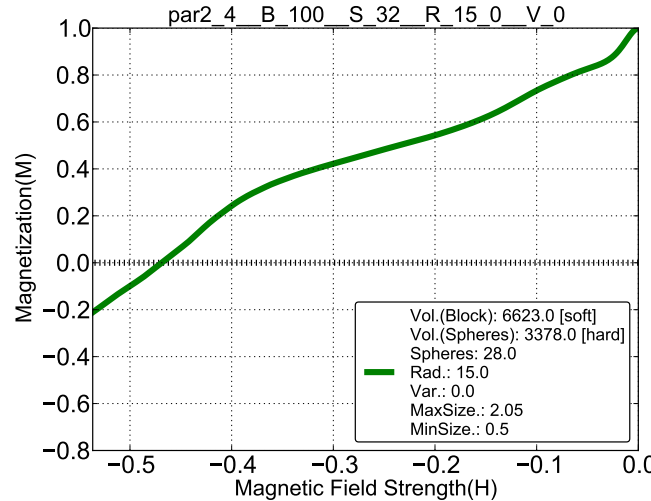


Figure 6.6b: Demagnetization curve for a nano composite magnet with volume fraction of hard about 0.3, hard sphere size with the radius of 15nm and max mesh size by 2.05nm.

Figure 6.6a up to 6.6b show some BH-loops of low density packed spheres with the second parameter set and some significant points where these curves differ because of different amount of elements at the mesh.

6.1.8 Low density packed spheres - Comparison of all BH-loops within the second parameter set (par2) (Spheres=28; Radius=15nm)

At this attempt most of the volume consist of soft magnetic material and approximately 30 percent of the cube is replaced by spheres which consist of hard magnetic material. At figure 6.7 all computations are compared with different mesh parameters to figure out the best parameters with low computation time but and high accuracy.

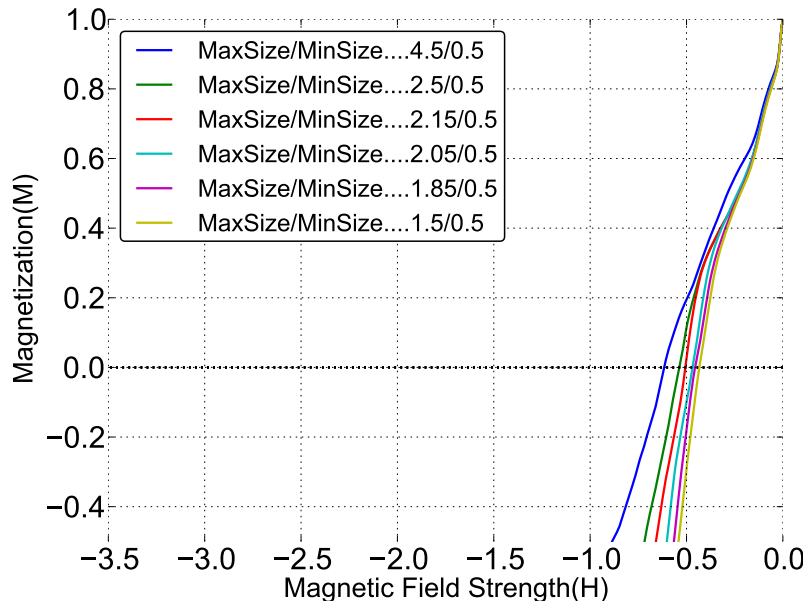


Figure 6.7: Comparison of all BH-loops within parameter set 2 with different tetrahedron count at this case the spheres consist of hard magnetic material and the intersected cube of soft magnetic material, approximately 30 percent of the total volume is replaced by spheres. The geometry is low density packed spheres, all spheres have equal sizes ($r=15\text{nm}$).

Conclusion

The hard magnetic part switched to soft magnetic material, so the volume of the intersected cube becomes soft magnetic. The difference between all these simulations isn't the same like at figure 6.5, but still high, all simulations are still normalized, so it's not carried out how much the grid size influences the accuracy of $(BH)_{\max}$ values. The BH-loop of the first simulation now hits the x-axis with the value of about 0.75 but simulations with higher tetrahedron count hit the x-axis around 0.5. This group of simulations also shows that the accuracy is not only influenced by mesh parameters also by material parameters. Nano composite magnets always consist of hard and soft magnetic phases, which means that the solver has to compute stiff systems, it leads to the problem that one part of the equation system is changing a lot more faster than the other one. At this group of simulations almost all volume of the cube consists of soft magnetic material which leads to the problem hard magnetic part influences the equation system less.

6.2 High density close packed spheres

This name has nothing to do with the real dense (P) of packed spheres from chapter 3 only with the alignment of those spheres.

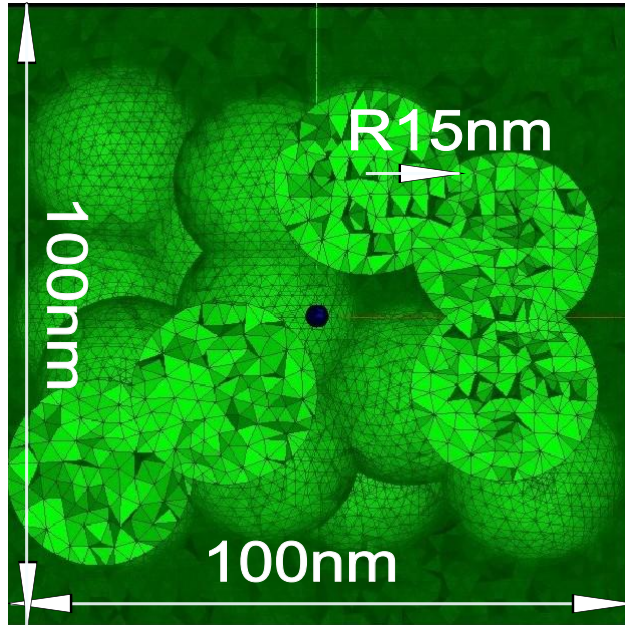


Figure 6.8: Top view - cut through the cube with high density close packed spheres, spheres now intersect with another spheres they are not separated which can lead to bad results at the BH-loops because of wide areas of soft magnetic material but the volume ratio is still the same like at the other simulations of chapter 4 and 5, all spheres have equal sizes ($r=15\text{nm}$).

Explanation

This was the second try but spheres within the cube are not separated from each other, some may touch another some not. This attempt is also done with different mesh sizes to get the best result but the geometry is still the same. According to the first run with low (random) density packed spheres it is recommended to use the same volume ratio, so 30 percent of the total volume is replaced by spheres the rest consist of the intersected cube, so it is possible to compare all simulations and figure out some differences with nearly same volume fractions. All spheres have the same size and the grain size with the radius of 15nm. At this try it was not clear how to replace much more space with spheres so the easiest solution was that those spheres are allowed to touch another one. All spheres are inside the cube, none of those hit the boundary of the cube. High density close packing is the easiest way to replace a lot space by spheres or with any shape, because of the fact that spheres are allowed to intersect them, this results into the worst case of all three attempts. All simulations show that the grade of areas about soft magnetic materials influences the BH-loop dramatically. The geometry of the soft magnetic material is one main factor of the strength of super magnets.

6.2.1 High density close packed spheres - Mesh of simulation 1 (57k)

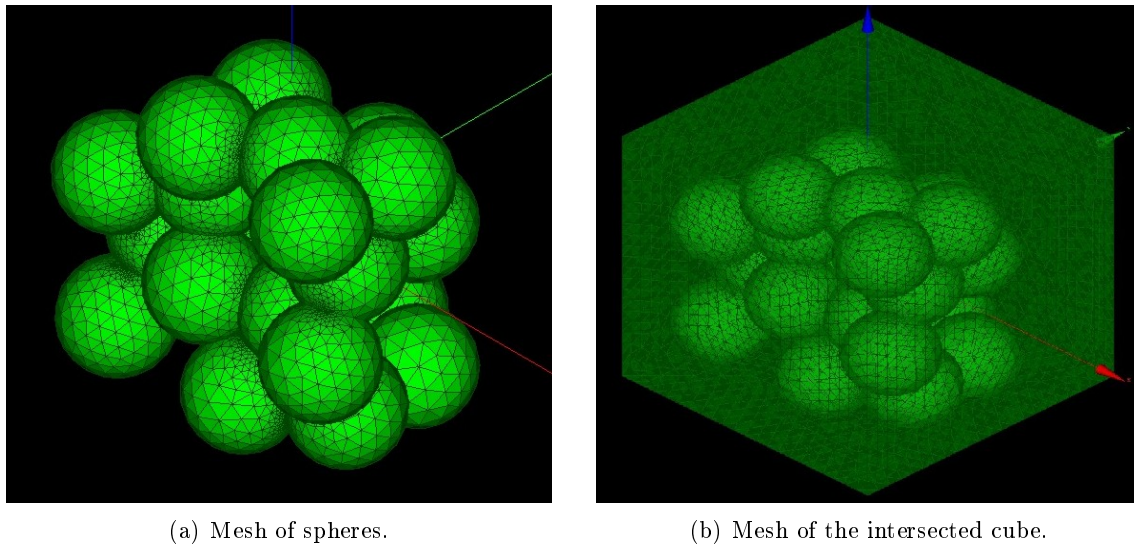


Figure 6.9: Shows the two meshes used for the first simulation of high density close packed spheres with lower mesh quality, this mesh is used to compare the computed results.

6.2.2 High density close packed spheres - Mesh of simulation 4 (362k)

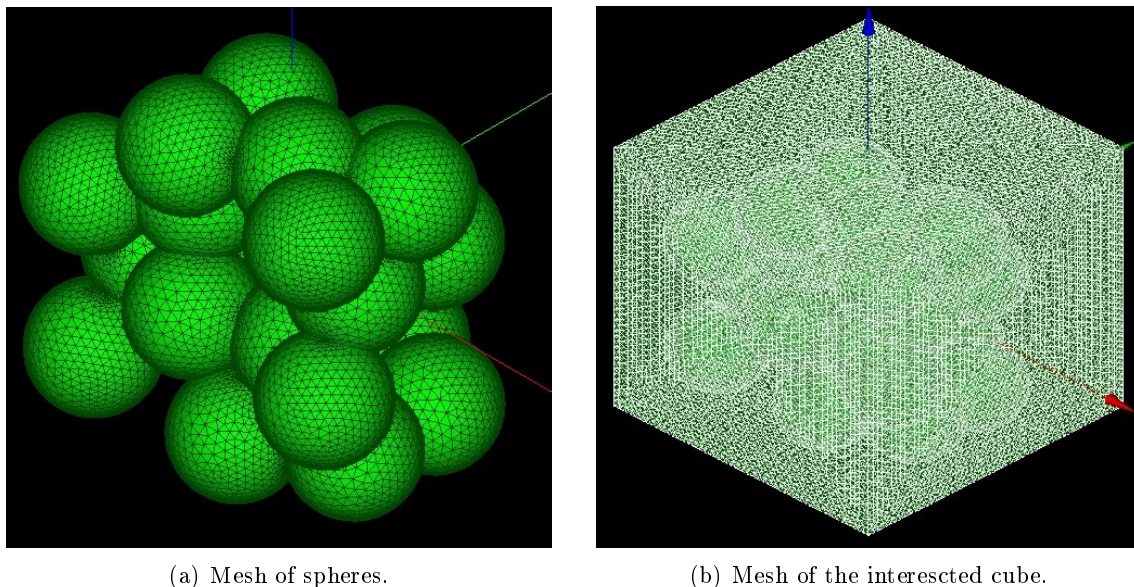


Figure 6.10: Shows the two meshes used for the fourth simulation of high density close packed spheres with higher mesh quality, this mesh is used to compare the computed results.

6.2.3 High density close packed spheres - BH-loops of first parameter set (par1) (Spheres=28; Radius=15nm)

At these simulations the geometry of high density close packed spheres is used. The intersected cube consist of hard magnetic material and 30 percent of space is replaced by soft magnetic material with spheres. All spheres are close together.

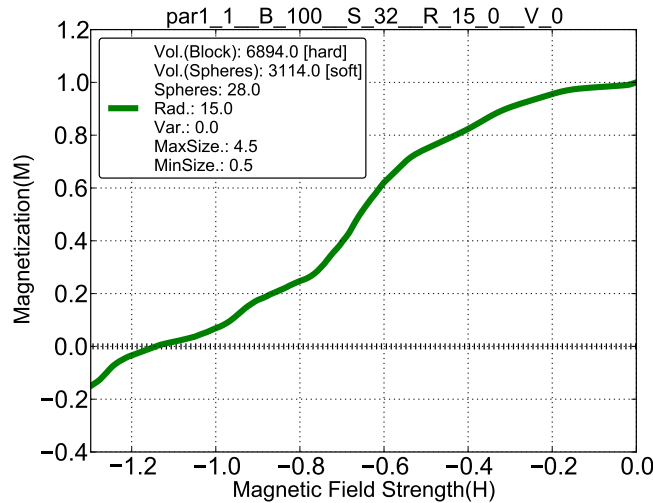


Figure 6.11a: Demagnetization curve for a nano composite magnet with volume fraction of soft about 0.3, soft sphere size with the radius of 15nm and max mesh size by 4.5nm.

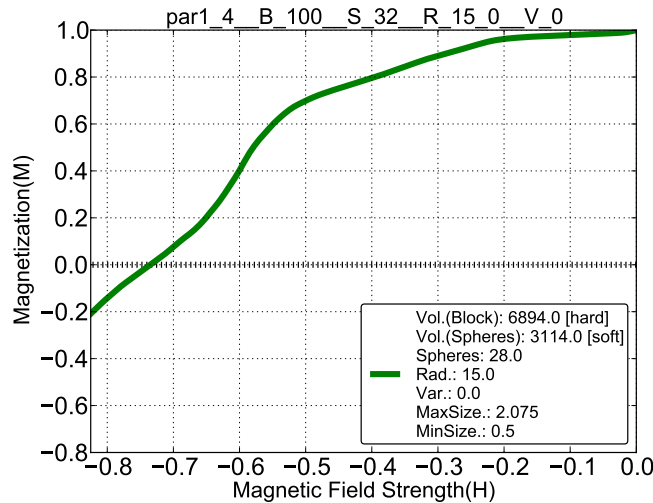


Figure 6.11b: Demagnetization curve for a nano composite magnet with volume fraction of soft about 0.3, soft sphere size with the radius of 15nm and max mesh size by 2.075nm.

Figure 6.11a up to 6.11b show some BH-loops of high density close packed spheres with the first parameter set and some significant points where these curves differ because of different amount of calculation elements at the mesh.

6.2.4 High density close packed spheres - Comparison of all BH-loops within the first parameter set (par1) (Spheres=28; Radius=15nm)

At this attempt most of the volume consist of hard magnetic material and approximately 30 percent of the cube is replaced by spheres which consist of soft magnetic material. At figure 6.12 all computations are compared with different mesh parameters to figure out the best parameters with low computation time but and high accuracy.

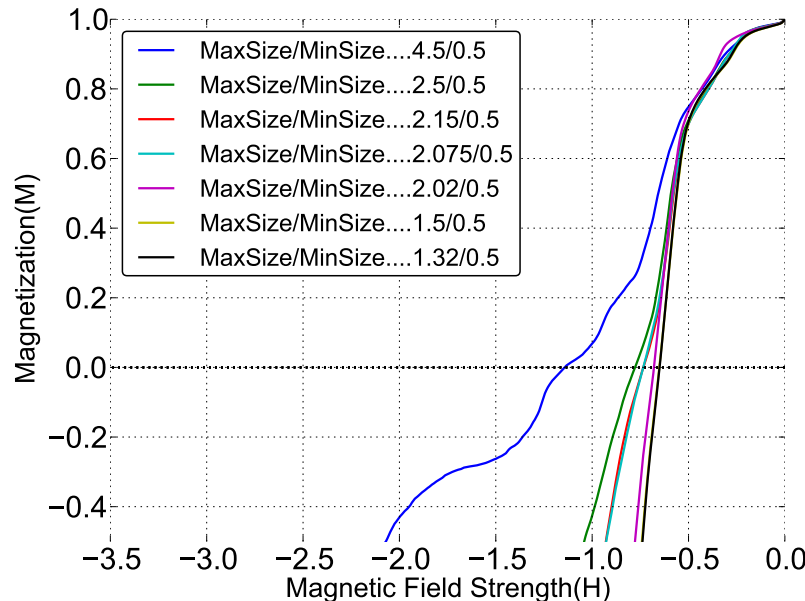


Figure 6.12: Comparison of all BH-loops within parameter set 1 with different tetrahedron count at this case the spheres consist of soft magnetic material and the intersected cube of hard magnetic material, approximately 30 percent of the total volume is replaced by spheres. The geometry is high density close packed spheres, all spheres have uniform sizes ($r=15\text{nm}$).

Conclusion

The new BH-loops show that the mesh size is still a big factor which influences the accuracy of computing finite elements. There is also a big difference between figure 6.5 and figure 6.12. At figure 6.12 it seems that the BH-loop response to soft-magnetic materials but it belongs to a hard magnetic material, so the geometry and distribution also influences the behaviour of all BH-loops. Just to mention most of the spheres are connected together, so there is no break between them. Simulations with higher tetrahedron count differ less but computations with higher accuracy take a lot more time to finish. There is always a trade off between higher accuracy and computation time, computation time is not relevant as long as the account of simulation is less, but if the number of simulations rises it could be a big problem if the accuracy is too high. Other simulations show that the best parameters for computation are still $\text{maxsize}=1.5/\text{minsize}=0.5$ of the mesh to achieve high accuracy.

6.2.5 High density close packed spheres - BH-loops of second parameter set (par2) (Spheres=28; Radius=15nm)

At these simulations the geometry of high density close packed spheres is used. The intersected cube consist of soft magnetic material and 30 percent of space is replaced by hard magnetic material with spheres. All Spheres are close together.

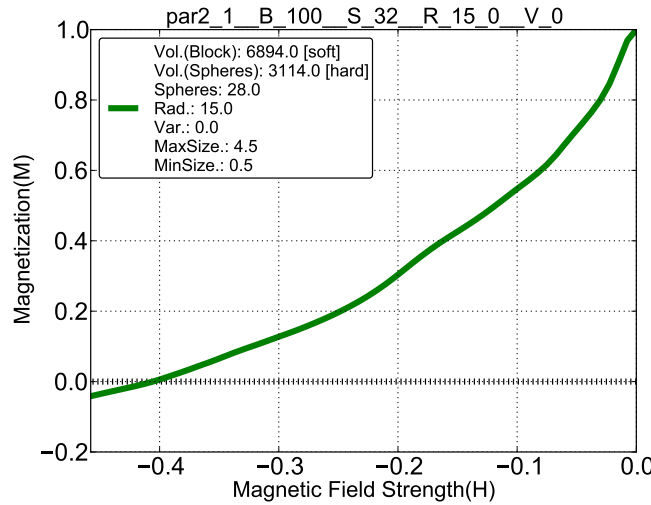


Figure 6.13a: Demagnetization curve for a nano composite magnet with volume fraction of hard about 0.3, hard sphere size with the radius of 15nm and max mesh size by 4.5nm.

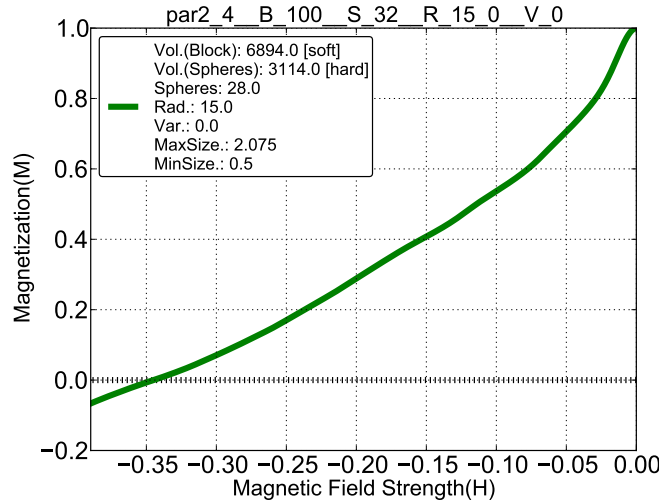


Figure 6.13b: Demagnetization curve for a nano composite magnet with volume fraction of hard about 0.3, hard sphere size with the radius of 15nm and max mesh size by 2.075.

Figure 6.13a up to 6.13b show some BH-loops of high density close packed spheres with the second parameter set and some significant points where these curves differ because of different amount of calculation elements at the mesh.

6.2.6 High density close packed spheres - Comparison of all BH-loops within the second parameter set (par2) (Spheres=28; Radius=15nm)

At this attempt most of the volume consist of soft magnetic material and approximately 30 percent of the intersected cube is replaced by spheres which consist of hard magnetic material. At figure 6.14 all computations are compared with different mesh parameters to figure out the best parameters with low computation time but and high accuracy.

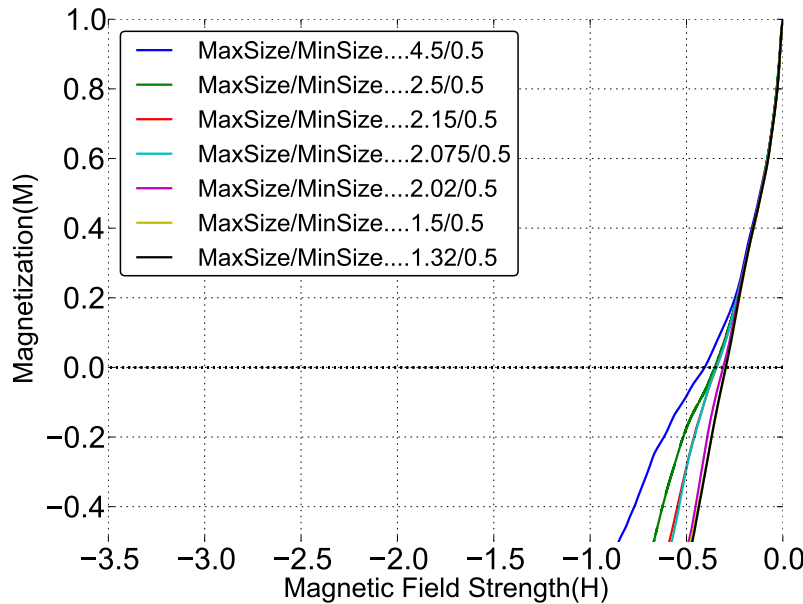


Figure 6.14: Comparison of all BH-loops within parameter set 2 with different tetrahedron count at this case the spheres consist of hard magnetic material and the intersected cube of soft magnetic material ,approximately 30 percent of the total volume is replaced by spheres. The geometry is high density close packed spheres, all spheres have uniform sizes ($r=15\text{nm}$).

Conclusion

The hard magnetic material switched to soft magnetic, so the intersected cube becomes soft. There is some difference over all simulations especially between simulation 4 with 350k tetrahedrons and 6 with 1.4 million elements (tetrahedrons). At these cases it's obvious that the accuracy also influences the calculations of $(BH)_{\max}$. The BH-loop with highest accuracy now hit's the x-axis beneath 0.25, all other curves clearly hit the x-axis with an value over 0.25. Nano composite magnets always consist of hard and soft magnetic phases, which means that the solver has to compute stiff systems, it leads to the problem that one part of the equation is changing fast and the other part is changing slow. At these group of simulations almost all volume of the cube consist of soft magnetic material. It's figured out if smaller step sizes of the mesh will improve the calculation accuracy and all converge to the same value. At this attempt spheres are allowed to touch another sphere.

6.3 High density loose packed spheres

This name has nothing to do with the real dense (P) of packed spheres from chapter 3 only with the alignment of those spheres.

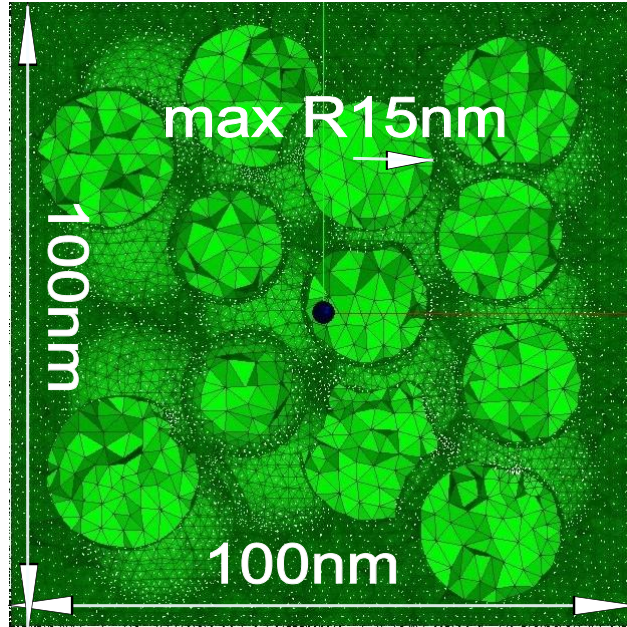
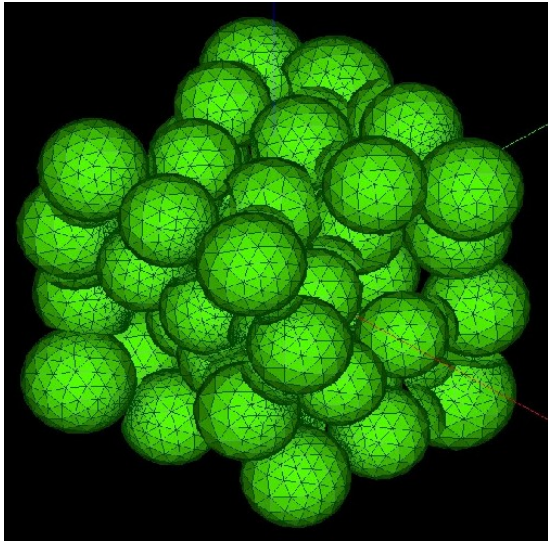


Figure 6.15: Top view - cut through the cube with high density loose packed spheres, all spheres are stacked together but each sphere is separated and don't touches another sphere. According to this fact they have different sizes, the volume ratio is still the same like at all other simulations of chapter 6, all spheres are limited to the maximum size ($r=15\text{nm}$).

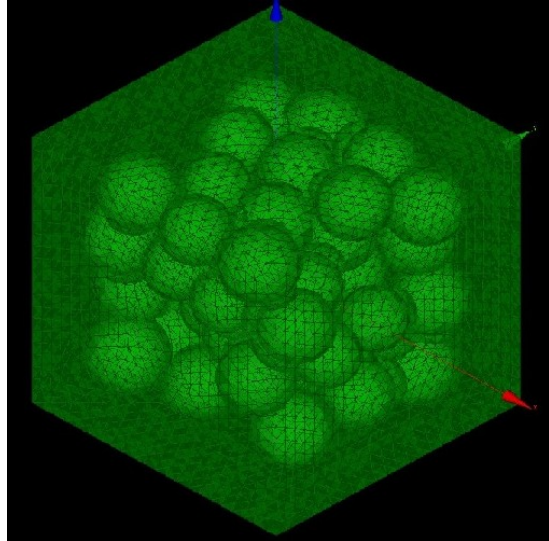
Explanation

At this attempt all spheres are dense packed but all they don't touch another one. Because of the fact that all spheres are dense packed together but with the requirement don't touch another sphere the sizes are not uniform. At this run all spheres are checked if they intersect with another sphere and also if the minimum distance of meshing is maintain. If they intersect with another one the size is shorten as long as they don't touch other spheres. All of those requirements lead to the problem to have the same volume ratios like at previous attempts and the usage of more spheres, so at this attempt 48 spheres are used with different sizes to achieve the same total volume ratio like at the previous runs. All spheres have different sizes with less than the radius of 15 nm. The result of this attempt shows that there is no response to the density how spheres are packed together as long as the area of the soft magnetic is small and the distance between those spheres is enough. Alignment of those spheres is still a problem because of the problem to accomplish the same volume ratio and simple requirements leads to use more spheres than to the contrary of previous formations.

6.3.1 High density loose packed spheres - Mesh of simulation 1 (57k)



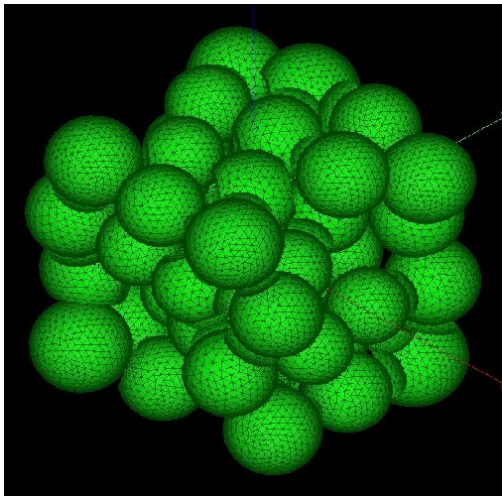
(a) Mesh of spheres.



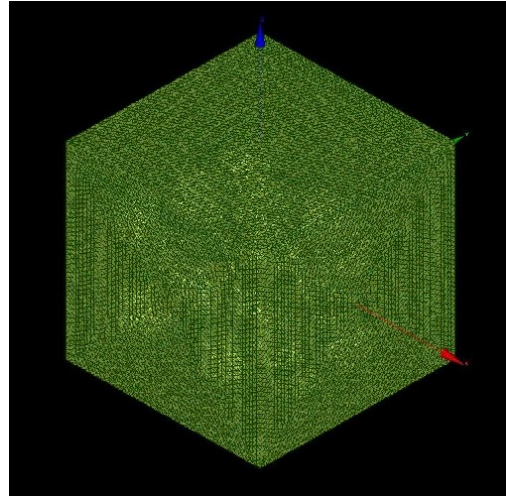
(b) Mesh of the intersected cube.

Figure 6.16: Shows the two meshes used for the first simulation of high density loose packed spheres with lower mesh quality, this mesh is used to compare the computed results.

6.3.2 High density loose packed spheres - Mesh of simulation 4 (326k)



(a) Mesh of spheres.



(b) Mesh of the intersected cube.

Figure 6.17: Shows the two meshes used for the fourth simulation of high density loose packed spheres with higher mesh quality, this mesh is used to compare the computed results.

6.3.3 High density loose packed spheres - BH-loops of first parameter set (par1) (Spheres=48;max Radius=15nm)

At these simulations the geometry of high density loose packed spheres is used. The intersected cube consist of hard magnetic material and 30 percent of space is replaced by soft magnetic material with spheres. All spheres are close together but separated.

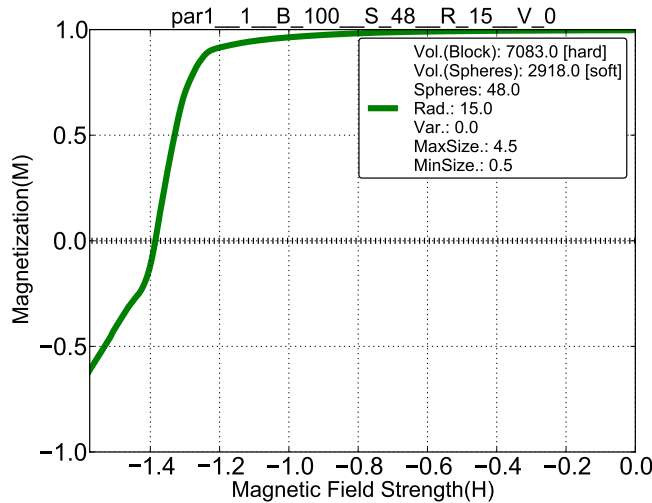


Figure 6.18a: Demagnetization curve for a nano composite magnet with volume fraction of soft about 0.3, soft sphere size with the max. $r = 15\text{nm}$ and max mesh size by 4.5nm .

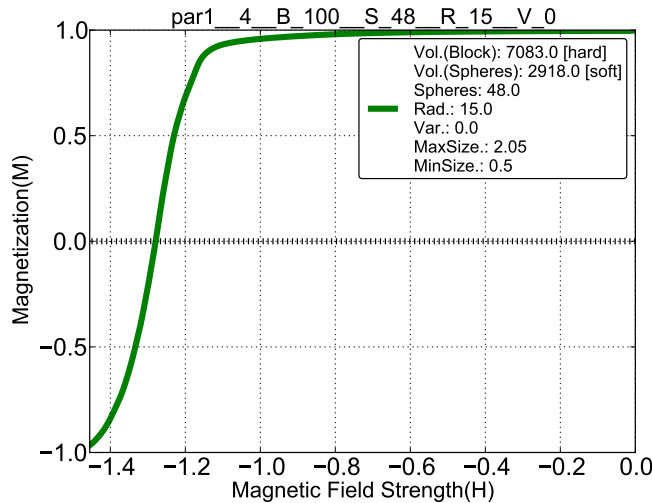


Figure 6.18b: Demagnetization curve for a nano composite magnet with volume fraction of soft about 0.3, soft sphere size with the max. $r = 15\text{nm}$ and max mesh size by 2.05nm .

Figure 6.18a up to 6.18b show some BH-loops of high density loose packed spheres with the first parameter set and some significant points where these curves differ because of different amount of calculation elements at the mesh.

6.3.4 High density loose packed spheres - Comparison of all BH-loops within the first parameter set (par1) (Spheres=48;max Radius=15nm)

At this attempt most of the volume consist of hard magnetic material and approximately 30 percent of the cube is replaced by spheres which consist of soft magnetic material. At figure 6.19 all computations are compared with different mesh parameters to figure out the best parameters with low computation time but and high accuracy.

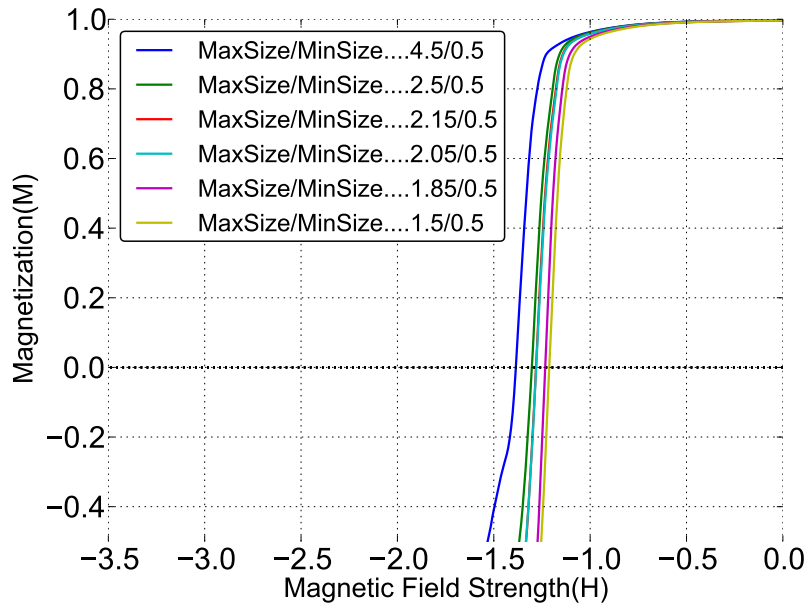


Figure 6.19: Comparison of all BH-loops within parameter set 1 with different tetrahedron count at this case the spheres consist of soft magnetic material and the intersected cube of hard magnetic material, approximately 30 percent of the total volume is replaced by spheres. The geometry is high density loose packed spheres. They all have none uniform sizes with the maximum radius of 15nm.

Conclusion

At these simulations it's obvious that the grid size influences the accuracy of computing finite elements, but with higher tetrahedron count there is only less difference between those simulations especially from simulation 5 and simulation 6 the behaviour is nearly the same. The value of $(BH)_{\max}$ becomes better in comparison to figure 6.5 because of the higher coercive force (H_C) In comparison to further simulations it's clear that not only the volume ratio influences the behaviour of magnets also the geometry effects the computed BH-loops. At this group of simulations it's obvious that with smaller step size for meshing the computations converge, just for example the simulation 5 with parameters of maxsize=1.85 / minsize=0.5 and simulation 6 with maxsize=1.5 / minsize=0.5 are nearly the same even when the amount of elements for computation is doubled.

6.3.5 High density loose packed spheres - BH-loops of second parameter set (par2) (Spheres=48; max Radius=15nm)

At these simulations the geometry of high density loose packed spheres is used. The intersected cube now consist of soft magnetic material and 30 percent of space is replaced by hard magnetic material. All spheres are close together but separated.

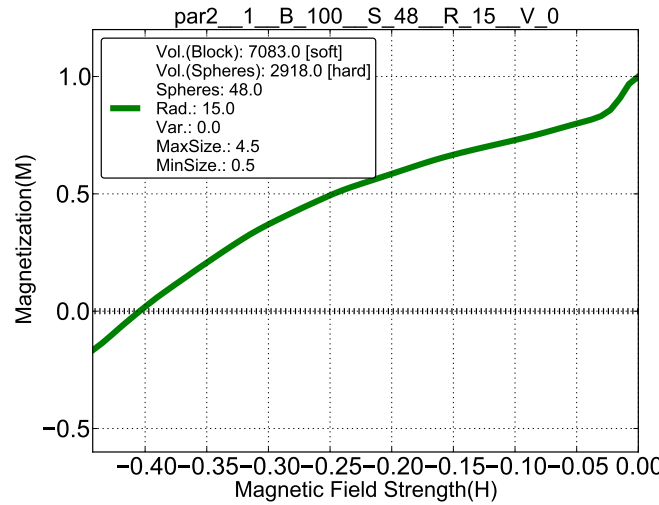


Figure 6.20a: Demagnetization curve for a nano composite magnet with volume fraction of hard about 0.3, hard sphere size with the max. $r=15\text{nm}$ and max mesh size by 4.5nm .

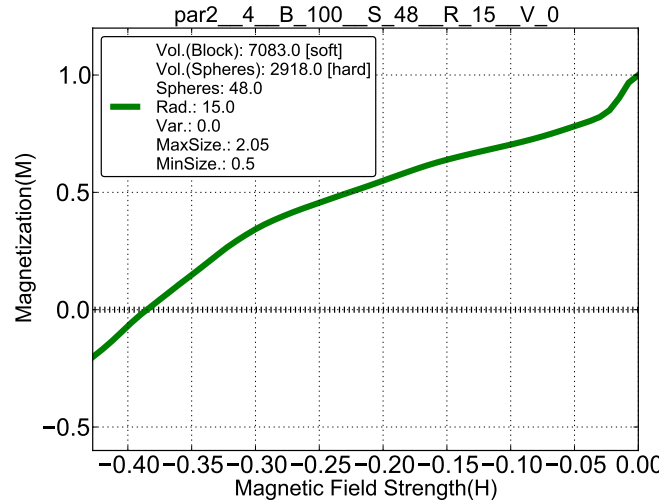


Figure 6.20b: Demagnetization curve for a nano composite magnet with volume fraction of hard about 0.3, hard sphere size with the max. $r=15\text{nm}$ and max mesh size by 2.05nm .

Figure 6.20a up to 6.20b show some BH-loops of high density loose packed spheres with the second parameter set and some significant points where these curves differ because of different amount of calculation elements at the mesh.

6.3.6 High density loose packed spheres - Comparison of all BH-loops within the second parameter set (par2) (Spheres=48;max Radius=15nm)

At this attempt most of the volume consist of soft magnetic material and approximately 30 percent of the cube is replaced by spheres which consist of hard magnetic material. At figure 6.21 all computations are compared with different mesh parameters to figure out the best parameters with low computation time and high accuracy.

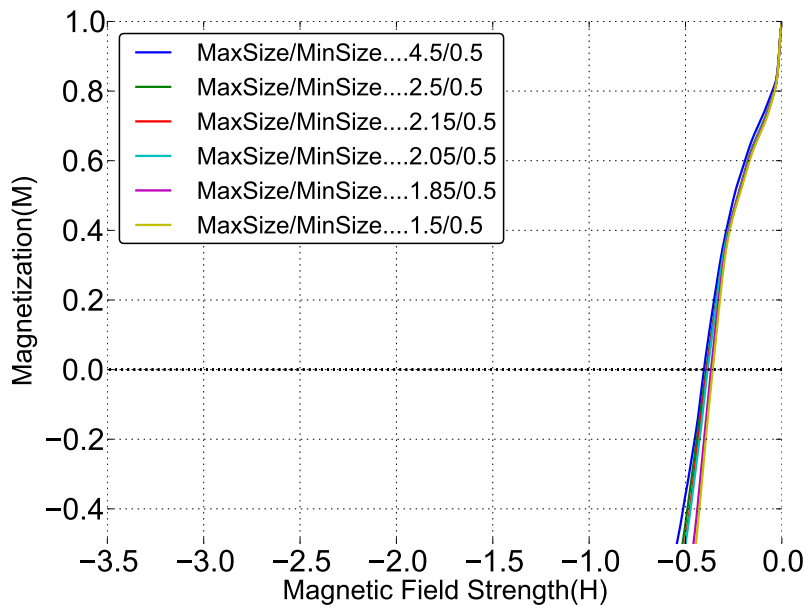


Figure 6.21: Comparison of all BH-loops within parameter set 2 with different tetragon count at this case the spheres consist of hard magnetic material and the intersected cube of soft magnetic material,approximately 30 percent of the total volume is replaced by spheres. The geometry is high density loose packed spheres, all spheres have none uniform sizes (maximum $r=15\text{nm}$).The BH-loops like to refer to soft magnetic material.

Conclusion

From the parameter set 1 to parameter set 2 the hard shell switched to soft soft magnetic, the cube now consists almost of soft magnetic material. At this attempt 70 percent of the total volume is soft magnetic material and 30 percent hard magnetic. There is no big difference between all computations with different accuracy and tetrahedron count, also the value of $(BH)_{\max}$ is not effected by the grid size and accuracy of these simulations. They hit the x-axis around the value of 0.35. All simulation seems to be equal even with higher amount of computation elements, it's because of the fact that most of the volume consists of soft magnetic material which also influences the accuracy of solving finite elements, because of the fact that the program still has to solve stiff equation systems but with low influence of hard magnetic materials and those properties.

6.3.7 What's the best mesh size ?

According to previous simulations with different mesh sizes, the best results can be achieved with following parameters. The max step of the mesh at every computation should not be greater than 1.85nm to achieve high accuracy and not smaller than 1.3nm because of the high amount of tetrahedrons and less effect to the accuracy. At all simulations the min step size of the grid is always the same like 0.5nm because this value leads to a fine mesh at the spheres and is still smaller as any used radius. If the amount of tetrahedrons is beyond 2.5 millions elements there is no real improvement to the accuracy of all computations. All simulations where the models are used to compute a row of different simulations the maximum mesh step size of 1.6 nm is used because the accuracy is high enough with the awareness to save some resources and computation time.

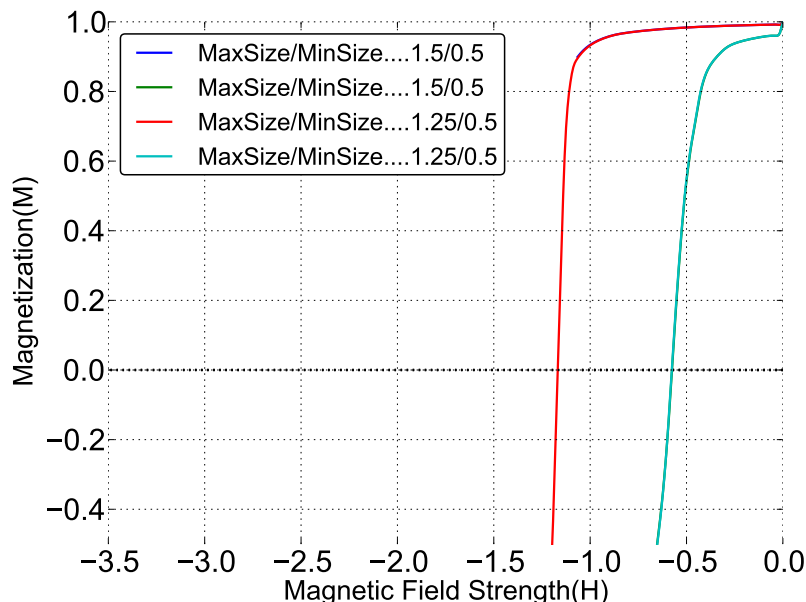


Figure 6.22: Comparison of different meshes at the same model (8.1), all computations are nearly equal so there is no improvement below the maximum step size of the grid with 1.5nm it only leads to higher computation time. This kind of model is often used at several computations, but at those models which are also used to calculate a row of computations a little bit greater max step size(1.6nm) is allowed because of really time and resources exhausted computations. This figure also shows that the accuracy because of different material properties is still no problem with these step sizes (max. 1.5nm / min 0.5nm) and below, so there is no change at it. At the green curve the cube consist of soft magnetic material and spheres of hard magnetic material, this case is often a problem to the accuracy and there is no big change at the computed curves.

Chapter 7

Comparison of high close/high loose/low-density packed spheres

7.1 Comments to the simulations

In this chapter there is a short summary of chapter 6 and 3. At the start of chapter 6 it wasn't clear how much simulations are to do for all the different cases and how hard it can be to align the spheres for the simulations. Another problem was meshing these shapes, because meshing requires that the geometries like spheres and the cube are not intersected and there are two main options to common the shapes or to cut them. Cutting the spheres means, u also have to rescale them and make the radius smaller so that those sphere don't touch them, on the other side, if u common two spheres this geometry will influence the behaviour of the BH-loop negatively. At the moment the first simulations show that it is still a lot better for the BH-loops and behaviour to make more loose packed spheres than close packed spheres, on the opposite more spheres (or any other geometry object), leads to more meshes even with same limits. Meshing shapes is also a problem if those shapes don't have enough space between them, because if two sphere are really close together the algorithm would fail to mesh them due the fact of overlapping elements. So there are only a few alignments to reach decent densities. This problem of a minimum distance between those shapes also leads to lower densities of packing spheres together. One another problem because of chapter 3 there is always a limitation because of the used geometry to cover space by any geometry with uniform sizes. One another way is to allow multi sized spheres and multiple sizes for the simulations or another alignment to achieve higher densities. These simulations also show that it is recommended to have more spheres with soft magnetic material which are not connected than bigger spheres or wide areas which leads to bad results at the computed BH-loops.

7.2 Comparison of different geometries

At this chapter all computed BH-loops from chapter 6 with different geometries are compared. At the moment there are just three kinds of used geometries like to separate all spheres well, to common them or to cut them if spheres are close together. At these simulations the fraction of the volumes which is replaced by spheres is always the same, spheres within the cube replace approximately 30 percent of the total space.

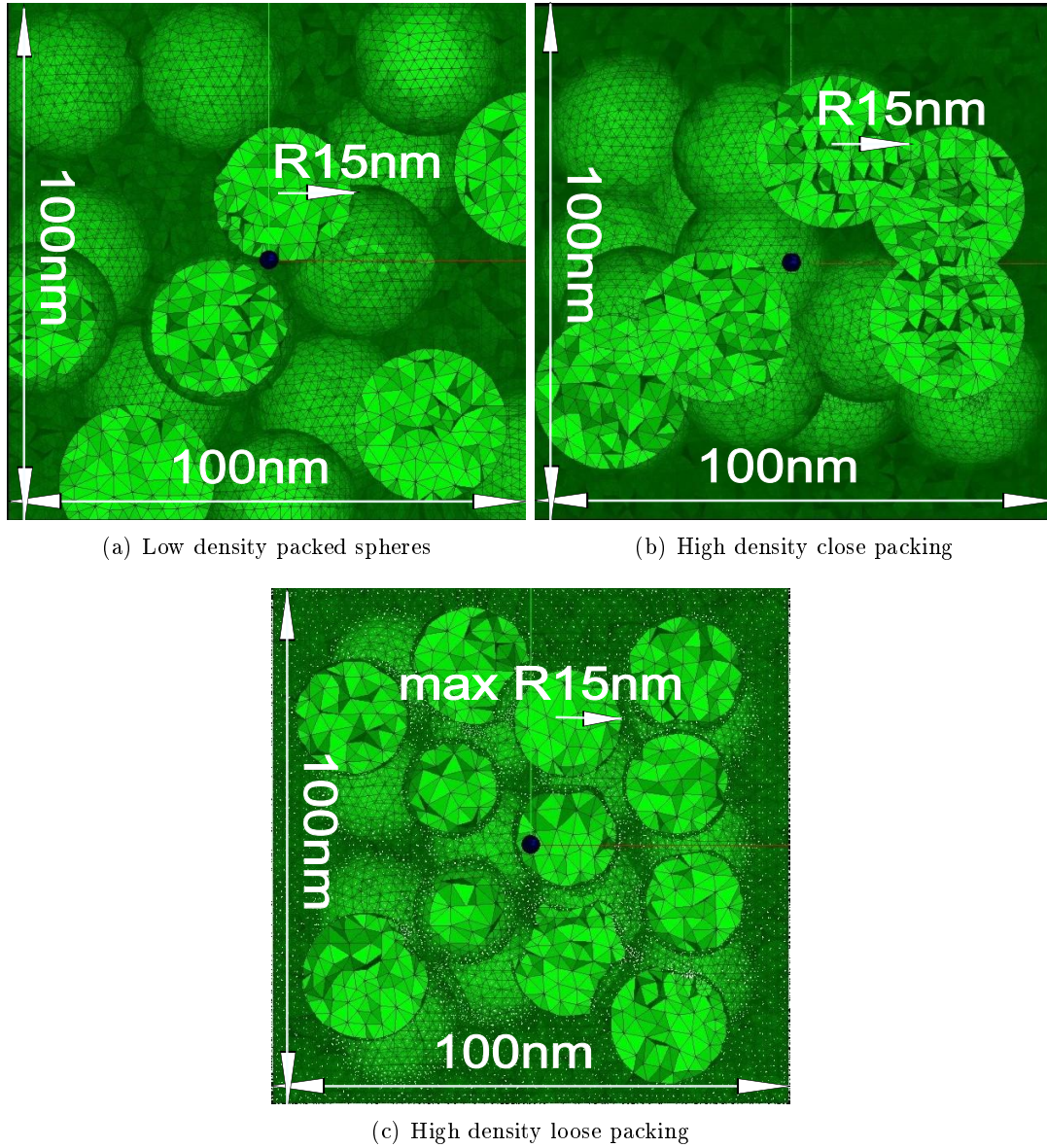


Figure 7.1: Comparison of all different geometries used in this work with approximately the same volume ratios, all spheres within the cube replace approximately 30 percent of the total space, the size of spheres is almost equal, except the sizes used at high density loose packing because all spheres are limited to radius of 15nm.

7.2.1 Comparison of low/high close/high loose - packed spheres (par1)

At all these attempts most of the volume consists of hard magnetic material and approximately 30 percent of the cube is replaced by spheres which is soft magnetic material. At figure 7.2 all computations are compared with the best accuracy to observe some differences because of the geometry and resulting behaviour at the BH-loops.

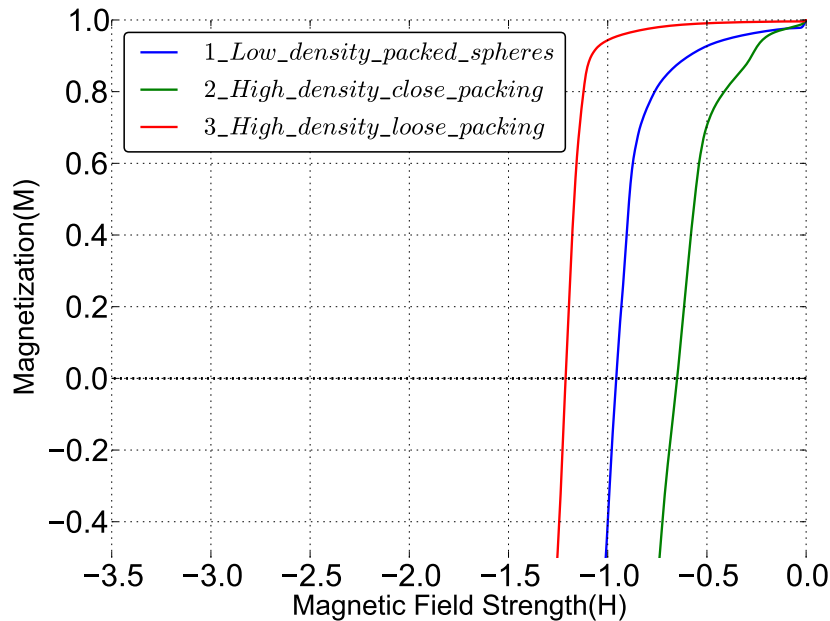


Figure 7.2: Comparison of low/high close/high loose packed spheres almost all space of the cube consists of hard magnetic material and spheres within the cube of soft magnetic material. Each alignment leads to own BH-loop, at all simulation approximately 30 percent of the total volume is replaced by soft magnetic material (spheres). This figure also shows that the alignment and geometry is really important.

Conclusion

Figure 7.2 shows that distribution of soft magnetic material is really important for the resulting BH-loops even though the volume ratio is nearly the same. These groups of attempts are done so that approximately 30 percent of the total volume consists of soft magnetic material. Distribution of soft magnetic material is really important, at simulation 2 all spheres are packed together and the result is the worst case of all computations. At simulation 1 all spheres are well separated, at this simulation all spheres have the radius of 15nm same at simulation 2. Simulation 3 shows the best behaviour, all spheres are still dense packed together but each is checked if they touch another one, spheres which intersect are shorten as long as they don't touch another one. It's the best result of all simulations another reason why perhaps bigger areas of soft magnetic material influences the behaviour of BH-loops negatively.

7.2.2 Comparison of low/high close/high loose - packed spheres (par2)

At all these attempts most of the total volume consists of soft magnetic material and approximately 30 percent of the cube is replaced by spheres which is hard magnetic material. At figure 7.3 all computations are compared with the best accuracy to observe some difference because of the geometry and resulting behaviour at the BH-loops.

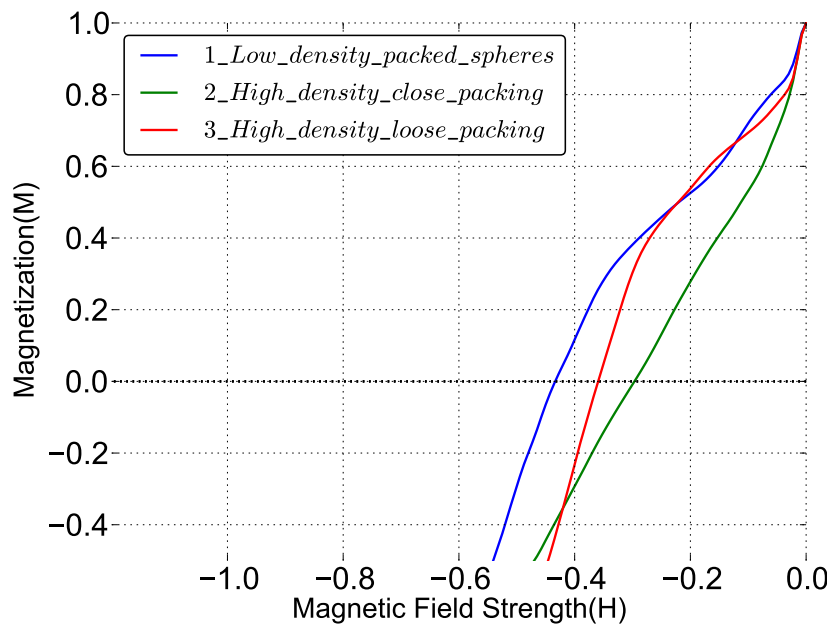


Figure 7.3: Comparison of low/high close/high loose packed spheres almost all space of the cube consist of soft magnetic material and spheres within the cube of hard magnetic materials. Each alignment leads to nearly same BH-loop's because of the fact that almost 70 percent of the total volume is soft magnetic material but only 30 percent consist of hard magnetic material. This figure also shows that the alignment and geometry is really important.

Conclusion

Figure 7.3 shows that high usage of soft magnetic materials negates the influence of the geometry and hard magnetic material nearly to zero. All simulations hit the x-axis around 0.4. So there is nearly no influence by the geometry and the hard magnetic material perhaps due the fact that most of cube is covered by soft magnetic material. Simulation 3 still has the worst behaviour and the lowest value of H_C which response to a bad $(BH)_{max}$, 30 percent of the total volume consist of hard magnetic material (spheres). Nano composite magnets always consist of hard and soft magnetic phases, which means that the solver has to compute stiff systems, which leads to the problem that one part of the equation is changing fast and the other part is changing slowly. It also means at this kind of simulations the low usage of hard magnetic material influences the stiff systems less.

Chapter 8

Influence of soft magnetic material

8.1 Effect of soft magnetic material at equal volume parts

At this chapter there are two simulations done, one simulation is where the hard magnetic material is at the outside and the soft magnetic material is inside. The other simulation is where the hard magnetic material is inside of the cube and soft magnetic material is at the outside. This pair of simulation is done to figure out, what's the best way to replace hard magnetic material by soft magnetic material, or in other words is there any big difference between those two possible alignments at the BH-loop. At this two simulations there is used the hexagonal grid where each sphere doesn't touch another sphere, the sphere within the cube replaces 47 percent of the space of the cube, where the rest of the volume is 53 percent. Figure 8.1 shows that each sphere is separated from each other sphere. Computations are not normalized at this chapter so the volume and material properties are respected.

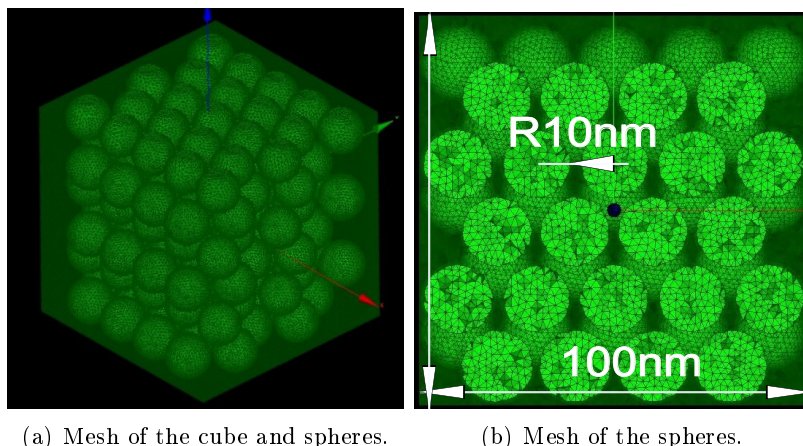


Figure 8.1: Shows the geometry of the cube and spheres with hexagonal lattice each sphere is separated from each other, hexagonal lattice gives the highest dense of sphere packing with equal sized spheres, at this case 47 percent of the volume is replaced by spheres all spheres have the same size with radius of 10nm and inside the cube there are appropriately 135 spheres.

8.1.1 Computed BH-loops with 135 spheres and grain size with radius of 10nm (volume ratio of intersected cube/spheres = 53/47)

At these simulations the geometry of hexagonal grid is used. The volume of the cube and spheres are nearly equal, these simulations are done to show the effect of different alignments because by the soft magnetic material.

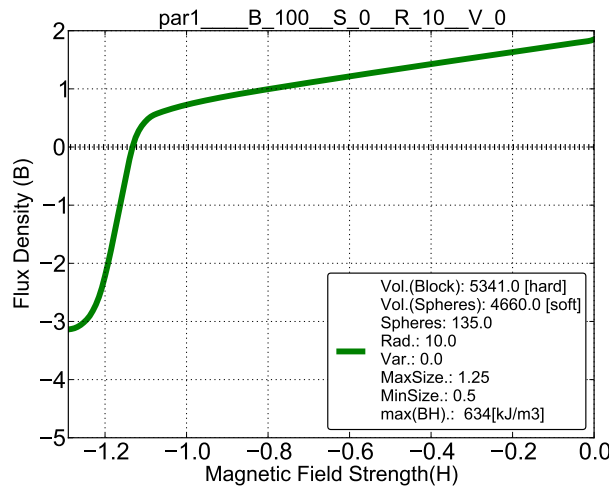


Figure 8.2: BH-loop of first attempt (par1) at this simulation the soft magnetic material (spheres) is separated by hard magnetic material (cube), the volume ratio is nearly equal of these two shapes, but the H_C is doubled in comparison to the second attempt (par2).

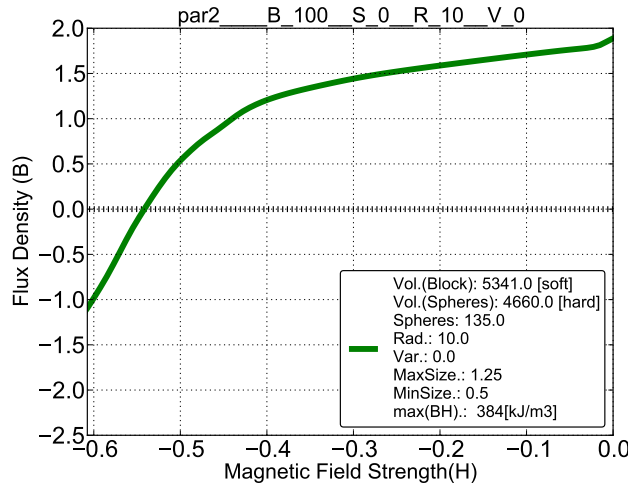


Figure 8.3: BH-loop of second attempt (par2) at this simulation the hard magnetic material (spheres) is separated by soft magnetic material (cube), the volume ratio is nearly equal of these two shapes, but the H_C is divided in comparison to the first attempt (par1).

Figure 8.2 and figure 8.3 show that there is a big difference at the response BH-loops.

8.1.2 Comparison of computed BH-loops with 135 spheres and grain size with radius of 10nm (volume ratio of intersected cube/spheres = 53/47)

At this attempt most of the volume is divided into equal parts so one part consists of hard magnetic material and the other part of soft magnetic material, it was possible to replace approximately 46 percent of the cube by spheres which consist at one simulation of soft magnetic material(figure 8.2) and another simulation by hard magnetic material (figure 8.7). At figure 8.4 those two simulations are compared.

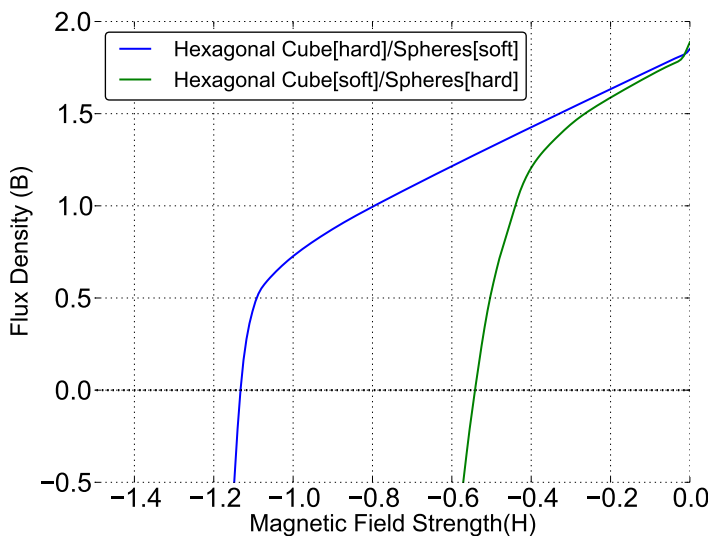


Figure 8.4: Comparison of computed BH-loops with hexagonal lattice, almost 53 percent of the cube is replaced by spheres, the blue curve shows the behaviour of the BH-loop with composition if spheres consist of soft magnetic material and on the opposite the green line shows the effect if the spheres consist of hard magnetic material.The spheres have the radius about 10nm.

Conclusion

According to figure 8.4 there is a big difference at these two BH-loops especially at the response of the coercive force (H_C) value. The curve where the hard magnetic material is at outside and 47 percent of space about the cube is replaced by soft magnetic material shows the best behaviour in comparison to the opposite, where the spheres consist of hard magnetic material, the $(BH)_{max}$ is approximately doubled in comparison to the curve with the second parameter set. All two computations are weighted with material parameters, also these two simulations show that wide areas of soft magnetic materials influence the H_C negatively and also the response to the BH-loops, so it's recommended to prevent big areas of soft magnetic material and intercept them as much as possible to improve the behaviour of nano composite magnets. These requirements make it really hard to find any geometry where as much as possible soft magnetic material is used but all areas of

soft magnetic material are disconnected from each other with the use of hard magnetic materials. One another fact about those two curves is that the value of the coercive force (H_C) is nearly doubled like maximum energy product $(BH)_{\max}$ with another alignment of the soft magnetic material. At the simulation with the first parameter set (par 1) the H_C is 1.2 and the simulation with the second parameter set (par 2) the H_C is 0.55 which means that the case where the hard magnetic material is outside is still a lot better than the opposite simulation. This two simulations are done with two different mesh sizes to figure out if there is still any big difference the first try was with 1.3 million tetrahedrons (maxsize=1.5, minsize=0.5) and the second mesh was with 2.5 million tetrahedrons (maxsize=1.25, minsize=0.5) the result of these two computations is equal.

8.2 Effect of unequal volume ratios

At these next two simulations there is as much possible volume replaced by spheres which don't touch them. At this attempt it was possible to replace almost 63 percent of space by spheres which all have the same dimensions, some spheres are cut which hit boundary of the cube. This attempt is done to show the effect if the volume of spheres and the cube are not equal. Figure 8.5 shows that all spheres are well separated from each other, this figure also shows that spheres are cut which intersect the boundary of the cube to replace as much volume as possible volume by spheres.

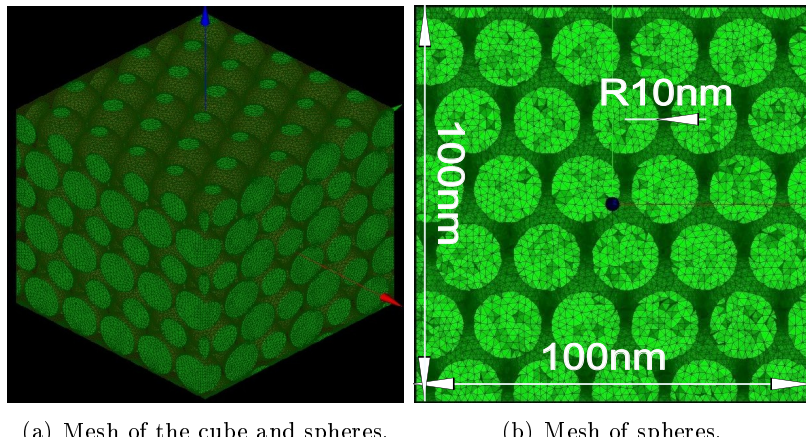


Figure 8.5: Shows the geometry of the intersected cube and spheres with hexagonal lattice each sphere is separated from each other, hexagonal lattice gives the highest dense of sphere packing with equal sized spheres at this case almost 60 percent of the volume is replaced by spheres. At these simulations there are 294 spheres used with the radius of 10nm.

This simulation are done to show the effect if the volume ratio of the hard magnetic and soft magnetic part is not equal, another goal was to replace as much space as possible by spheres. Figure 8.7 and figure 8.6 show that it is possible to achieve the same $(BH)_{\max}$ values with different volume ratios but with the awareness of the right geometry. So it is possible to decrease the amount of hard magnetic material due the fact that it is still a lot better to separate soft magnetic material by hard magnetic material.

8.2.1 Computed BH-loops with 294 spheres and grain size of radius with 10nm (volume ratio of intersected cube/spheres = 40/60)

At these simulations the geometry of hexagonal grid is used. The volume of the cube and spheres are not equal, these simulations are done to show that there are some possibilities to achieve same $(BH)_{max}$ values.

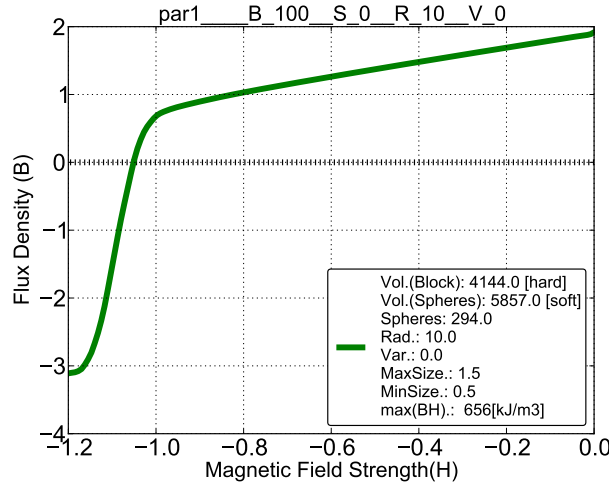


Figure 8.6: BH-loop of first attempt (par1) at this simulation the soft magnetic material(spheres) is separated by hard magnetic material(cube), the volume ratio is not equal of these two shapes, but all two simulations achieve nearly same $(BH)_{max}$ values.

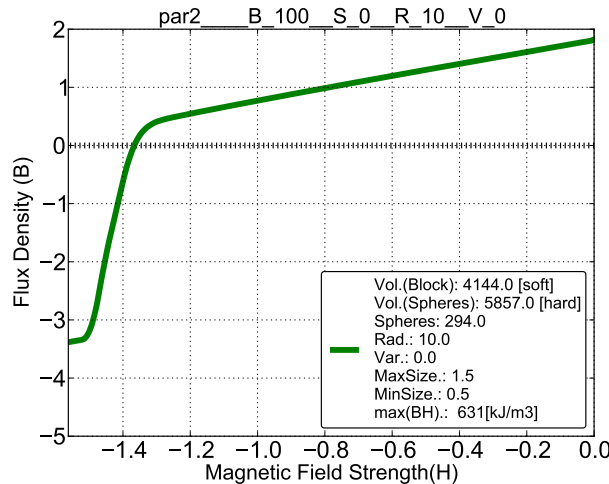


Figure 8.7: BH-loop of second attempt (par2) at this simulation the hard magnetic material(spheres) is separated by soft magnetic material(cube), the volume ratio is not equal of these two shapes, but all two simulations achieve nearly same $(BH)_{max}$ values.

Figure 8.6 and figure 8.7 show that there is a big difference at the response BH-loops.

8.2.2 Comparison of computed BH-loops with 294 spheres and grain size of radius with 10nm and volume ratio of 40/60

At this attempt most of the volume is divided into two parts so one part consist of hard magnetic material and the other part of soft magnetic material. It was possible to replace approximately 63 percent of the cube by spheres which consist at one simulation of soft magnetic material (figure 8.6) and another simulation of hard magnetic material (figure 8.7). At figure 8.8 those two simulations are compared.

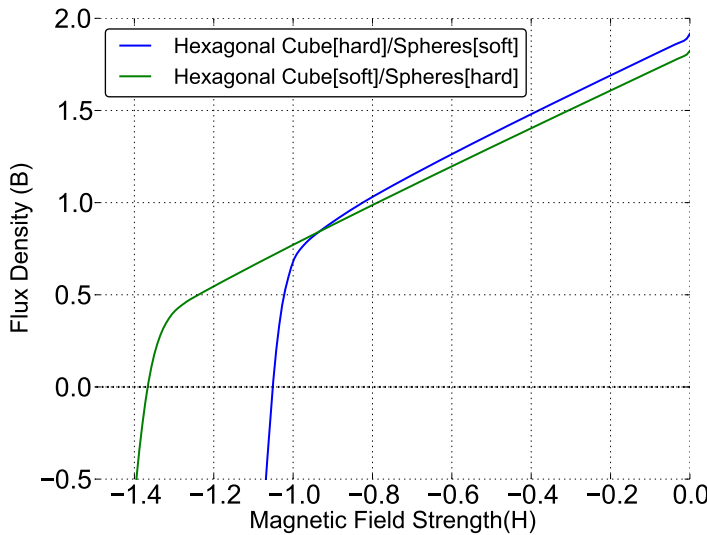


Figure 8.8: Comparison of computed BH-loops with hexagonal lattice, almost 60 percent of the cube is replaced by spheres, the blue curve shows the behaviour of the BH-loop with composition where spheres consist of soft magnetic material and on the opposite the green line shows the behaviour if the spheres consist of hard magnetic material.

Conclusion

According to figure 8.6 and 8.7 the best behaviour is diverse, because at the first computation 8.6 almost 60 percent of the nano composite magnet consist of soft magnetic material which are intersected by hard magnetic material (40 percent), this composition results to a little higher $(BH)_{max}$ value but to worse coercive force (H_C). On the opposite the $(BH)_{max}$ of the second simulation is slightly worse but the curve hits the x-axis with a higher H_C value due the usage of high amount of hard magnetic material. The grain boundaries of the soft magnetic material just influence the shifting point of all BH-loops. This comparison also shows that it is possible to achieve nearly same $(BH)_{max}$ values with the usage of less hard magnetic material and high usage of soft magnetic material. At these two simulations spheres have equal distances to each other sphere. Just to mention at figure 8.6 the curve hits x-axis around 1.1 and at figure 8.7 the curve hits the x-axis around 1.4, so 20 percent less hard magnetic material decreases the value of H_C only about 20 percent.

Chapter 9

Influence of grain size and volume ratio

9.1 Description

At this chapter the influence of the grain size and volume ratio is observed. All simulations are computed with the following parameters for the mesh with max step size = 1.6nm and min size step=0.5, to achieve high accuracy but with less computation time in awareness of the computation time. According to the following simulations the grain size of the soft magnetic materials effects the value of H_C a lot. At this case it is novelty that the grain size of soft phase is observed in complex models (great equation systems). At all next simulations the intersected cube consists of hard magnetic material, where some volume is replaced by spheres which consist of soft magnetic material. All simulations achieve similar $(BH)_{max}$ values (maximum energy product), some values are above or beneath the average value but at all simulations the coercive force (H_C) differs due the usage of different grain sizes and volume ratios. The value of H_C is decreasing at all computations as well with increasing the amount of $\alpha - \text{Fe}$, but the value of the energy product ($(BH)_{max}$) is similar at all simulations. It is recommend to achieve a high coercive force (H_C) because of the problem that with increasing the surrounding temperature of those magnets the coercive force also decreases which leads to a bad energy product. So to gain a high coercive force (H_C) and energy product ($(BH)_{max}$) is one of the most important goals of designing super magnets.

Grain size.	sim1	sim2	sim3	sim4	sim5	
10nm	9%	12%	27%	33%	58%	$\alpha - \text{Fe}$ (usage of Iron in percent)
12.5nm	8%	19%	29%	32%	60%	$\alpha - \text{Fe}$ (usage of Iron in percent)
15nm	7.5%	18%	25%	34%	62%	$\alpha - \text{Fe}$ (usage of Iron in percent)

Table 9.1: This table gives a short overview about the most important parameters which are used in this chapter for all simulations. There are three different grain sizes (soft magnetic material) used and several volume fractions at the soft and hard magnetic phase.

9.2 Influence of grain size and volume ratio

At all these simulations the influence of soft magnetic material is observed especially the effect of the grain size and volume ratio. From figure 9.1 up to 9.3 all simulations are computed with three different grain sizes like 10nm, 12.5nm, 15nm and different volume fractions at the soft magnetic material. Some volume of the cube is replaced by spheres which consist of soft magnetic material, all spheres are separated by hard magnetic material.

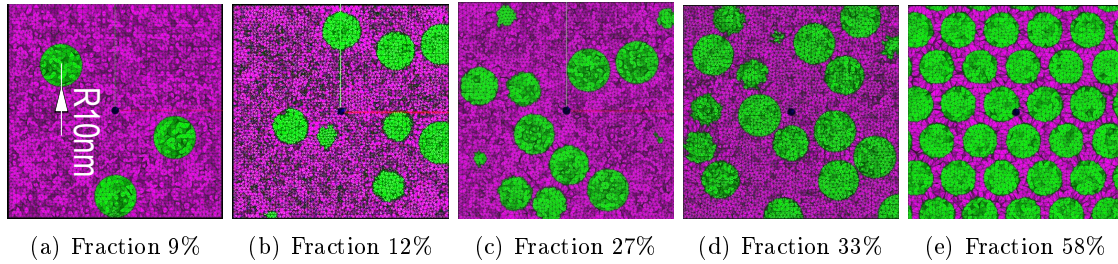


Figure 9.1: Top view - cut through the intersected cube (hard magnetic material) which shows the spheres (soft magnetic material) with the grain size of **radius = 10nm** and different volume fractions due to the usage of different amount of soft magnetic material.

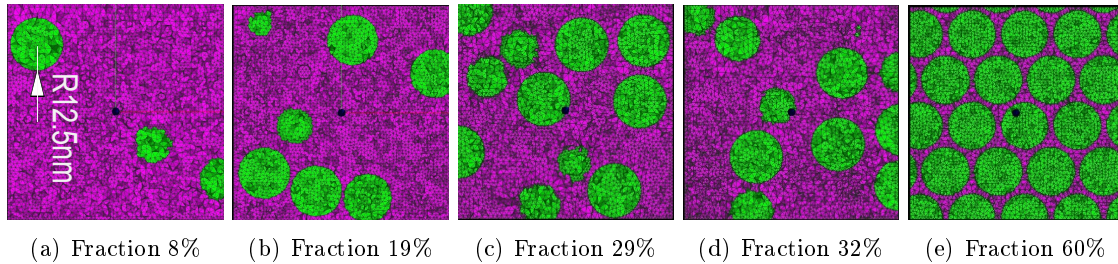


Figure 9.2: Top view - cut through the intersected cube (hard magnetic material) which shows the spheres (soft magnetic material) with the grain size of **radius = 12.5nm** and different volume fractions due to the usage of different amount of soft magnetic material.

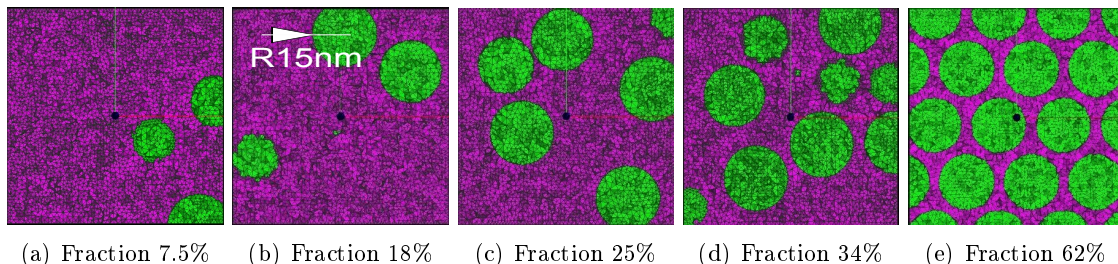


Figure 9.3: Top view - cut through the intersected cube(hard magnetic material) which shows the spheres (soft magnetic material) with the grain size of **radius = 15nm** and different volume fractions due to the usage of different amount of soft magnetic material.

9.2.1 Soft magnetic material with grain size of $r=10\text{nm}$ and different volume ratios

At this group of simulations, all spheres within the cube have a **grain size of 10nm**. All simulations are computed with different amount of iron ($\alpha-\text{Fe}$). The fist simulation starts with about 9 percent iron and the last simulation is computed with 59 percent.

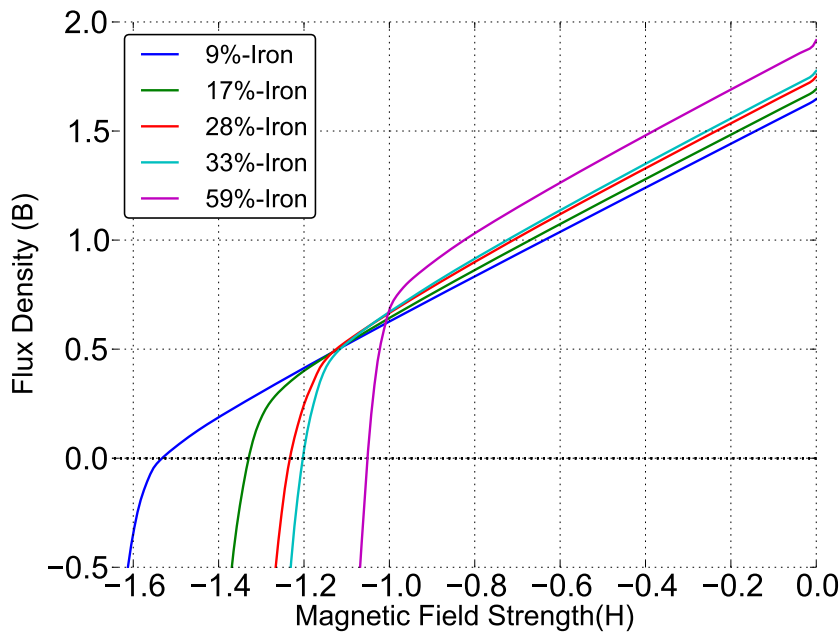


Figure 9.4: Comparison of different BH-loops with equal sized spheres (radius=10nm) and several counts, at all soft simulations different amount of soft magnetic material is used. The intersected cube consists of hard magnetic material and spheres within the boundary are soft magnetic material. At the last simulation with the highest amount of iron the hexagonal lattice is used because of the limitation of random dense packing with equal spheres, all computations achieve nearly same $(BH)_{\max}$ values (higher than 500kJ/m^3) but with a higher ratio of soft magnetic material the value of H_C is decreasing

Conclusion

According to figure 9.4 all computed graphs hit the x-axis between 1.6 and 1.2, and it's obvious that the grain size of the soft magnetic material influences the BH-loop a lot especially the value of H_C . The value of $(BH)_{\max}$ of all computations with grain size of **10nm is especially the best** in comparison to higher grain sizes. All values are not normalized in this graph because the so flux density (B) is shown and not the magnetization (M), so the volume ratio of the soft and hard magnetic part is respected, which leads to the point that all curves start with different y-values because of the different amount of soft magnetic material. The value of the coercive force (H_C) is mainly effected by the grain size of the soft magnetic material but as well the volume ratio of soft and hard magnetic material is still important.

9.2.2 Soft magnetic material with grain size of $r=12.5\text{nm}$ and different volume ratios

At this group of simulations, all spheres within the cube have the **grain size of $r=12.5\text{nm}$** . All simulations are computed with different amount of iron($\alpha - \text{Fe}$). The fist simulation starts with about 8 percent iron and the last simulation is computed with 60 percent.

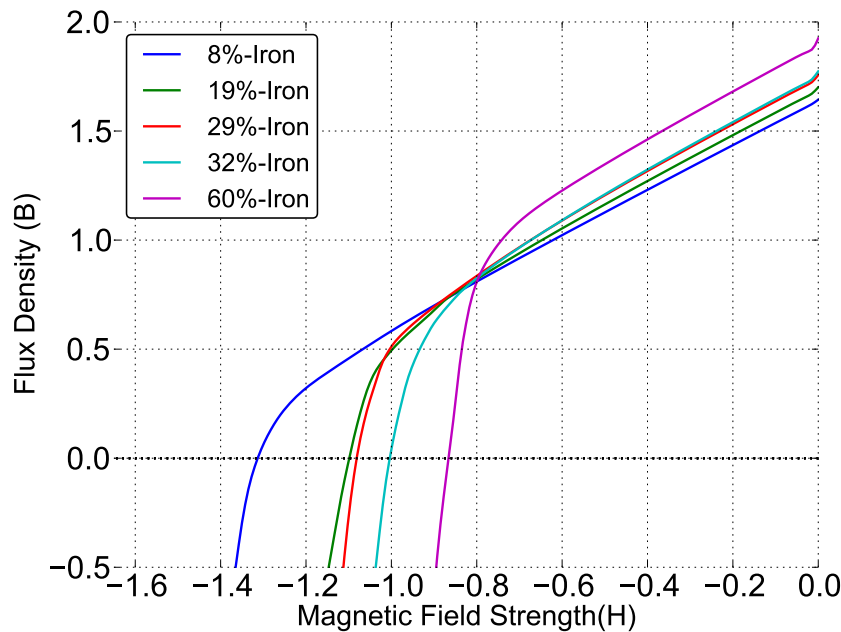


Figure 9.5: Comparison of different BH-loops with equal sized spheres (radius=12.5nm) and several counts, at all soft simulations different amount of soft magnetic material is used. The intersected cube consists of hard magnetic material and spheres within the boundary are soft magnetic material. At the last simulation with the highest amount of iron the hexagonal lattice is used because of the limitation of random dense packing with equal spheres, all computations achieve nearly same $(BH)_{\max}$ values (less than 500kJ/m^3) but with a higher volume ratio of soft magnetic material the value of H_C is decreasing.

Conclusion

According to figure 9.5 all computed graphs hit the x-axis between 1.4 and about 0.85, and it's obvious that the grain size of the soft magnetic material influences the BH-loop a lot especially the value of H_C . The value of $(BH)_{\max}$ of all computations with grain size of **12.5nm is average** in comparison to other simulations. All values are not normalized in this graph because the flux density (B) is shown and not the magnetization (M), so the volume ratio of the soft and hard magnetic part is respected, which leads to point that all curves start with different y-values because of the different amount of soft magnetic material. The value of the coercive force (H_C) is mainly effected by the grain size of the soft magnetic. All computed curves are shifted in the middle in comparison to figure 9.4 and 9.6 due the usage of a average grain size at the soft magnetic material.

9.2.3 Soft magnetic material with grain size of $r=15\text{nm}$ and different volume ratios

At this group of simulations, all spheres within the cube have the **grain size of $r=15\text{nm}$** . All simulations are computed with different amount of iron($\alpha - \text{Fe}$). The fist simulation starts with about 8 percent iron and the last simulation is computed with 63 percent.

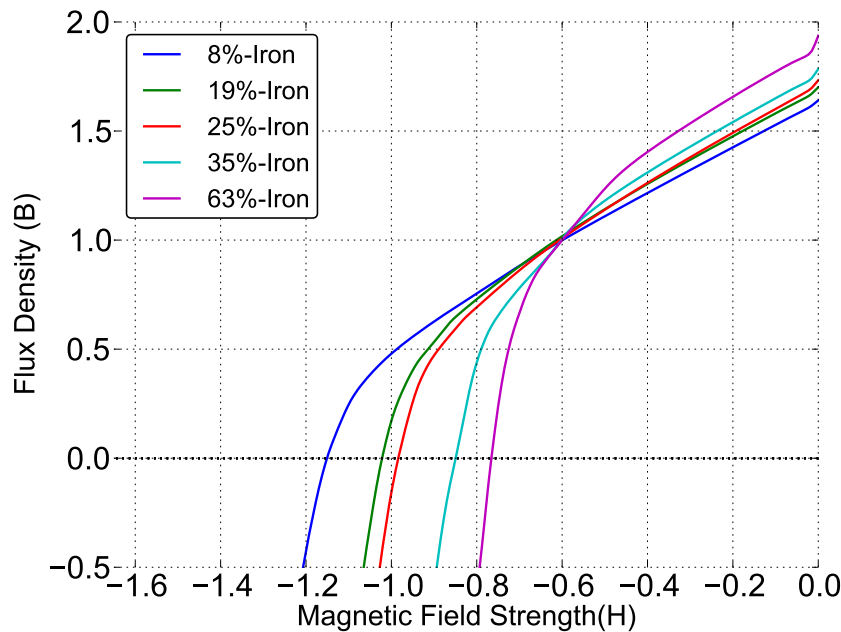


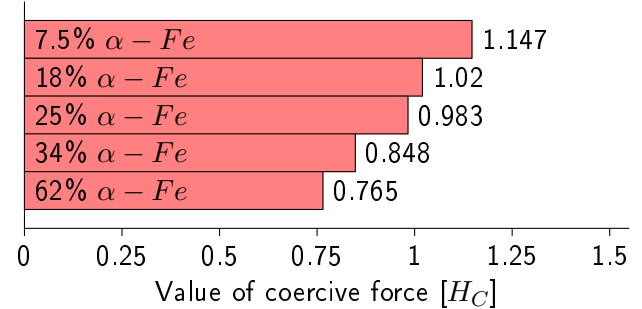
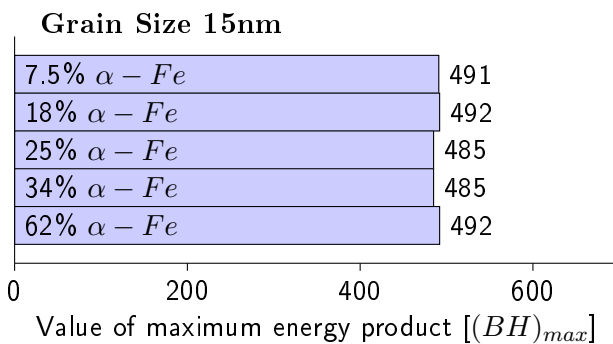
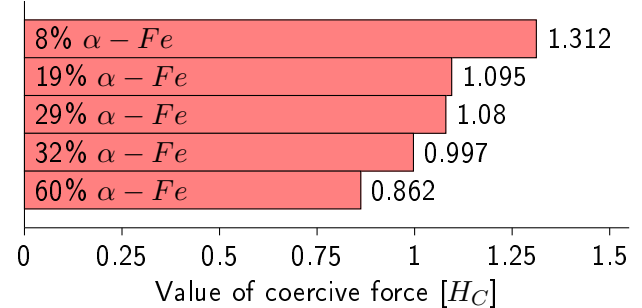
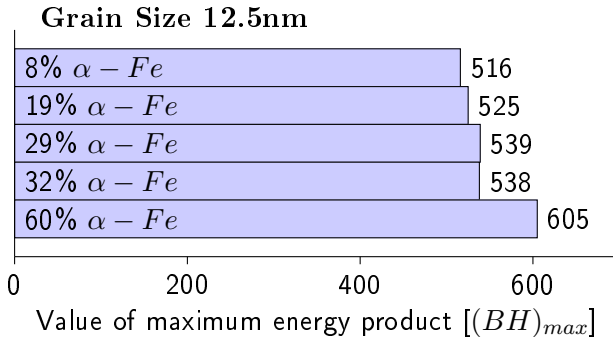
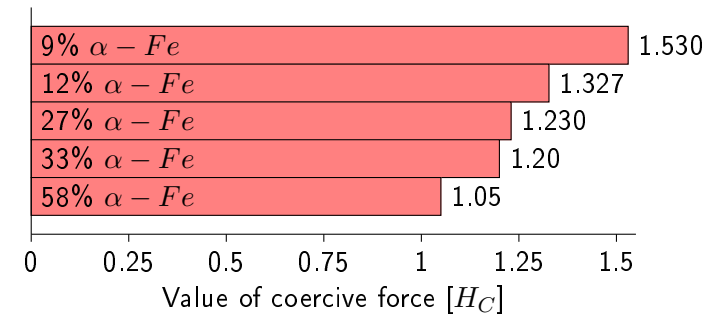
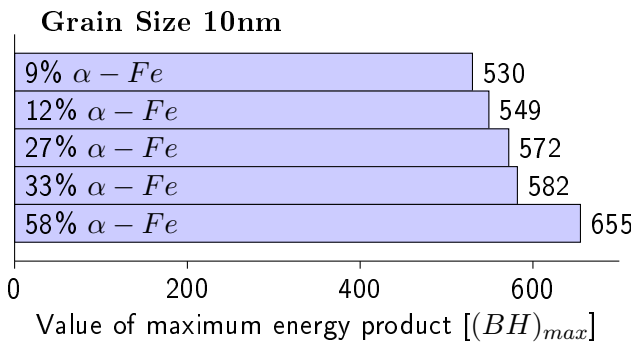
Figure 9.6: Comparison of different BH-loops with equal sized spheres (radius=15nm) and several counts, at all soft simulations different amount of soft magnetic material is used. The intersected cube consists of hard magnetic material and spheres within the boundary are soft magnetic material. At the last simulation with the highest amount of iron the hexagonal lattice is used because of the limitation of random dense packing with spheres, all computations achieve nearly same $(BH)_{\max}$ values (less than 500kJ/m^3) but with higher volume fraction of soft magnetic material the value of H_C is decreasing.

Conclusion

According to figure 9.6 all computed graphs hit the x-axis between 1.2 and 0.8, and it's obvious that the grain size of the soft magnetic material influences the BH-loop a lot especially the value of H_C . The value of $(BH)_{\max}$ of all computations with grain size of **15nm is even the worst** in comparison to other simulations. All values are not normalized in this graph because the flux density (B) is shown and not the magnetization (M), so the volume ratio of the soft and hard magnetic part is respected, which leads to point that all curves start with different y-values because of the different amount of soft magnetic material. The value of the coercive force (H_C) is mainly effected by the grain size of the soft magnetic material. All computed curves are shifted in right direction in comparison to figure 9.4 and 9.5 due the usage of a rough grain size.

9.2.4 Comparison of $(BH)_{max}$ and corresponding H_C values

Short summary about those simulations all important data are collected from each simulation like grain size, maximum energy product ($(BH)_{max}$) and coercive force (H_C) to show the correlation between all parameters and variables. The grain size of the soft magnetic material is really important to the coercive force (H_C) like the amount of α -Fe. The value of $(BH)_{max}$ is increasing if the amount of α -Fe is increased but at the opposite the value of H_C is decreased because of higher amount of soft magnetic material. At all simulations smaller grain sizes of α -Fe lead to higher H_C values and higher amount of soft magnetic material evaluates the maximum energy product ($(BH)_{max}$)..



9.2.5 Summary

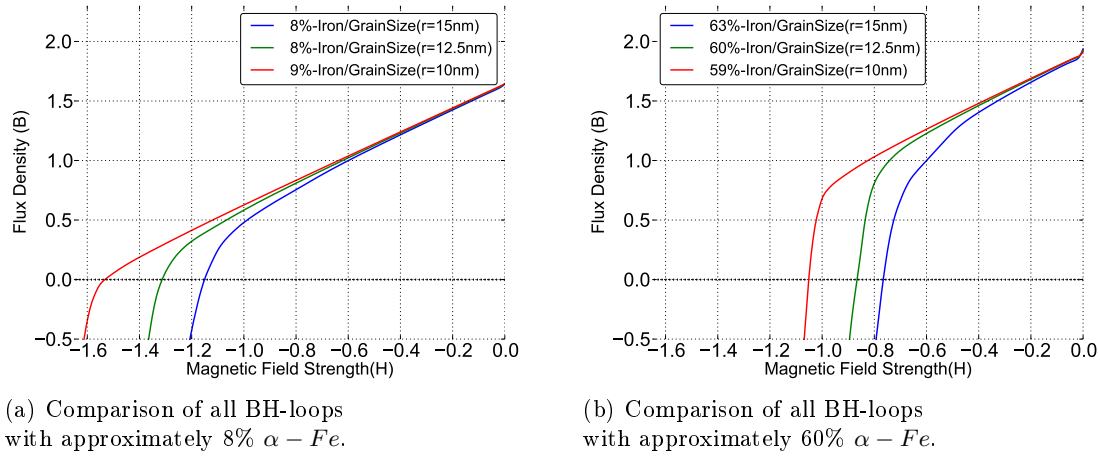


Figure 9.7: This two figures show the effect of different grain sizes even with less amount of Iron the hysteresis loop is crucial effected by the grain size of the soft magnetic material. 60% of α -Fe are natural used at Nd-Fe-B magnets, so the strength of those super magnets can be evaluated by smaller grain sizes and maybe some alloys. The value of H_C is crucial to the value of the maximum energy product $((BH)_{\max})$ and the associated temperature dependency. Smaller grain sizes lead to less temperature dependency. Maybe there is a grain size where there is no negative effect to the proper hysteresis loops especially with the usage of higher amount of Iron (α -Fe). Smaller grain sizes lead to higher shifting points where the curves are starting to hit the x-axis.

According to figure 9.4, 9.5 and 9.6, the grain size has a serious impact on the behaviour of all BH-loops and especially to the value of H_C and the associated maximum energy product $((BH)_{\max})$. So there are some possibilities how to control the behaviour of the hysteresis loop. The best way to improve the performance data of super magnets is to use smaller grain sizes for the soft magnetic part. It also includes that the area of all soft phases is really small in comparison to the hard magnetic material, so this phase must split the areas of all soft phases as much as possible. All simulations achieve different $((BH)_{\max})$ values. The fraction of the soft phase is not important as long as the value of H_C is high enough. Nearly all simulations with the grain size of 10nm achieve better H_C values than simulations with the grain of 15nm, because all hit the x-axis above 1. It's also obvious that the ratio of soft magnetic material influence the value of the coercive force H_C , but the grain size of the soft phase influences the behaviour a lot more. At the first simulation and the usage of only 8 percent iron with the grain size of 10nm the curve hits the x-axis about 1.55 in comparison to the nearly same amount of iron the simulation with a rougher grain size of 15nm the x-axis get hit by the value of 1.2. The goal must be to use smaller grain sizes so the influence of the soft phase decreases like the temperature dependency and it's possible to use more iron which reduces the cost of super magnets.

Chapter 10

Compendium and prospects

This work is about simulation nano composite magnets. Super magnets always consist of two phases like the hard magnetic phase and on the opposite the soft magnetic part. The goal must be to use as much soft magnetic material as possible to decrease the overall costs but with less disadvantages. There are some simulations in this work to show the effect of soft magnetic material with different geometries and volume ratios. In all simulations the geometry and the grain sizes of this material are really important. Beside the problem of the right usage of the soft phase also some chapters about the main issue, computing finite elements and basic principles about nano composite magnets are shown. There are a lot of different problems which make it difficult to replace hard magnetic material by soft magnetic material especially the geometry and grain size of the soft phase is really important by this way. The problem of sphere packing mentioned in this work is the main issue of replacing space by any geometry body. There is often a limitation of replacing space which makes it impossible to replace any volume as far as wanted, it even becomes harder if there is any requirement like spheres or shapes are not allowed to touch another shape. In this work there are also some simulations to figure out what's the best way to replace hard magnetic material by soft magnetic material, like to avoid wide areas of soft phases. One last point in this work is to show the effect with different grain sizes and volume ratios of the soft magnetic phase. The aim of new super magnets must be to decrease the influence of the soft magnetic phase, it's possible to achieve the same energy product $(BH)_{\max}$ with different grain sizes and different volume fractions which influence the coercive force (H_C) too. This value must be in focus at most applications because a higher (H_C) value means that super magnets are still powerful if the surrounding temperature is high. One way to decrease the temperature dependency is to use smaller grain sizes for the soft magnetic phase which increase the value of (H_C). It is also possible to use a geometry where the influence of the soft magnetic material is nearly negated. This study also shows the with the awareness of the right alignment of the soft magnetic phase the behaviour of nano composite magnets can be influenced in a positive way especially if the volume fraction is the same. There are also some simulations to show that smaller grain sizes about the soft magnetic material evaluates the strength of super magnets positive.

Bibliography

- [1] Close-packing of equal spheres. http://readtiger.com/wkp/en/Close-packing_of_equal_spheres.
<http://readtiger.com>, last visited: June 2, 2013.
- [2] History of magnetism. http://www.gitam.edu/eresource/Engg_Phys/semester_2/magnetic/intro.htm.
GITAM, Department of Engineering Physics, last visited: June 2, 2013.
- [3] Manufacturer of high-performance rare earth magnets, ndfeb, smco. the stable production and supply of high-quality, high-precision rare earth magnet.
<http://www.shinetsu-rare-earth-magnet>.
- [4] Nanocomposite magnets. <http://www.ifm.eng.cam.ac.uk/research/cip/hiwi/>. Institute for Manufacturing, Dept. of Engineering , last visited: June 2, 2013.
- [5] Hicham Badri, Mohammed El Hassouni, and Driss Aboutajdine. Kernel-based laplacian smoothing method for 3d mesh denoising. In Abderrahim Elmoataz, Driss Mammass, Olivier Lezoray, Fathallah Nouboud, and Driss Aboutajdine, editors, *Image and Signal Processing*, volume 7340 of *Lecture Notes in Computer Science*, pages 77–84. Springer Berlin Heidelberg, 2012. ISBN 978-3-642-31253-3.
- [6] Stephen B. Castor. *Rare Earth Deposits of North America*, volume 58. Resource Geology, Nevada Bureau of Mines and Geology, University of Nevada, Reno, Nevada, USA, November 2008. DOI:10.1111/j.1751-3928.2008.00068.x.
- [7] Michael Diggles. Rare earth elements critical resources for high technology.
<http://pubs.usgs.gov/fs/2002/fs087-02/>. U.S. Geological Survey, last visited: June 2, 2013.
- [8] Peter Fleischmann. <http://www.iue.tuwien.ac.at/phd/fleischmann/node25.html>. TU Vienna, last visited: June 2, 2013.
- [9] Carl F. Gauss. Besprechung des buchs von l. a. seeber: Untersuchungen über die eigenschaften der positiven ternären quadratischen formen usw. *Göttingische Gelehrte Anzeigen*, 2:188–196, 1831. 1876.
- [10] J.P. Gregoire, C. Rose, and B. Thomas. Direct and iterative solvers for finite-element problems. *Numerical Algorithms*, 16(1):39–53, 1997. <http://dx.doi.org/10.1023/A>
- [11] Thomas C. Hales. The sphere packing problem. *Journal of Computational and Applied Mathematics*, 44:41–76, November 1992.

- [12] Thomas C. Hales. A proof of the kepler conjecture. *Math. Intelligencer*, 16:47–58, 1994.
- [13] Sabine Hoefinger Josef Fidler, Thomas Schrefl and Maciej Hadjuga. Recent developments in hard magnetic bulk material. *Journal of Physics:Condensed Matter*, 16(2):455–469, January 2004. DOI:10.1088/0953-8984/16/5/007.
- [14] M. Jurczyk. Nanocomposite Nd-Fe-B type magnets. *Journal of Alloys and Compounds*, 299:283–286, November 2000.
- [15] Professor Emeritus Karl J.Strnat. Modern permaneten magnets for application in electro-technology. *Journal of Physics:Condensed Matter*, 78(6):923 – 946, 1990. DOI:10.1109/5.56908.
- [16] S. Harrell M. Beals, L. Gross. Cell aggregation and sphere packing. <http://www.tiem.utk.edu/~gross/bioed/webmodules/spherepacking.htm>. The institute for Environmental Modelling, last visited: June 2, 2013.
- [17] T. Schrefl R. W. Chantrell, J. Fidler and M. Wongsam. Micromagnetics: Finite element. *Encyclopedia of Materials: Science and Technology*, pages 5651+5661, 2001. ISBN: 0-08-0431526, <http://magnet.atp.tuwien.ac.at/ts/papers/ema108005.pdf>.
- [18] M. Radi and S. Selberherr. Three-dimensional adaptive mesh relaxation. In Kristin Meyer and Serge Biesemans, editors, *Simulation of Semiconductor Processes and Devices 1998*, pages 193–196. Springer Vienna, 1998. ISBN 978-3-7091-7415-9.
- [19] Daniel Rypl. Mesh quality. <http://mech.fsv.cvut.cz/~dr/papers/Thesis/node23.html>. University of Leeds, last visited: June 2, 2013.
- [20] Joachim Schöberl. <http://www.hpfem.jku.at/netgen/>. Johannes Kepler University Linz, last visited: June 2, 2013.
- [21] Mark S. Shephard and Marcel K. Georges. Automatic three-dimensional mesh generation by the finite octree technique. int. j. numer. meth. engng. *International Journal for Numerical Methods in Engineering*, 32(4):709–749, 1991. DOI: 10.1002/nme.4503.
- [22] Jonathan Richard Shewchuk. What is a good linear element ? interpolating, conditioning and quality measure. *University of California at Berkeley,Berkeley*. <http://www.cs.berkeley.edu/~jrs/papers/elem.pdf>.
- [23] Ralph Skomski and J.M.D.Coey. Giant energy product in nanostructred two-phase magnets. *Journal of Physics:Condensed Matter*, 48(24):15812–15816, November 1993.
- [24] Mysid Slffea. Unstructured grid. http://commons.wikimedia.org/wiki/File:Unstructured_grid.svg. Wikipedia, last visited: June 2 2013.
- [25] Wayne Storr. Electronics tutorial about magnetic hysteresis. <http://www.electronics-tutorials.ws/electromagnetism/magnetic-hysteresis.html>. Basic Electronics Tutorials, last visited: June 2, 2013.

- [26] George G. Szpiro. *Kepler's conjecture : how some of the greatest minds in history helped solve one of the oldest math problems in the world.* John Wiley & Sons, Inc., Hoboken, New Jersey, November 2003. ISBN 0-471-08601-0.
- [27] Damien; Schlenker Michel (Eds.) Tremolet de Lacheisserie, E.; Gignoux. *Magnetism, Materials and Applications*, volume 24. First Springer Science + Business Media, Inc. softcover printing, 2005, 233 Spring Street, New York, NY 10013, USA, November 2005. E-book ISBN 0-387-27063-7.
- [28] Eric W. Weisstein. Sphere packing problem. <http://mathworld.wolfram.com/SpherePacking.html>. Wolfram MathWorld, last visited: June 2, 2013.
- [29] D.H. Ping Y.Q. Wu and A.Inoue K. Hono, M.Hamano. Microstructural characterization of an nanoncomposite /Nd-Fe-B magnet with a remaining amorphouse phase. *International Journal for Numerical Methods in Engineering*, 32(4):3295–3297, September 1999. ISSN : 0018-9464, DOI: 10.1109/TMAG.1984.1063214, [http://www.nims.jp/apfim/apfim/pdf/NdFeBCuNb-\]JAP.pdf](http://www.nims.jp/apfim/apfim/pdf/NdFeBCuNb-]JAP.pdf).

Appendices

.1 First Appendix

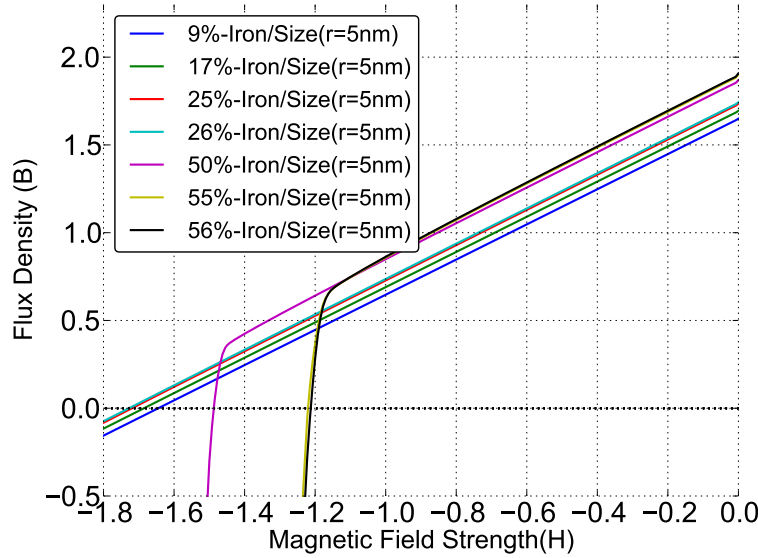


Figure 1: Comparison of all BH-loops with the grain size of $r=5\text{nm}$ and different fractions of the soft magnetic part , at 8% $\alpha - \text{Fe}$ up to 32% $\alpha - \text{Fe}$ random packed spheres and 45% $\alpha - \text{Fe}$ up to 58% $\alpha - \text{Fe}$ hexagonal packed spheres are used.

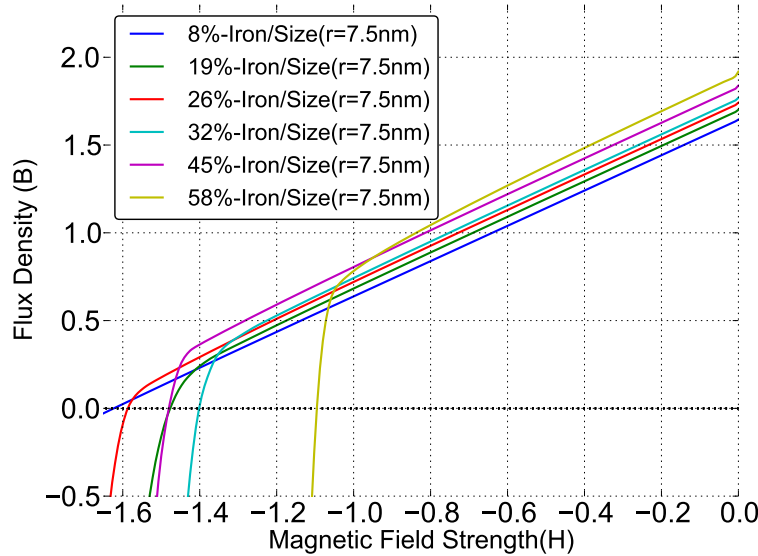


Figure 2: Comparison of all BH-loops with the grain size of $r=7.5\text{nm}$ and different fractions of the soft magnetic part , at 8% $\alpha - \text{Fe}$ up to 32% $\alpha - \text{Fe}$ random packed spheres and 45% $\alpha - \text{Fe}$ up to 58% $\alpha - \text{Fe}$ hexagonal packed spheres are used.

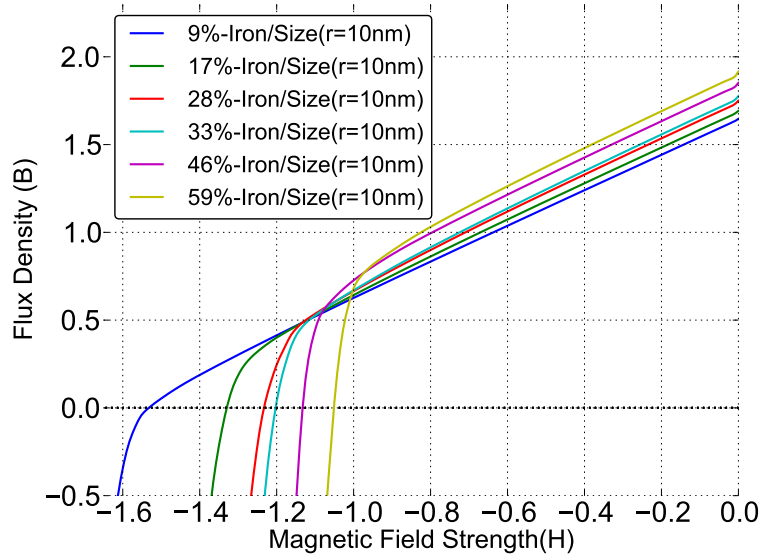


Figure 3: Comparison of all BH-loops with the grain size of $r=10\text{ nm}$ and different fractions of the soft magnetic part , at 9% $\alpha - Fe$ up to 33% $\alpha - Fe$ random packed spheres and 46% $\alpha - Fe$ up to 59% $\alpha - Fe$ hexagonal packed spheres are used.

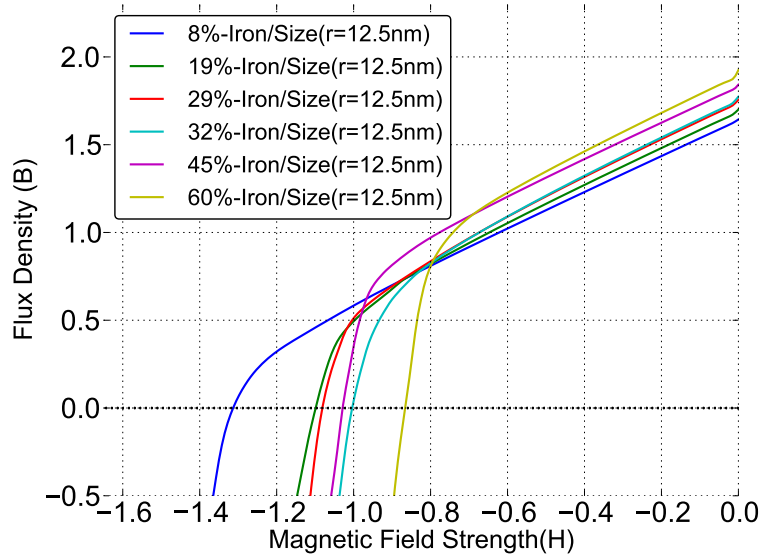


Figure 4: Comparison of all BH-loops with the grain size of $r=12.5\text{ nm}$ and different fractions of the soft magnetic part , at 8% $\alpha - Fe$ up to 32% $\alpha - Fe$ random packed spheres and 45% $\alpha - Fe$ up to 60% $\alpha - Fe$ hexagonal packed spheres are used.

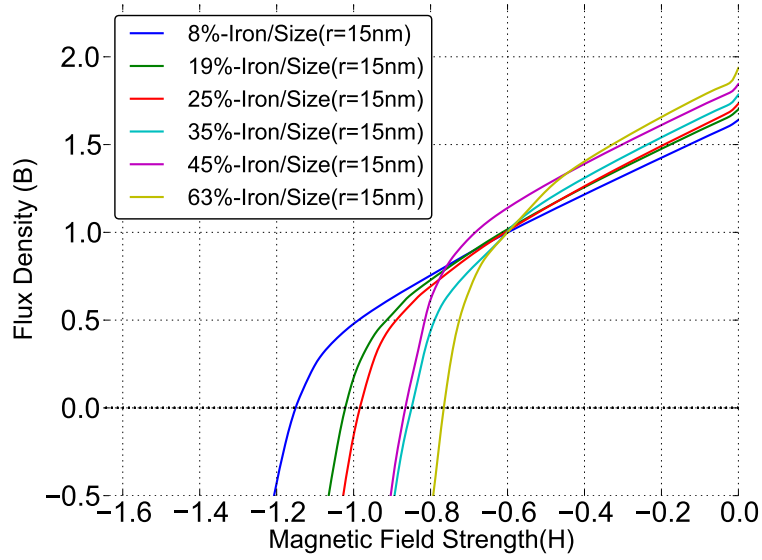


Figure 5: Comparison of all BH-loops with the grain size of $r=15\text{nm}$ and different fractions of the soft magnetic part , at 8% $\alpha - \text{Fe}$ up to 35% $\alpha - \text{Fe}$ random packed spheres and 45% $\alpha - \text{Fe}$ up to 63% $\alpha - \text{Fe}$ hexagonal packed spheres are used.

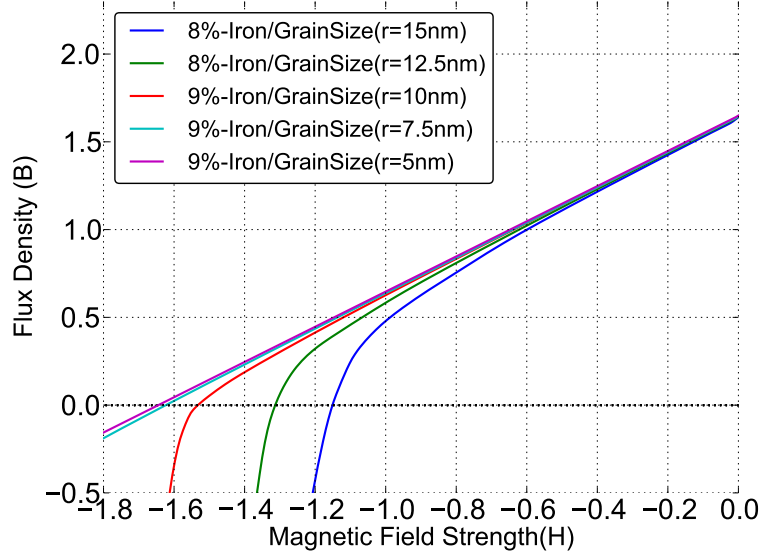


Figure 6: Comparison of all BH-loops with approximately 8% $\alpha - \text{Fe}$, at this case the intersected cube consists of hard magnetic material and all spheres within with soft magnetic material, three simulations with different grain sizes ($r=5, 7.5\text{nm}, 10\text{nm}, 12.5\text{nm}, 15\text{nm}$) are compared with nearly same amount of volume fractions.(random packed spheres)

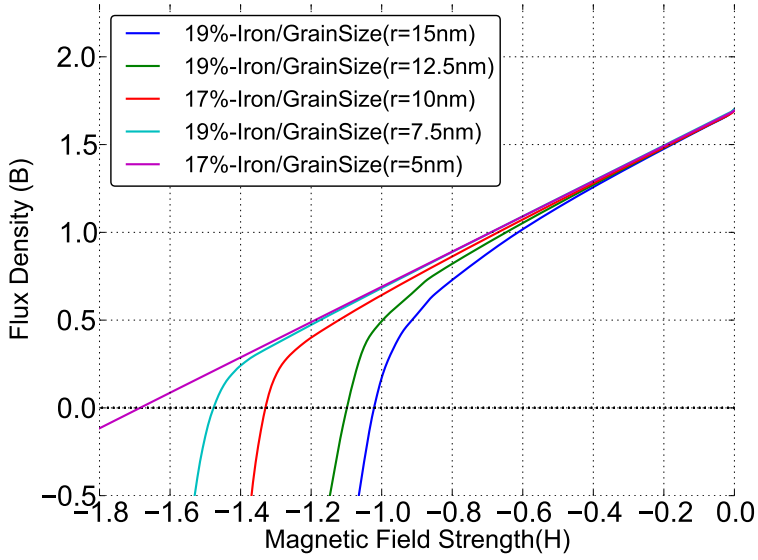


Figure 7: Comparison of all BH-loops with approximately 19% α -Fe, at this case the intersected cube consists of hard magnetic material and all spheres within with soft magnetic material, three simulations with different grain sizes ($r=5, 7.5\text{nm}, 10\text{nm}, 12.5\text{nm}, 15\text{nm}$) are compared with nearly same amount of volume fractions. (**random packed spheres**)

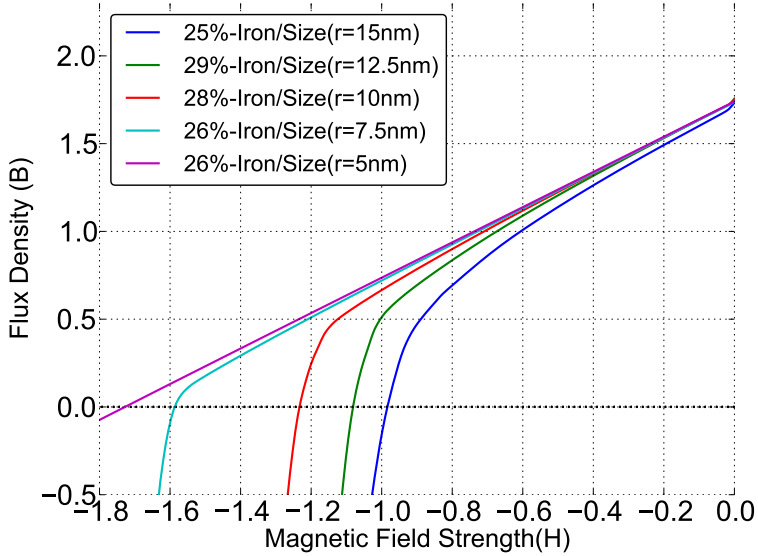


Figure 8: Comparison of all BH-loops with approximately 28% α -Fe, at this case the intersected cube consists of hard magnetic material and all spheres within with soft magnetic material, three simulations with different grain sizes ($r=5, 7.5\text{nm}, 10\text{nm}, 12.5\text{nm}, 15\text{nm}$) are compared with nearly same amount of volume fractions. (**random packed spheres**)

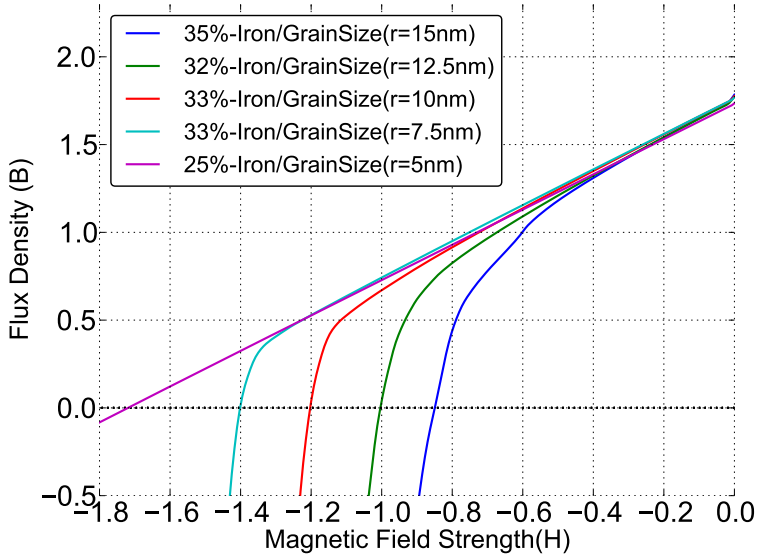


Figure 9: Comparison of all BH-loops with approximately 33% α -Fe, at this case the intersected cube consists of hard magnetic material and all spheres within with soft magnetic material, three simulations with different grain sizes ($r=5, 7.5\text{nm}, 10\text{nm}, 12.5\text{nm}, 15\text{nm}$) are compared with nearly same amount of volume fractions. (**hexagonal packed spheres**)

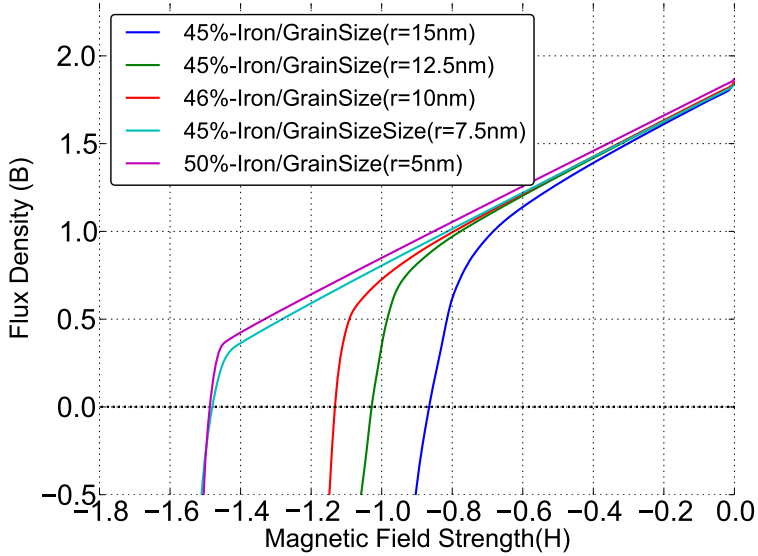


Figure 10: Comparison of all BH-loops with approximately 45% α -Fe, at this case the intersected cube consists of hard magnetic material and all spheres within with soft magnetic material, three simulations with different grain sizes ($r=5, 7.5\text{nm}, 10\text{nm}, 12.5\text{nm}, 15\text{nm}$) are compared with nearly same amount of volume fractions. (**hexagonal packed spheres**)

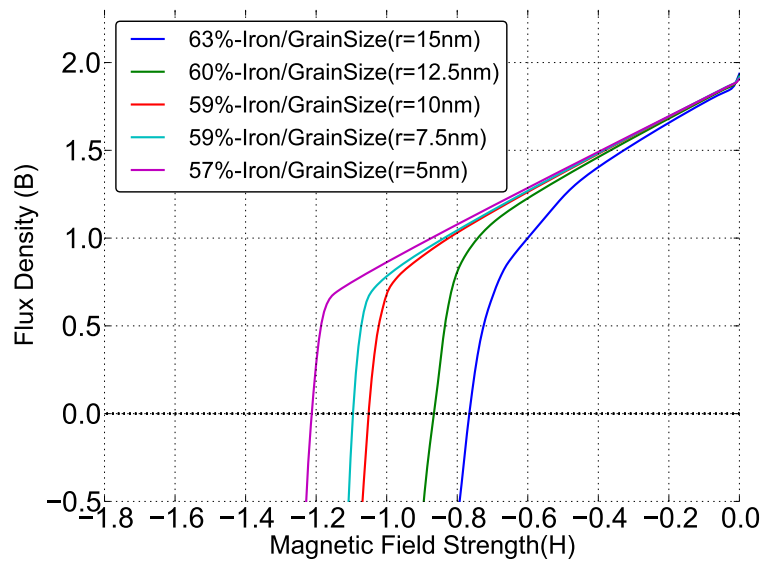


Figure 11: Comparison of all BH-loops with approximately 60% α -Fe, at this case the intersected cube consists of hard magnetic material and all spheres within with soft magnetic material, three simulations with different grain sizes($r=5, 7.5\text{nm}, 10\text{nm}, 12.5\text{nm}, 15\text{nm}$) are compared with nearly same amount of volume fractions. (**hexagonal packed spheres**)